DISSERTATION

submitted to the

Combined Faculties for the Natural Sciences and for Mathmatics

of the Ruperto-Carola University of Heidelberg, Germany

for the degree of

Doctor of Natural Sciences

presented by

Hitomi Sanno

born in Shiga, Japan

oral examination: ……

The generation and characterization of transgenic mice expressing modifiers of Rho GTPases

Gutachter: Prof. Dr. Hilmar Bading

PD. Dr. Ralph Nawrotzki

Hiermit erkläre ich, daß ich die vorliegende Dissertation selbst verfaßt und mich dabei keiner anderen als der von mir ausdrücklich bezeichneten Quellen and Hilfen bedient habe. Des Weiteren erkläre ich, daß ich an keiner anderen Stelle ein Prüfungsverfahren beantragt oder die Dissertation in dieser oder einer anderen Form bereits anderweitig als Prüfungsarbeit verwendet oder einer anderen Fakultät als Dissertation vorgelegt habe.

Heidelberg, ...

Hitomi Sanno

Acknowledgements

I would like to express my sincere gratitude to the following people:
Dr. Kerry Lee Tucker for this interesting project, for his enthusiastic scientific support, and for immensely helpful advice, criticism and suggestions during all my Ph.D years.
Prof. Dr. Achim Kirsch for providing a wonderful working space and scientific support.
Prof. Dr. Hilmar Bading and PD. Dr. Ralph Nawrotzki for valuable ideas and suggestions, as well as for evaluating this thesis.
Prof. Dr. Karin Gorgas and Dorde Komljenovic for their help in analysis of the brain sections.
Dr. Silvia Arber from University of Basel, Switzerland, for the loxP vector construct.
Dr. Klaus Aktories from University of Frieburg for the C3 cDNA.
Prof. Dr. Stefan Offermanns for the EIIa and Nestin CRE mice.
All the members of the Tucker group for their advice and kind support.
Mark Evans for his critical reading and suggestion for Figure 2.

I would like to show my sincere gratitude to all my family for their support throughout my entire study.

This work was financially supported by the SFB 488 (to Dr. K.L. Tucker).

Summary

In developmental neurobiology, it is a fundamental topic but it is not still well investigated how newborn neurons elaborate axonal and dendrite processes to navigate complicated pathways and travel long distances before they reach their target. Recent studies have suggested that Rho family GTP-binding proteins are important components of the signalling pathways that link the reception of extracellular cues to the cytoskeleton. Rho family GTP-binding proteins regulate many different aspects of the actin cytoskeleton in a wide variety of organisms. Small GTPases of the Rho family have been suggested to be involved in the regulation of formation of neurites and their differentiation into axons and dendrites, but the function of Rho GTPases is not still clear in terms of axonal and dendritic growth during mammalian development. There are numerous data suggesting the important role of Rho GTPases in axonal guidance *in vitro*, however, there has been little direct evidence of these proteins in the *in vivo* context in mammals. To modulate the activity of Rho during early nervous system development, we expressed either a RhoA dominant negative (N19-RhoA) mutant, a constitutively active (V14-RhoA) mutant, or a natural inhibitor, C3 transferase from *Clostridium botulinum*, in neuborn neurons under the control of the tau gene. Their protein expression in neurons can be activated by application of Cre recombinase. The tau gene was used because it is known to drive the high expression of genes specifically in neurons (Binder *et al.*, 1995). We used this transgenic strategy to analyze the effects of Rho family GTP-binding proteins on axonal outgrowth in early nervous system and the effect of long-term inhibition of Rho function in the adult brain. The recombinant protein of N19-RhoA was expressed in the postnatal mouse brain, and we found that the somatosensory cortex in the adult mouse brain contained more severe involutions and aggregations of the cells in specific area of somatosensory cortex in brain, particularly in layer IV. Also, the barrel-like discontinuous pattern was more extended toward the posterior part of the brain in the mice that have expressed a dominant negative RhoA.

Zusammenfassung

Wie neugeborene Neurone ihre axonalen und dendritischen Fortsätze einsetzen um komplizierte Signalwege zu steuern und um weite Entfernungen zu überwinden bevor sie ihr Ziel erreichen, ist ein fundamentales aber noch nicht ausreichend erforschtes Thema in der Entwicklungsbiologie. Jüngste Studien zeigen, dass GTP-bindende Proteine der Rho Familie wichtige Bestandteile von Signalkaskaden sind, welche das Cytoskelett modulieren können. GTP-bindende Proteine der Rho Familie regulieren viele verschiedene Aspekte des Aktin Cytoskelettes in einer Vielzahl von Organismen. Es wird angenommen, das kleine GTPasen der Rho Familie an der Regulation und Entstehung von Neuriten und ihrer Differenzierung in Axone und Dendriten beteiligt sind. Die Funktion der Rho GTPasen beim axonalen oder dendritischen Wachstum während der Entwicklung ist aber bisher noch ungeklärt. Verschiedene Daten weisen darauf hin das Rho GTPasen in der axonalen Zielführung in vitro eine Rolle spielen, doch liegen für diese Proteine und deren Funktion, in vivo bei Säugetieren, deutlich weniger Daten vor. Um die Aktivität von Rho während der frühen Entwicklung des Nervensystems zu modulieren, wurden entweder eine RhoA dominant negative Mutante (N19-RhoA), eine konstitutiv aktive (V14-RhoA) Mutante, oder ein natürlicher Inhibitor, die C§ Transferase aus Clostridium botulinum, in neugeborenen Neuronen unter der Kontrolle des Tau Gens exprimiert. Die Protein Expression kann in diesem System durch die Zugabe einer Cre Recombinase aktiviert werden.
Hierbei wurde das Tau-Gen benutzt weil es dafür bekannt ist, eine hohe Expression von Genen, speziell in Neuronen, zu ermöglichen. In dieser Arbeit wurde diese transgene Strategie angewendet, um die Effekte der GTP-bindenden Proteine der Rho Familie auf das axonale Wachstum im frühen neuronalen System, und um den Effekt der Langzeitinhibierung von Rho im adulten Gehirn zu untesuchen.
Mit dieser Arbeit konnte gezeigt werden, das die Expression des rekombinanten Proteins N19-RhoA im postnatalen Gehirn der Maus zu einer erhöhten Aggregation von Zellen, in der Schicht IV im somatosensorischen Kortex der adulten Maus, führt. Weiterhin wurde beobachtet das dass barrel-field, bei den dominant negativen RohA Mutanten, weiter in Richtung einer posterioren Region verschoben war.

Table of contents

1 INTRODUCTION

In developmental neurobiology, it is a fundamental topic but it is not still well investigated how newborn neurons elaborate axonal and dendrite processes to navigate complicated pathways and travel long distances before they reach their target. Recent studies have suggested that Rho family GTP-binding proteins are important components of the signalling pathways that link the reception of extracellular cues to the cytoskeleton.

Rho family GTP-binding proteins, Rho GTPases, regulate many different aspects of the actin cytoskeleton in a wide variety of organisms. Small GTPases of the Rho family have been suggested to be involved in the regulation of formation of neurites and their differentiation into axons and dendrites, but the function of Rho GTPases is not still clear in terms of axonal and dendritic growth during mammalian development *in vivo*. There are numerous data suggesting the important role of Rho GTPases in axonal guidance *in vitro*, however, there has been little direct evidence of these proteins in the *in vivo* context in mammals.

In general, Rho inhibits neurite outgrowth, and when Rho is bound to GTP, Rho causes the actin cytoskeleton to become rigid, causing the inhibition of axonal elongation and growth cone collapse followed by the formation of stress fibers and focal adhesions. The importance role of Rho GTPases in neuronal development has been suggested and Rho GTPases thereby could possibly lead to defects in neuronal migration. Therefore, not only in the early nervous system, the importance of Rho GTPases and the effect of long-term inhibition of Rho function in the adult brain was also analyzed.

1.1 Small GTPases of the Rho family

The small G protein superfamily (small GTPase) is composed of more than 100 members and has been divided into six families: Ras, Rho, Rab, Arf, Sar and Ran. Ras and Rho GTPases regulate many important aspects of cell behaviour including decisions to proliferate or differentiate, cell polarity, modifications to the actin cytoskeleton, cell shape, cell movement, gene transcription, and microtubule dynamics (reviewed by Kaibuchi *et al.*, 1999; Aspenstrom, 1999a and 1999b; Dickson, 2001; Ramakers, 2002). Rab, Arf, and Sar GTPases are involved in the regulation of intracellular vesicle transport, and the Ran subfamily plays an important role in transport through the nuclear membrane (reviewed by Takai *et al.,* 2001). Most members of the small GTPase family possess the ability to bind to and hydrolyze GTP. They thereby act as binary molecular switches cycling between an active and an inactive conformation. In the GTP-bound active form, the protein can interact with one or more cellular targets to promote a response until hydrolysis of GTP to GDP brings the switch to the "off" inactive conformation (Figure 1). Even though members of the small G protein superfamily are described as small GTPases in my thesis, a common usage, it is important to understand that although GTPase activity is essential to stop the functions of small G proteins in most cases, GTP does not always need to be bound for the G protein to be functional. There are examples of small GTPases that are constitutively active, such as Rnd3/RhoE and RhoH/TTF (reviewed by Rossman *et al.*, 2005). This simple mechanism of Rho GTPase acitivity regulation is carefully controlled by more than 60 activators and over 70 inactivators (Figure 1).

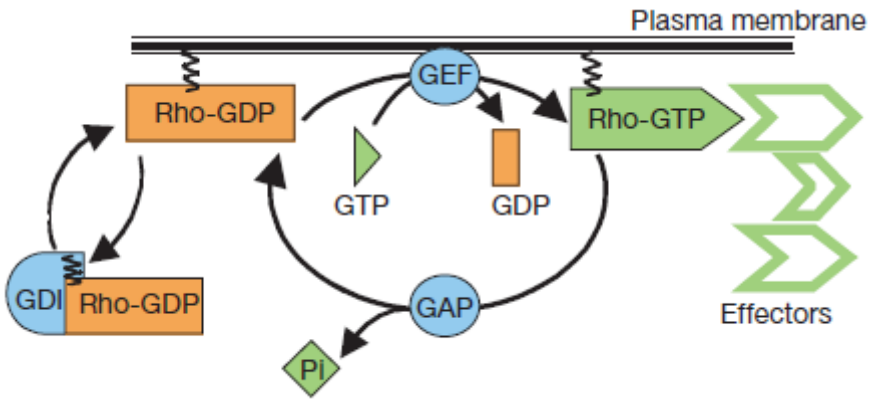

Figure 1. ***The GTPase molecular switch:*** *In the GTP-bound active state, Rho-GTPases regulate the activity of their binding partners or one of over 60 target effectors to promote a cellular responses and influence the actin cytoskeleton organization, gene expression, or cell cycle progression. The cycle is highly regulated by three classes of protein: in mammalian cells, around 60 guanine nucleotide exchange factors (GEFs) catalyze nucleotide*

exchange and mediate activation; more than 70 GTPase-activating proteins (GAPs) stimulate GTP hydrolysis, leading to inactivation; and guanine nucleotide exchange inhibitors (GDIs) bind the switch regions and the C-terminal isoprenyl moiety of Rho GTPases to sequester them in the cytosol. (taken from Etienne-Manneville and Hall, 2002)

Rho GTPases are key signaling proteins which regulate intracellular signals in response to extracellular signals and participate in many physiological processes. Rho was first isolated as a small GTP-binding protein related to Ras (Madaule and Axel, 1985). The Ras-related gene family was found in a wide variety of organisms, including plants, *Saccharomyces cerevisiae*, *Drosophia melanogaster*, mouse, rat, and human (DeFeo-Jones *et al.*, 1983; Reymond *et al.*, 1984; Fukui and Kiziro, 1985; Mozer *et al*., 1985; Avraham and Weinberg, 1989). In mammals, they include Rho (RhoA, RhoB, and RhoC), Rac (Rac1, Rac2, and Rac3), Cdc42, Rnd1/Rho6, Rnd2/Rho7, Rnd3/RhoE, RhoD/HP1, RhoG, TC10 and RhoH/TTF. An exception to the previously-described GTPase cycle pattern is found only in Rnd and RhoH/TTH proteins which are known to be unable to hydrolyze GTP *in vitro* so that they are constitutively active (reviewed by Etienne-Manneville and Hall, 2002; Rossman *et al.*, 2005). Like the ras genes, the rho genes encode proteins of 21 kilodaltons in size. Different mammalian Rho GTPases are at least 40% identical to each other at the amino-acid level, and the most well-studied GTPases among them are Rho, Rac, and Cdc42. RhoA, RhoB, and RhoC are three highly homologous isoforms of Rho in mammals and, at the amino-acid level they share more than 85% identity.

Two regions, the switch I and switch II domains, are highly conserved within most of the small GTPases. These regions surrounding the γ-phosphate of GTP have been determined by comparing the structure of Ha-Ras in the GTP- and the GDP-bound conformations (reviewed by Takai *et al.*, 2001).

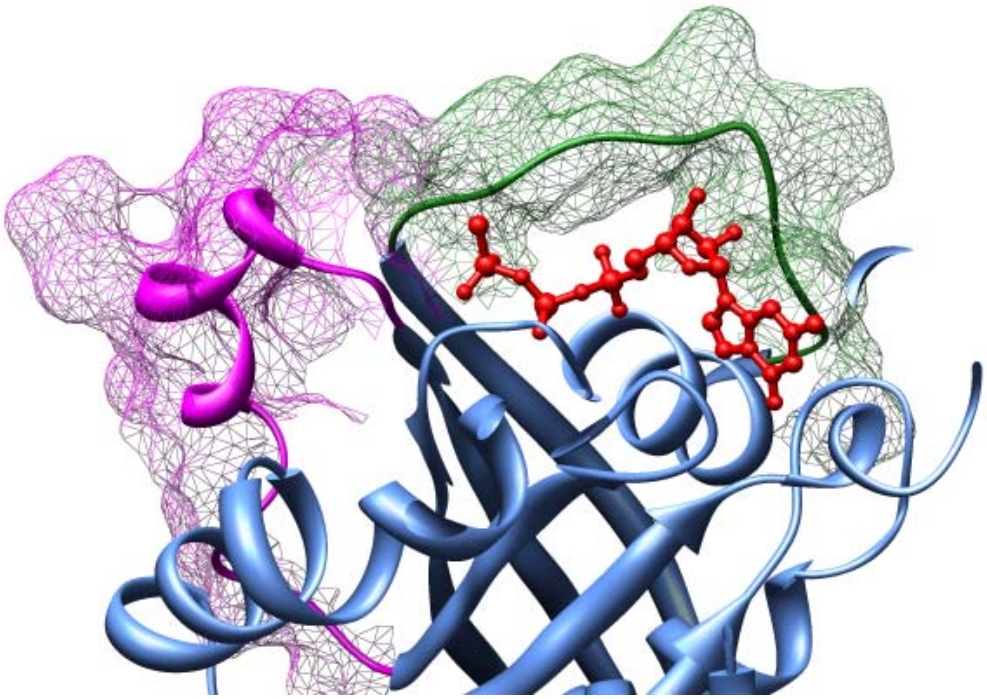

Figure 2. ***RhoA and GTP crystallographic structure:*** *The switch I (green) and switch II (purple) loops are highlighted. The structure was generated using the 3D imaging software from http://www.cgl.ucsf.edu/chimera/. The sequence to generate the 3D imaging structure was based on the Protein Data Bank model 1A2B (Ihara et al., 1998)*

The switch I region is within loop L2 and β2, which is the effector region, and the switch II region is within loop L4 and helix α2 (Figure 2). Together they encircle the γ-phosphate of GTP. Most small GTPases have consensus amino acid sequences for specific GDP/GTP-binding and GTPase activity, and there is a separate region for the downstream effectors (Figure 3). Moreover, all Rho GTPases are modulated by a post-translational lipid modification (prenylation) and a C-terminal carboxymethylation of four amino acids (i.e. Cys-A-A-X box) so that the last three amino acids are cleaved (Adamson *et al.*, 1992). These modifications are required for their localization to the plasma membrane and for the activation of downstream effectors. Only post-translationally modified Rho proteins interact with the regulators of Rho GTPases. These modifications serve functional roles, for example, by preventing the dissociation of guanine nucleotide dissociation inhibitors (GDIs) from Rho GTPases (Hori *et al.*, 1991; Read *et al.*, 2000).

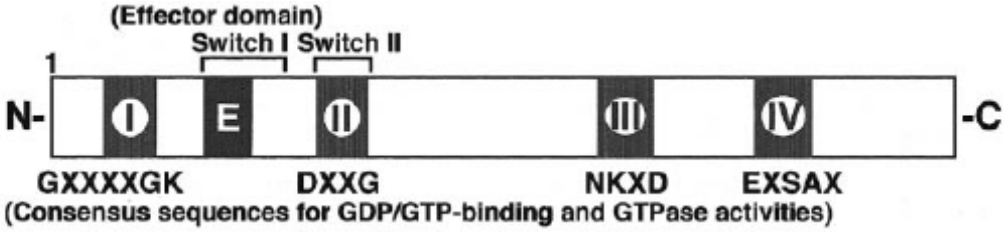

Figure 3. ***Structure of small GTPases:*** *Most of the GTPases conserve Switch I and Switch II of the consensus sequences responsible for GDP/GTP-binding interaction and GTPase activities. A, Ala; D, Asp; E, Glu; G, Gly; K, Lys; N, Asn; S, Ser; X, any amino acid (taken from Takai et al., 2001)*

Two Rho protein mutant forms, constitutively active and dominant negative forms of Rho GTPases, have been commonly used for experimental purposes to study their role in axonal arborization (Threadgill *et al.*,1997; Nakayama *et al.*, 2000), dendritic growth (Threadgill *et al.*, 1997; Ruchhoeft *et al.*, 1999; Nakayama *et al.*, 2000; Li *et al.*, 2000), neuronal remodeling (Luo *et al.*, 1996; Ruchoeft *et al.*, 1999; Li *et al.*, 2000), and growth cone motility (Jin and Strittmatter, 1997; Kozma *et al.*, 1997; Ruckhoeft *et al.*, 1999; Kuhn *et al.*, 2000; Nakayama *et al.*, 2000; Wahl *et al.*, 2000).

1) A constitutively active form made by mutation of glycine (G) at position 12 for Ras/Rac/Cdc42 or 14 for RhoA to valine (V) is not able to hydrolyze GTP, and therefore signals are continuously sent to downstream targets. It reduces the essential GTPase activity and GAPs become inaccessible to the GTP-bound Rho (Garrett *et al.*, 1989; Ridley and Hall, 1992a and 1992b). In fibroblasts, the constitutively active mutant of Rho (V14-Rho) was shown to stimulate the assembly of focal adhesion and stress fibers induced by growth factors such as platelet derived growth factor (PDGF), epidermal growth factor (EGF), or those found in bovine fetal calf serum (FCS) (Ridley and Hall, 1992a). Microinjection of active Rac into fibroblasts led to the formation of lamellipodia and membrane ruffles (Ridley *et al.*, 1992), while active Cdc42 stimulated the formation of filopodium in Swiss 3T3 fibroblasts resulting from actin polymerization (Nobes *et al.*, 1995). Transfection of constitutively active Rho, Rac, or Cdc42 increased the numbers of dendrites in cortical neurons *in vitro* (Threadgill *et al.*, 1997) but caused growth cone collapse in the neuroblastoma cell line NIE-115 (Kozma *et al.*, 1997; Jin and Strittmatter, 1997) and in the case of Rac, in chick DRG neurons as well (Kozma *et al.*, 1997). Mice expressing constitutively active Rac1 in cerebellar Purkinje cells showed dendritic morphology changes (Luo *et al.*, 1996).

2) A dominant negative mutant made by mutation of threonine (T) at amino acids 17 (Rac/Cdc42) and at 19 (RhoA) to asparagine (N) or by mutation of serine (S) to asparagine (N)

at amino acids 17 (Ras), is predicted to block the GTPase activity of endogenous Rho GTPases through the competition in binding to GEF exchange factors (Feig *et al.*, 1994), and it has been suggested that this substitution of the amino acid to asparagine possibly disturbs the Rho GTPase activity by interfering with an essential Mg^{2+} ion required for guanine nucleotide binding in all Ras superfamily GTP-binding proteins (Farnsworth *et al.*, 1991). When dominant negative RhoA was transfected, the numbers of dendrites in cortical neurons was decreased *in vitro* (Threadgill *et al.*, 1997). Transfection of dominant negative Rac showed the inhibition of outgrowth in PC12 phaeochromocytoma cells (Lamoureux *et al.*, 1997). Serum-induced outgrowth was inhibited by dominant negative Rac and Cdc42 in neuroblastma NIE-115 cell (Kozma *et al.*, 1997).

Experimental models using neuronal cell lines do not always necessarily reproduce the activities of primary neurons. The neurite outgrowth in PC12 and N1E-115 cells showed the same result, but embryonic chick DRG neurons showed different data. In general, Rho inhibits neurite outgrowth while Cdc42 induces filopodia and Rac promotes lamellipodia (reviewed by Gallo and Letourneau, 1998a). The Rho GTPases possibly activate each other sequentially, and therefore activation hierarchies may exist amongst these proteins (Kozma *et al.*, 1995; Nobes and Hall, 1995). It has been suggested that when both Rho and Rac1 are active, slow outgrowth occurs and the collapse of growth cones, but when Rho is active and Rac1 is inactive, moderate outgrowth occurs with growth cones extending lamellipodia and filopodia. Finally, when Rho is inactive and Rac1 is in either the active or the inactive form, rapid growth and collapse of growth cones are seen respectively (reviewed by Gallo and Latourneau, 1998a).

1.2 C3 transferase

Rho was found to be the target of the *Clostridium botulinum* exoenzyme C3 transferase, which ADP-ribosylates Rho at amino acid 41 (asparagine) and thereby inactivates it (Sekine *et al.*, 1989; Aktories and Frevert, 1987; Morii *et al.*, 1991). Subsequently, various C3-family members have been identified including the exoenzyme ADP-ribosyltransfarase from *Clostridium limosum*, *Bacillus cereus*, and epidermal differentiation inhibitor (EDIN) (reviewed by Kaibuchi *et al.*, 1999) that share the same functionality. All C3 transferases are highly specific inhibitors of all the three Rho member isoforms, RhoA, RhoB, and RhoC (Just *et al.*, 1992), and C3 is believed not to ADP-ribosylate Rac or Cdc42 (Just *et al.*, 1995). Nucleotide binding of GDP/GTP and inherent or GAP- activated GTPase activity are not affected by ADP-ribosylation of Rho, and it has been suggested that modified Rho possibly binds to alternate effectors to sequester activation (reviewed in the book “GTPases” by Aktories, Schmidt, and

Hofmann, 10. GTPases targeted by bacterial toxins, Oxford University Press). The C3 transferase has been shown to inhibit the LPA activity, suggesting that Rho mediates the length of neurites induced by the LPA in neuroblastoma cells (Jalink *et al.*, 1994).

Toxin and source	Modification to Rho	Effect on cells (cell type)
C3 from *Clostridium botulinum*[53,54]	ADP ribosylates Asn41, inactivates Rho	*Rounding of Swiss 3T3 fibroblasts *Blocks migration of neutrophils, but stimulates fMLP-induced actin polymerization *Decreases F-actin content of resting HL60 cells, increases fMLP-stimulated F-actin
CNF1 *Escherichia coli*[60]	Unknown modification activates Rho	*Increases total actin (F-actin pool) but also cell volume of HEp-2 cells
Toxin A and toxin B from *Clostridium difficile*[56,59]	Glucosylates and inactivates Rho, Rac and Cdc42	*Rounding of cells and cell death
C3-related toxin from *Bacillus cereus*[58]	ADP ribosylates Asn41, inactivates Rho	Same as C3
Exoenzyme from *Clostridium linosum*[61,62]	ADP ribosylates Asn41, inactivates Rho	Same as C3
EDIN from *Staphylococcus aureus*[63]	ADP ribosylates Asn41, inactivates Rho	Same as C3
DNT from *Bordetella bronchiseptica*[57]	Rho mobility-shift on gels, activates Rho	*Inhibits differentiation of MC3T3-E1 cells (osteoblast-like) *Inhibits cytokinesis *Stimulates stress fibres, focal adhesions *Stimulates protein and DNA synthesis *Prevents ADP-ribosylation of Rho by C3

Figure 4. ***Rho is the target for covalent modification by many pathogenic bacteria:*** *Characterized toxins acting on Rho and their effects on various cell types. CNF1, Cytotoxic necrotizing factor 1; EDIN, epidermal differentiation inhibitor; DNT, dermonecrotizing toxin (taken from Machesky and Hall, 1996)*

Because several bacterial toxins and exoenzymes modify Rho GTPases (Figure 4), it is suggested that there is an important and ubiquitous Rho function including cell flattening and neurite outgrowth in neuronal cells (reviewed by Machesky. and Hall, 1996). Dramatic changes in the actin cytoskeleton have been shown upon introduction of C3 transferases into cells, causing most cell types to round up in mammalian cell culture (Wiegers *et al.*, 1991; Paterson, *et al.*, 1990; Chardin *et al.*, 1989). In neuronal cells, C3 transferase treatment flattens cells and expresses neurite-like cell processes. C3 transferase stimulated growth cone formation in N1E-115 cells (Kozma *et al.*, 1997). On the other hand, C3 transferase induce axonal outgrowth from DRG neurons but lamellipodia and filopodia in the growth cones of DRG are missing under these conditions (Jin and Strittmatter, 1997). Incubation with C3 exoenzyme in cultured rat

pheochromocytoma PC-12 cells inhibited cell growth and induced neurites (Nishiki *et al.*, 1990), and microinjection of C3 exoenzyme induced neurite outgrowth but co-injection of a dominant negative Rac1 or Cdc42 blocked that outgrowth (Kozma *et al.*, 1997). C3 transferases cause the loss of actin stress fibres and integrin adhesion plaques.

Thymi isolated from C3 exoenzyme-expressing transgenic mouse were smaller, reflecting a 90% decrease in cell number. A transgenic mouse expressing C3-exoenzyme showed disrupted fiber cell morphology, cytoskeletal regulation, and fiber cell interactions in developing eyes (Henning *et al.*, 1997; Maddala *et al.*, 2004).

All the studies using the C3 exoenzyme or C3 transgenic mice have shown an important need for Rho GTPase function, and thereby C3 exoenzyme is widely used for Rho function studies.

1.3 Nucleotide exchange and exchange factors GEFs (Guanine nucleotide exchange factors)

Guanine nucleotide exchange factors (GEFs) promote activation of the small GTPases stabilizing the nucleotide-free form of the GTPase and thereby facilitating its association with GTP, which is the more abundant nucleotide. Different GEFs are recruited to membranes and/or growth factor receptors. The first mammalian Rho GEF was found in diffuse B-cell-lymphoma cells (Dbl), and more than 30 potential GEFs for small GTPases have since been discovered (reviewed by Rossman, 2005). All of them have a conserved exchange factor domain, the Dbl homology (DH) domain, which is generally adjacent to a pleckstrin homology (PH) domain and which interacts with the switch regions of Rho GTPases (Figure 5) (reviewed by Cerione and Zheng, 1996). The heterotrimeric small GTPases bind to the Dbl domain of GEF and as a result become activated to mediate their downstream effector targets. Many Rho GEFs are constitutively activated by the N-terminal truncation of sequences which lie upstream of the DH domain (Schmidt and Hall, 2002). The function of the PH domain is not well investigated, but it seems to play a role in cellular localization together with the DH domain to activate Rho GTPases (van Aelst *et al.*, 1997).

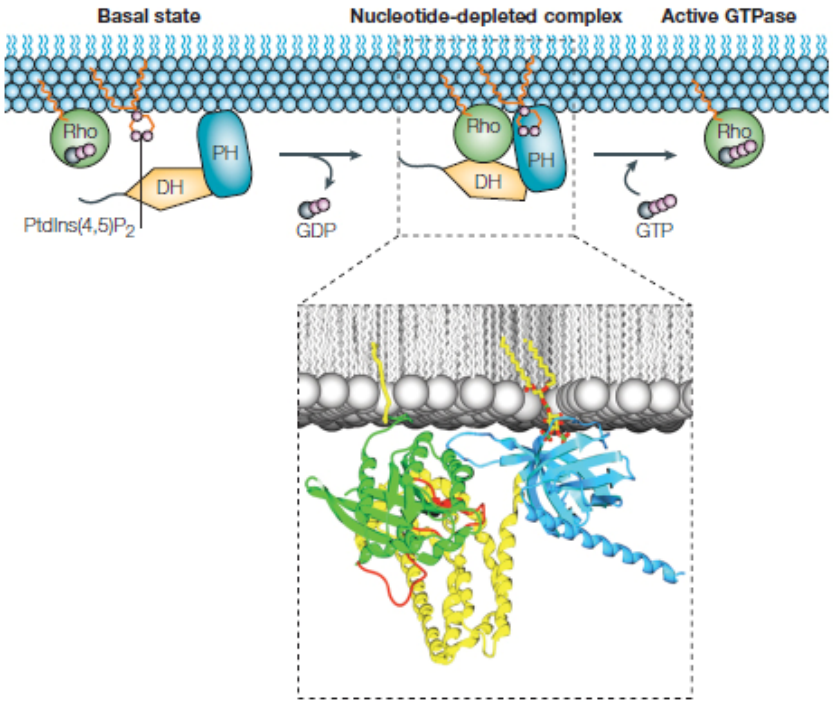

Figure 5. ***Model of PH-domain-assisted guanine nucleotide exchange:*** *GDP-bound Rho interacts with GEFs (as indicated by DH and PH). GEFs promote GDP and* Mg^{2+} *dissociation from Rho GTPases. (taken from Rossmann et al., 2005)*

Genetic analyses have shown that GEFs are important for the regulation of cell motility and morphology (Barrette *et al.*, 1997). Among GEFs that have already been studied, Dbl is expressed in brain, ovary and testis and mice lacking the Dbl gene showed defective dendrite elongation (Hirsch *et al.*, 2002). Trio, a GEF for the Rho GTPases, is known to play a role in embryonic lethality, skeletal development, and neuronal-tissue development (reviewed by Rossman *et al.*, 2005), and it also has been shown that Trio is expressed along axons in the CNS of embryos and in the subsets of brain regions and has an essential role in axonal and dendritic development in *Drosophila* (Newsome *et al.*, 2000; Awasaki *et al.*, 2000; Bateman *et al.*; 2000, Liebl *et al.*, 2000). It is possible that the actin cytoskeleton is regulated through the local activation or recruitment of GEFs with the guidance cues by Rho GTPases.

1.4 GTP hydrolysis and GAPs (GTPase activating proteins)

GTPase activating proteins (GAPs) promote the hydrolysis of the bound GTP by enhancing the intrinsic GTPase activity of the Rho protein and thus bring it to the inactive state. Once Rho

proteins are activated and bound to GTP, their activity is terminated by GTP hydrolysis, yielding a bound GDP and free phosphate. Approximately 70 GAPs have been identified and are assumed to specifically promote GTPase activities for individual members of the small G-protein superfamily. There are several Ras and Rho GAPs and each GAP is possibly specific for different cell types. Many Ras and Rho GAPs contain membrane interacting domains and have been found in transient protein complexes formed as a result of incoming membrane signals. It has been suggested that different GAPs target specific GTPases and that the interactions with certain membrane compartments or signaling complex proteins may regulate the GTPases (reviewed by Bernards, 2005).

There are suggestions that GAPs play an important role in neuronal development or nervous system function from the evidence that multiple GAPs for the small GTPases are expressed in the brain at high levels (reviewed by Bernards *et al.*, 2005). An example of GAPs involvement in processing external signal transduction in neurons comes from studies that indicate p250GAP is possibly involved in the downstream activity of the neurotransmitter N-methyl-d-aspartate (NMDA) receptor (Nakazawa *et al.*, 2003; Taniguchi *et al.*, 2003). NMDA receptors regulate actin reorganization in dendritic spines (Engert and Bonhoeffer, 1999; Maletic-Savatic *et al.*, 1999). Another function GAPs may have is that of bridging multiple signaling pathways. A Rho GAP, p190RhoGAP, may link the Rho and Ras signaling pathways thorough its binding to p120RasGAP (reviewed by Machesky and Hall, 1996).

Mice deficient in p190-B RhoGAP showed similar phenotypes to the CREB transcription factor deficient mice in that they have a reduced body size as well as cell size during development (Sordella *et al.*, 2002). Rho and CREB have both been suggested to play a role in the differentiation of thymocytes and neurons (Henning *et al.*, 1997; reviewed by Luo, 2000). It has been found that the brain and thymus defects in p190-B RhoGAP-deficient mice are associated with a failure in cell differentiation (Sordella *et al.*, 2002). From this it is suggested that increased activity of ROK (Rho kinase) in p190-B Rho GAP deficient cells downregulates the insulin/IGF signal and therefore several downstream pathway factors including MAP kinases and JNK (c-jun N-terminal kinase) resulting in increased CREB activity (Figure 6).

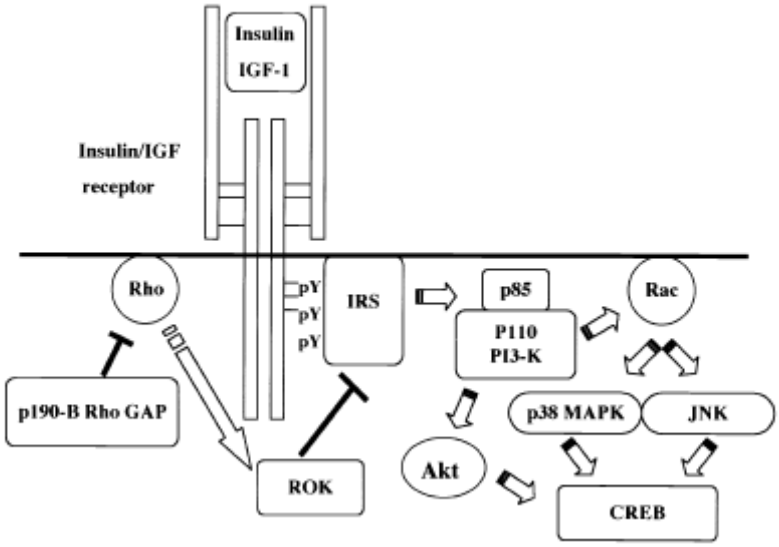

Figure 6. ***Model of the predicted role of p190-B RhoGAP in modulating insulin/IGF-1 signaling to CREB****. Increased ROK (ROCK) activity in mutant cells downmodulates insulin/IGF signal into downstream pathway factors, MAP kinases and JNK, promoting CREB activity (taken from Sordella et al., 2002)*

In summary, the activity balance between the GEFs and GAPs has been shown to be important in the regulation of Rho GTPases, and therefore it is interesting to see the relationship between them in axonal outgrowth and in neuronal development.

1.5 GDIs (Guanine Nucleotide Dissociation Inhibitors)

The GDP-bound form of the Rho GTPase specifically interacts with proteins in the cytoplasm known as guanine nucleotide dissociation inhibitors (GDIs), which keep Rho in an inactive form in cells (reviewed by Olofsson, 1999). The Rho-GDI family consists of at least three isoforms: Rho-GDIα, Rho-GDIβ, and Rho-GDIγ. Rho-GDIs are active on all Rho, Cdc42, and Rac proteins (Abo *et al.*, 1992, Leonard *et al.*, 1992; Hart *et al.*, 1992). Ubiquitously expressed proteins, GDIs are so named for their function of inhibiting the dissociation of GDP from Rho proteins (Ueda *et al.*, 1990) and therefore prolonging the time Rho GTPases spend in the inactive form, preventing GDP/GTP exchange activity by GEFs (Figure 1). Another biochemical characteristic of GDIs is a weak interaction with the GTP-bound Rho to inhibit GTP hydrolysis, resulting in a blockage of intrinsic and GAP-mediated GTPase activity (reviewed by DerMardirossian and Bokoch, 2005; Hart, *et al.*, 1992; Chuang *et al.*, 1993; Sasaki *et al.*, 1993; Hancok and Hall, 1993). Therefore, GDIs are capable of blocking the GDP binding/GTP cycle both at the GDP/GTP exchange step and at the GTP hydrolysis step (reviewed by Van Aelst and D'Souza-Schorey, 1997).

GDIs are also involved in controlling the distribution of the Rho GTPases cycling between the cytosol and the plasma membrane (Figure 1, reviewed by DerMardirossian and Bokoch, 2005). The inactive Rho GTPases bound to Rho-GDI stay in the cytosol. When GDIs release the inactive Rho, it then incorporates into the plasma membrane lipid layer, where it is converted to the active GTP-bound form by interaction with membrane-associated Rho-GEFs. After GTP hydrolysis, a membrane associated, GDP-bound Rho may bind to a GDI. Once this occurs, the newly formed complex dissociates from the membrane and returns to the cytosol (reviewed by Sasaki and Takai, 1998). Therefore, GDIs help to terminate GTPase signaling at the membrane and serve to sequester inactive GTPases in the cytosol. The formation of the Rho-GDI complex has been shown to be required for the suppression of Rho signaling (Yamashita and Tohyama, 2003).

1.6 The neurotrophin family

The neurotrophin family consists of nerve growth factor (NGF), brain-derived neurotrophic factor (BDNF), neurotrophin-3 (NT-3), and neurotophin-4/5 (NT4/5). The neurotrophin family of neurotrophic factors are known for their effects on neuronal survival and growth. Neurotrophins help to stimulate and control neurogenesis, and one of their most important abilities is to support the survival of a wide variety of peripheral nervous system neuronal populations (reviewed by Bibel and Barde, 2000). These trophic factors are released from target cells, retrogradely transported along their axons, and rapidly degraded upon arrival in cell bodies.

NGF is important for the survival and maintenance of sympathetic and sensory neurons. NGF binds to and activates its high affinity receptor TrkA. It is then internalized into the responsive neuron. The NGF/TrkA complex is subsequently trafficked back to the cell body and this NGF movement from axon tip to soma is thought to be involved in the long-distance signaling of neurons. NGF accelerates neurite outgrowth from embryonic rat hippocampal neurons (Brann *et al.*, 1999) and chick ciliary ganglion neurons (Yamashita *et al.*, 1999) NGF is suggested to be important in later stages of innervations of nerve because NGF is strongly expressed in epithelial targets.

BDNF plays important roles in proliferation, differentiation and survival of neurons during development, as well as in the synaptic activity and plasticity in mature neurons. Regulation of the local availability of BDNF at the cell soma, dendrites, axons, and spines gives spatial and temporal specificity of the different effects. BDNF deficient mice do not have slowly adapting mechanoreceptors (Carroll *et al.*, 1998). Mutations in the gene encoding MeCP2

(methyl-CpG binding protein 2) cause Rett syndrome (RTT) which is an X-linked postnatal neurodevelopmental disorder and BDNF was found to be the first mammalian neuronal target gene for MeCP2 (Chen *et al.*, 2003; Martinowich *et al.*, 2003). A functional interaction between BDNF and MeCP2 was shown *in vivo* that BDNF protein levels decrease in *Mecp2*$^{-/y}$ cortex by 21%, cerebellum by 41%, and the rest of the brain by 55% of wild-type levels. The decrease of BDNF levels in the absence of MeCP2 is surprising, knowing that BDNF is a target of repression by MeCP2 (Chang *et al.*, 2006). The forebrain-specific BDNF deficient mice mimicked the phenotypes seen in the MeCP2 deficient mice in that they have a decreased brain weight, smaller olfactory and hippocampal neuronal sizes, and a clasped hindlimb. Overexpression of *Bdnf* did not rescue these phenotypes shared by these two deficient mice, while the phenotypes of *Mecp2*$^{-/y}$ mice that are rescued by BDNF are not detected in BDNF deficient mice. Therefore, BDNF has extensive modulatory effects in neurons throughout the brain, some of which are in common with MeCP2 function (reviewed by Sun and Wu, 2006)

NT-3 was the third neurotrophic factor in the NGF-family of neurotrophins characterized after NGF and BDNF. It has activity on certain neurons of the peripheral and central nervous system; it supports existing neurons to survive and differentiate and encourages new neurons and synapses to grow and differentiate. NT-3 is unique in the number of neuron types it can potentially stimulate, given its ability to activate two of the receptor tyrosine kinase neurotrophin receptors TrkB and TrkC. Mice deficient in the NT-3 gene have shown a loss of proprioceptive and subsets of mechanoreceptive sensory neurons (Ernfors *et al.*, 1994; Tessarollo *et al.*, 1994). Both BDNF and NT-3 play an important role in growth cone turning in embryonic *Xenopus laevis* spinal cord neurons (Song *et al.*, 1997; Ming *et al.*, 1997).

Neurotrophins regulate neuronal differentiation, axon extension, guidance, arborization, and synaptogenesis (Gundersen and Barrett, 1979; Cohen-Cory and Fraser, 1995; Gallo *et al.*, 1997; Lom and Cohen-Cory, 1999; Ming *et al*., 1999; Yamashita *et al.*, 1999; Alsina *et al.*, 2001; Frost, 2001; Tucker *et al.*, 2001). The neurotrophin activating pathways also regulate the cytoskeleton, which affects growth cone behaviors (Gallo and Letourneau, 1998b, 2000). Neurotrophins stimulate both axonal and dendritic growth and axonal outgrowth from CNS neurons has been shown to depend on neurotrophic factors *in vitro* (Lentz *et al.*, 1999; Goldberg *et al.*, 2002; reviewed by McAllister *et al.*, 1999; Markus *et al.*, 2002, Tucker, 2002). Additionally, neurotrophic factors may be important in stimulating axon growth after CNS injuries to the spinal cord (Coumans *et al.*, 2001). *In vivo*, injection of NGF increased the ingrowth of sympathetic and sensory nerves in brain (Menesini Chen *et al.*, 1978). NGF or TrkA deficient mice showed that more than 80% of DRG neurons are lost (Crowley *et al.*, 1994;

Smeyne *et al.*, 1994; Silos-Santiago *et al.*, 1995). All DRG neurons that die in the absent of NGF/TrkA signaling survive when BAX is eliminated. Crossing NGF null or Trk null mice with the pro-apoptotic gene BAX deficient mice showed the inhibition of apoptosis in peripheral neurons (Patel *et al.*, 2000). Peripheral axons were found to be extended toward ectopic sources of neurotrophins and its growth was reduced by function-blocking antibodies, suggesting that neurotrophins are involved in axonal elongation during development (Tucker *et al.*, 2001).

1.7 The neurotrophin receptors, p75 and the Trks

Two classes of receptors for neurotrophins are p75 ($p75^{NTR}$) and the Trk family of Tyrosine kinases receptors. $p75^{NTR}$ is a membrane glycoprotein and a low affinity neurotrophin receptor to which all neurotrophins bind (reviewed by Bothwell, 1995). The Trk family includes TrkA, TrkB, and TrkC. Trks bind to specific neurotrophins with a much higher affinity than $p75^{NTR}$; NGF acts via TrkA, BDNF and NT4/5 act via TrkB, and NT3 acts via TrkC (reviewed by Barbacid, 1993) (Figure 7). Coactivation of the phosophoinositide-3-kinase and phospholipase C-γ pathways is important for chemotrophic responses through Trk receptors (Ming *et al.*, 1999)

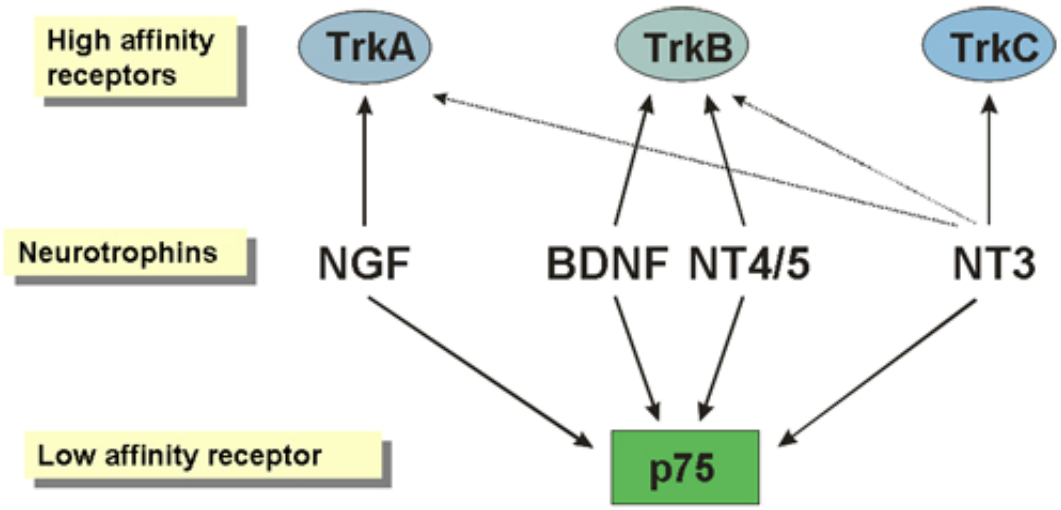

Figure 7. ***Neurotrophins and their receptors:*** *Trks bind to specific neurotrophins with a much higher affinity; NGF acts via TrkA, BDNF and NT4/5 act via TrkB, and NT3 acts via TrkC while p75 binds to all neurotrophins. (Courtesy of Tucker)*

The expression of $p75^{NTR}$ has been implicated in many different biological roles including cell death, cell migration, and modulation of synaptic transmission and functional regulation of sensory neurons. $p75^{NTR}$ is highly expressed in motor neurons in the spinal cord, most sympathetic and sensory neurons in the peripheral nervous system, cerebellar Purkinje cells and retinal ganglion cells during outgrowth of axons from these cells (von Bartheld *et al.*, 1991).

Neurotrophin binding to p75 decreases RhoA signaling, which promotes the extension of filopodia (reviewed by Gallo and Letourneau, 2004). In migrating cells of the nervous system, the neural crest cells also express $p75^{NTR}$ from the beginning of their separation from the dorsal neural tube (Stemple and Anderson, 1992). A link between $p75^{NTR}$, Rho and the actin cytoskeleton has been suggested (Figure 8 and 9), and $p75^{NTR}$ may have an important role in axon guidance during the development (Dechant and Barde, 2002). $p75^{NTR}$ is suggested to be a growth inhibitory protein for NGF-dependent neurons and functions in concert with myelin to prevent axonal growth in the adult brain (Kohn *et al.*, 1999).

$p75^{NTR}$ is expressed at high levels in subplate neurons with a low-rostral to high-caudal gradient form throughout the period of thalamocortical innervations, therefore $p75^{NTR}$ is suggested to play a role in thalamic innervations of cortex (Lee *et al.*, 1992, 1994). NT3 binding to $p75^{NTR}$ increases neurite length and filopodial formation of immunopurified subplate neurons *in vitro*.

Interestingly, RhoA was identified as a protein that interacts with the neurotrophin $p75^{NTR}$ through a yeast two-hybrid screen. It was found that the predominant GDP-bound form of wild-type RhoA associates with $p75^{NTR}$ while constitutively active RhoA does not interact with $p75^{NTR}$ (Yamashita *et al.*, 1999), suggesting that RhoA activation was dependent upon the interaction of RhoA and $p75^{NTR}$. However, later it was found that Rho-GDI, not RhoA, interacted directly with the $p75^{NTR}$ acting as a displacement factor to release RhoA from Rho GDI, an activity that can be enhanced by MAG and Nogo (Yamashita and Tohyama, 2003). $p75^{NTR}$ integrates diverse growth-regulating cues, including those from neurotrophins and myelin proteins, which may be important for both development and maintenance of neuronal circuitry.

The neurotrophin receptor $p75^{NTR}$ has been described as having Rho-GDI displacement activity, resulting in the activity to release RhoA from Rho-GDI (Yamashita and Tohyama, 2003). The Nogo receptor (NgR) associates with the $p75^{NTR}$ receptor in the absence of Myelin-associated glycoprotein (MAG) or Nogo. In this state, axonal growth and regeneration will occur, partly due to the fact that Rho-GDI remains complexed with Rho-GDP in the cytosol (Figure 8). However, in the presence of MAG or Nogo, the cytoplasmic domain of the NgR preferentially binds Rho-GDI, resulting in the release and subsequent activation of the Rho GTPase. In this state, activated Rho-GTP interacts with other signaling proteins such as Rho kinase (ROK/ROCK) resulting in no growth (Figure 8). Supporting evidence for this mechanism comes from reports that neurite outgrowth in postnatal cerebellar neurons was inhibited by MAG and Nogo, but overexpression of Rho-GDI reversed their inhibitory effects resulting in neurite growth (Yamashita and Tohyama, 2003).

In myelin-independent mechanisms, $p75^{NTR}$ activated by BDNF can suppress axonal growth probably because of the inhibition of nerve growth factor (NGF)-induced TrkA growth signaling to MAP kinase (MAPK) or Rac. Or it is possible that other unidentified growth inhibitory proteins could play a role in this signaling to cause the inhibition of growth (Figure 8).

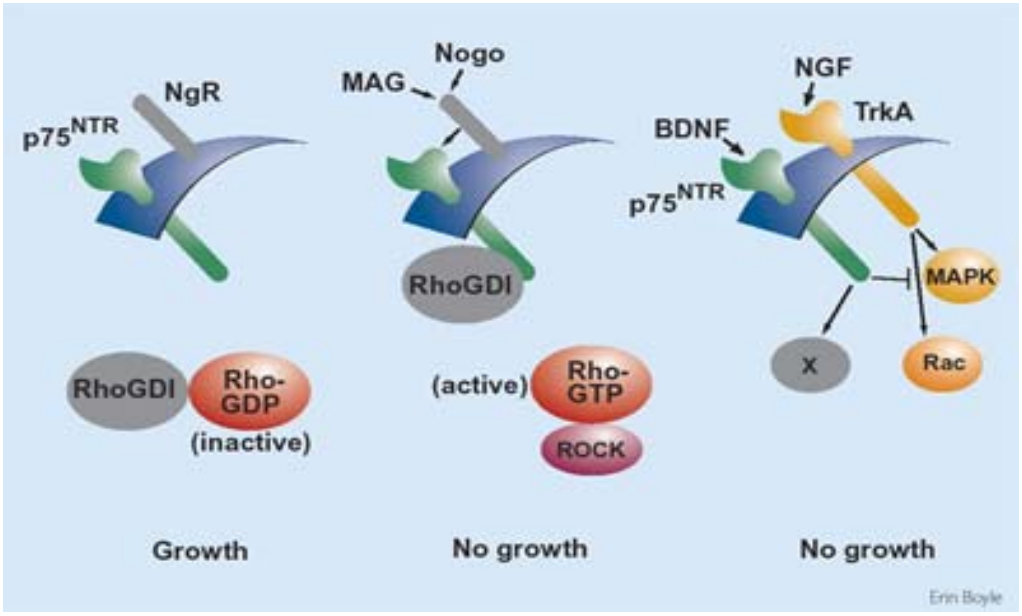

Figure 8. ***Mechanisms of axonal outgrowth inhibition****: $p75^{NTR}$ associates with RhoGDI and causes the inhibition of growth (taken from Kaplan and Miller, 2003)*

Neurotrophin binding to $p75^{NTR}$ inactivates RhoA in HN10 cells and cerebellar neurons (Yamashita *et al.*, 1999). However, $p75^{NTR}$ activate RhoA in transfected HEK293 cells independently from the ligand neurotrophin (Figure 9). $p75^{NTR}$ is suggested not to be a constitutive activator of RhoA in the cells expressing endogenous $p75^{NTR}$ (Yamashita and Tohyama, 2003). Whole-mount of $p75^{NTR}$-deficient mice carrying a targeted deletion in the third exon encoding the neurotrophin-binding domain were stained with anti-TuJ1 (beta-tubulin III), showing that outgrowth of spinal and sensory axonal elongation was retarded during embryonic development. This phenotype is probably caused by the loss of neurotrophin binding ability in a $p75^{NTR}$–dependent manner (Figure 10, Yamashita *et al.*, 1999).

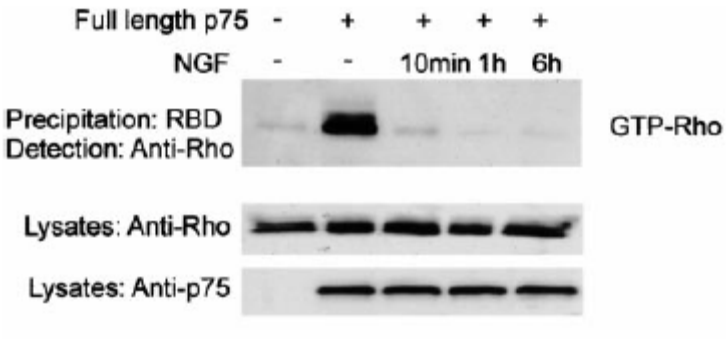

Figure 9. ***p75 activates RhoA in the absence of ligand NGF*** *The levels of GTP-bound Rho were increased with coexpression of full-length p75^{NTR} with RhoA. 10min of the neurotrophin NGF application already showed the decrease of the GTP-bound Rho. (taken from Yamashita et al., 1999)*

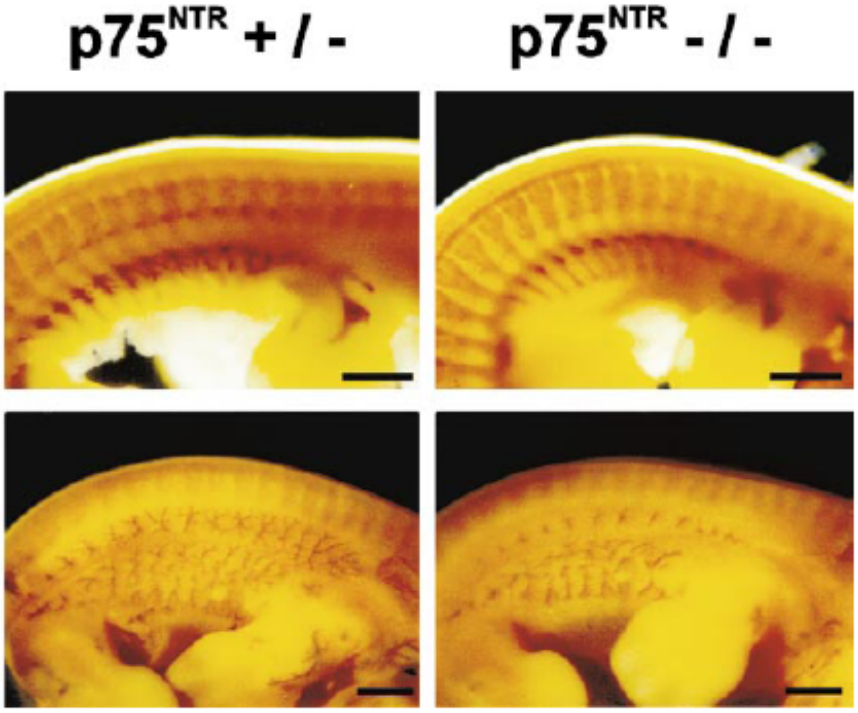

Figure 10. ***Intercostal nerve outgrowth slowed in p75-/- at 12.0 d.p.c. (Whole mount Tuj1 (beta tubulin III) Ab):*** *Outgrowth of spinal and sensory axonal elongation was retarded during the development in p75^{NTR}-deficient mice carrying a targeted deletion in the third exon encoding the neurotrophin-binding domain. (taken from Yamashita et al., 1999)*

p75^{NTR} plays an important role in the death of superior cervical ganglion neurons in the sympathetic system (Bamji *et al.*, 1998, Brennan *et al.*, 1999). The absence of p75^{NTR} resulted in contradictory reports demonstrating an increase, a decrease, or no change in the number of basal forebrain neurons (Yeo *et al.*, 1997, Peterson *et al.*, 1999; Ward and Hagg, 1999), but one consistent result is that p75^{NTR} activated by a neurotrophin can cause apoptosis in the absence of

Trk receptor (Dechant and Barde, 1997). The apoptosis mechanism of $p75^{NTR}$ is suggested to include Rac GTPase and JNK (Harrington *et al.*, 2002).

1.8 Use of the tau locus for gene expression in newborn neurons

The assembly of microtubules is regulated by microtubule-associated proteins known as MAPs. MAPs have been largely divided into two categories: Type I including MAP1 proteins and type II including MAP2, MAP4 and TAU/MAPT. The MAP1 family, comprised of MAP1a and MAP1b, binds to microtubules differently than other MAPs, utilizing charged interactions (reviewed by Mandelkow and Mandelkow, 1995). In general, the MAP C-terminal domains bind the microtubules while the N-terminal domains of the MAPs bind other parts of the cytoskeleton or the plasma membrane, resulting in spacing of the microtubule in the cells. The MAP1 family is found in axons and dendrites, tau is found in the axon, and MAP2 in the dendrites. *In vitro* activities of tau suggest a role in the neural outgrowth and the neuronal polarity development. Tau proteins stabilize microtubules by interacting with tubulin. However, mice deficient in the gene encoding tau are healthy, and neuronal development is almost normal both in structure and function. Using the cDNA for EGFP targeted into the locus encoding tau, strong EGFP was expressed throughout the embryonic central nervous system (Figure 11; Tucker *et al.*, 2001).

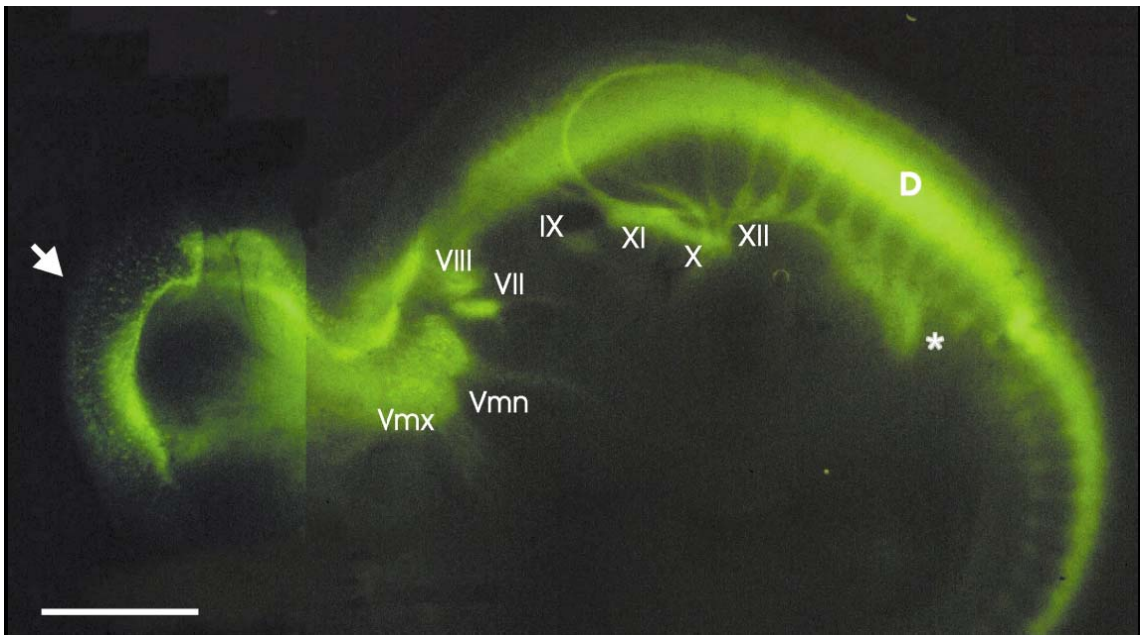

Figure 11. ***Targeting of the EGFP cDNA to the tau locus Homozygous mutant embryo at 10.75 d.p.c. with epi-fluorescence.*** *Labelled structures are as follows, proceeding caudally: arrow, trigeminal mesencephalic nucleus; Vmx,maxillary branch of trigeminal nerve; Vmn, mandibular branch of trigeminal nerve; VII, geniculate ganglion; VIII, vestibulocochlear ganglion; IX, glossopharyngeal ganglion;*

*X, vagus nerve; XI, spinal accessory nerve; XII, hypoglossal nerve; D, dorsal root ganglion and spinal cord; *spinal nerves growing into forelimb. Scale bar, 500 μm. (taken from Tucker et al., 2001).*

Using the tau locus as a target for other expression constructs, the effect of having various genes under the control of neuron-specific promoter has been tested. For example, MeCP2 which is thought to be responsible for the cause of the neurodevelopment abnormality called Rett syndrome, was engineered into the tau locus and resulted in the rescue of Rett syndrome in the transgenic mice (Luikenhuis *et al.*, 2004). Other examples of using tau locus include two ETS transcriptional factors of the Pea3 family, Er81 and Pea3, which were introduced into the DRG sensory and spinal motor neurons in the mouse. They showed that the late start of ETS signaling is crucial for the development of normal sensory afferent protrusions in the proprioceptive sensory neurons of the spinal cord (Hippenmeyer *et al.*, 2005).

1.9 Rho GTPases and neurite outgrowth development

During embryogenesis, axons must arrive at their targets properly in order to establish the complex neural networks in the adult nervous system. As neuronal precursors differentiate into neurons, one of the first obvious neuron-specific incidents is axon outgrowth. As a growth cone travels along its path, the growth cone of the axon specifically reacts to environmental extracellular signals to determine its next move during navigation. Growth cones travel toward attractant sources and away from repellent sources (Figure 12). The process of neurite formation and differentiation into axons and dendrites needs to precisely regulate the cytoskeleton. The actin cytoskeleton needs to cycle between the polymerization and depolymerization states for the growth of axon, thereby blockage of either state would inhibit axonal growth. Extension and retraction of growth cones are caused by the rearrangements of the actin cytoskeleton during axonal development. Growth cones respond to the extracellular cues by selectively stabilizing (polymerization) or destabilizing (depolymerization) the actin cytoskeleton in filopodia and lamellipodia resulting in extension or retraction of the growth cone to achieve directional growth (reviewed by Luo *et al.*, 1997). Blockage of either state would inhibit axonal growth. Extracellular cues, attractants and repellents, guide the local reorganization of the actin cytoskeleton in the filopodia and lamellipodia. Complicated regulations of the cytoskeleton in the axon produce the development of neurons including axonal branching, turning and orientation in chemotactic gradients, growth cone collapse and elongation, and the regulation of neurotransmitter release.

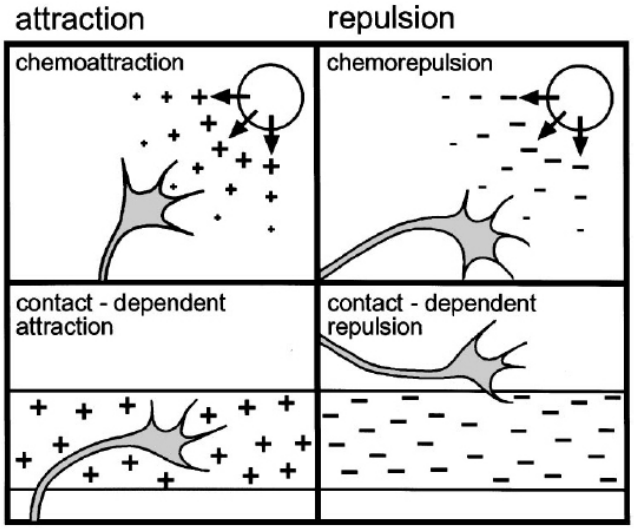

Figure 12. ***Growth cone guidance categorized into four different mechanisms; long-range (chemoattraction and chemorepulsion) or short-range distance (contact-mediated attraction or contact-mediated repulsion).*** *Growth cones travel toward attractant sources and away from repellent sources (taken from Mueller, 1999)*

Rho GTPases play an important role in the regulation of actin in the growth cones (reviewed by Luo *et al.*, 1997; Tapon and Hall, 1997; Gallo and Letourmeau, 1998a; Aspenstrom, 1999a, Mueller, 1999; Song and Poo, 1999; Bishop and Hall, 2000). When Rho is bound to GTP, Rho causes the actin cytoskeleton to become rigid, thereby inhibiting axonal elongation and causing growth cone collapse followed by the formation of stress fibers and focal adhesions (Figure 13). In neuroblastoma NIE-115 and phaechoromacytoma PC12 cell lines as well as in primary neuronal cultures, both LPA and thrombin causes growth cone collapse, neurite retraction and neuronal cell rounding (Suidan *et al.*, 1992; Jalink and Moolenaar, 1992; Jalink *et al.*, 1994). It has been suggested that thrombin and LPA signal through Rho GTPases to regulate myosin activity causing growth cone collapse and neurite retraction (reviewed by Luo *et al.*, 1997).

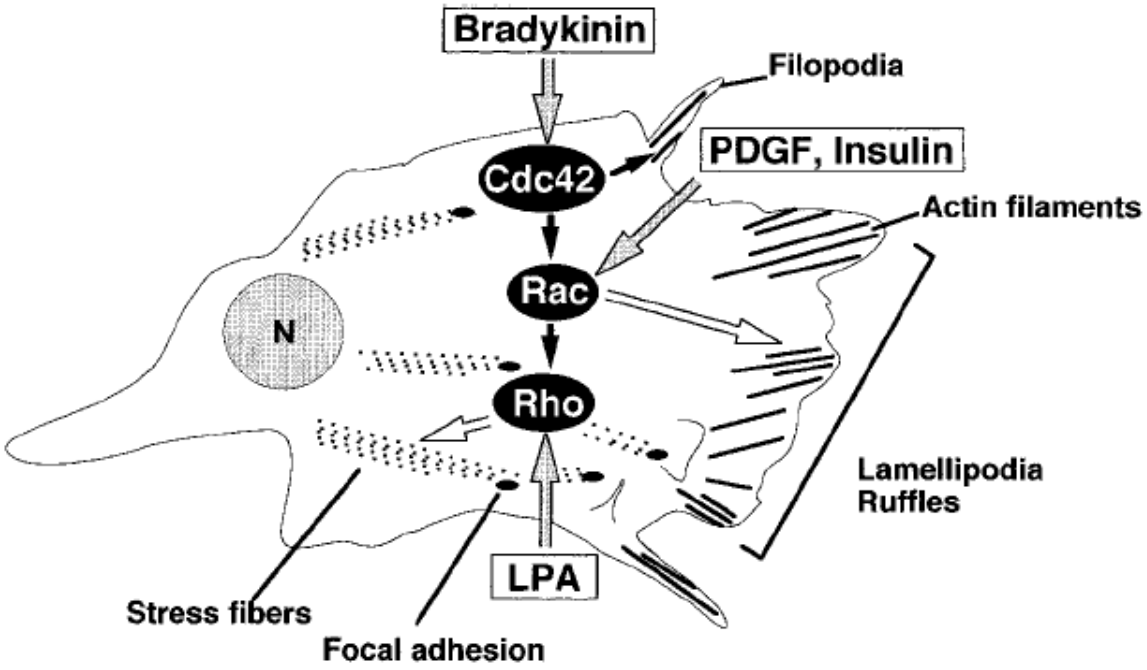

Figure 13. ***Rho, Rac, and Cdc42 signal cascade in cytoskeletal organization in Swiss 3T3 fibroblasts****. LPA (lysophosphatitic acid) activates Rho, which regulates actin stress fiber and focal adhesion formation. Rac regulates membrane ruffling and the formation of lamelipodia. Cdc42 regulates the formation of filopodia containing bundled F-actin (taken from Takai et al., 2001)*

Growth cone collapse in chick embryonic DRG neurons caused by the repellent guidance cue collapsin/Semaphorin is mediated through Rac1 and not Rho or Cdc42, but growth cone collapse occurred induced by LPA or myelin was not prevented in a dominant negative Rac1 mutant, indicating that Rac1 does not always act on all guidance cues to collapse DRG growth cones (Jin *et al.*, 1997). Formation of dendrites was decreased by inhibition of Rho GTPases and dendrite number was increased by the expression of constitutively active Rho, Rac, or Cdc42 in cortical neurons *in vitro* (Threadgill *et al.*, 1997). Although Rho GTPases play an important role in growth cone morphology and axon outgrowth in both neuronal cells and primary neurons, the functional results with neuronal cell lines and between neuronal types may be different, as summarized in Figure 14.

GTPase	Activity	Cell type	Effect on neurites
Rho	Dominant-negative (inactive) mutant	Cortical neurons	Decreased numbers of dendrites
	C3 toxin injection (inactivation)	NIE-115 cell line	Stimulation of growth cone motility and outgrowth
	C3 toxin injection (inactivation)	DRG neurons	Stimulation of outgrowth
	Constitutively active	Cortical neurons	Increased numbers of dendrites
	Constitutively active	NIE-115 cell line	Growth cone collapse
Rac	Dominant-negative (inactive) mutant	PC12 cell line	Inhibition of outgrowth
	Dominant-negative (inactive) mutant	Cortical neurons	Decreased numbers of dendrites
	Dominant-negative (inactive) mutant	NIE-115 cell line	Inhibition of C3- or serum-induced outgrowth
	Constitutively active	Cortical neurons	Increased numbers of dendrites
	Constitutively active	NIE-115 cell line	Growth cone collapse
	Constitutively active	DRG neurons	Growth cone collapse
Cdc42	Dominant-negative (inactive) mutant	Cortical neurons	Decreased numbers of dendrites
	Dominant-negative (inactive) mutant	NIE-115 cell line	Inhibition of C3- or serum-induced outgrowth
	Constitutively active	Cortical neurons	Increased numbers of dendrites
	Constitutively active	NIE-115 cell line	Growth cone collapse

Figure 14. ***Summary of Rho, Rac, and Cdc42 effects on neurite outgrowth*** *(taken from Gallo and Letourneau, 1998a)*

In vitro experiments using cerebellar granule neurons showed that constitutive activation of Rho by expression of the V14RhoA mutant or ROCK by expressing a constitutively active ROCK-Delta3 mutant inhibited axon outgrowth and decreased the number of axons generated from one neuron. In addition, inactivation of Rho by C3 transferase or ROCK by Y-27632 augmented axonal processes, leading to the suggestion that the Rho/ROCK pathway functions as an initiation point for axonogenesis (Bito *et al.*, 2000).

It has also been shown that RhoA mRNA is localized to developing axon and growth cones, and that its axonal translation regulates the signaling of Sema3A in many aspects of neuronal morphogenesis, especially growth cone collapse (Wu *et al.*, 2005). Rho GTPase activities are responsible for stimulating neurite outgrowth on laminin through the assembly of integrin-dependent adhesion sites and membrane extension stability in the growth cone (Woo and Gomez, 2006). Axonal RhoA mRNA knock-down studies using RNAi resulted in elimination of Sema3A-dependent growth cone collapse (Hengst *et al.*, 2006). In neuronal cell lines, Rho GTPases are also shown to be involved in synapse formation and plasticity (reviewed by Ramakers, 2002; Negishi and Katoh, 2005). Rho GTPases modulate neurite outgrowth in response to extracellular guidance signals such as myelin (Kuhn *et al.*, 1999), collapsin-1/Sema3A (Jin and Strittmatter, 1997; Vastrik *et al.*, 1999), Ephrin-A5 (Wahl *et al.*, 2000), and neurotrophins (Ozdinler and Erzurumlu, 2001; Yamashita *et al.*, 1999). Rac also plays a role in axonal patterning *in vivo* (Hakeda-Suzuki *et al.*, 2002; Ng *et al.*, 2002).

Given the importance of the actin cytoskeleton in growth cone steering, it has been suggested that Rho GTPases are important in neuronal development, thereby can lead to defects in neuronal migration, axonal growth, guidance, and dendritic morphogenesis (reviewed by Luo *et al.*, 1997; reviewed by Mueller, 1999)

Another suggested important role of Rho is in cell survival. Inactivation of Rho by C3 transferase induces apoptosis in hematopoeitic cells (Moorman *et al.*, 1996), C3 modified or dominant negative Rho expression causes adhesion-dependent or –independent apoptosis respectively (Bobak *et al.*, 1997), *Clostridium difficile* toxin B, a specific inhibitor of Rho, Rac, and Cdc42, induced cerebellar granular neurons apoptosis *in vitro* (Linseman *et al.*, 2001), and transgenic mice expressing dominant negative RhoA caused apoptosis in motor neurons of spinal cord (Kobayashi *et al.*, 2004), suggesting that Rho GTPases play a role in cell survival signaling. Although balanced signaling of Rho GTPases RhoA, Rac1 and Cdc42 results in cytoskeleton maintenance, cell survival appears to be controlled by a Rho-mediated pathway (Moorman *et al.*, 1999).

The presence of Rho GTPases in the adult brain as determined by *in situ* hybridization and Western blot analysis suggests a functional regulatory role in the adult brain. The synaptic remodeling areas in adult rat brain showed expression of RhoA, RhoB, Rac1 and Cdc42 in pyramidal cells of the CA1-CA4 regions and granule cells of the dentate gyrus (DG), hilar cells of the hippocampus, Purkinje and granular cells of the cerebellum, in addition to the brainstem, thalamus and neocortex (Figure 15) (Olenik *et al.*, 1997).

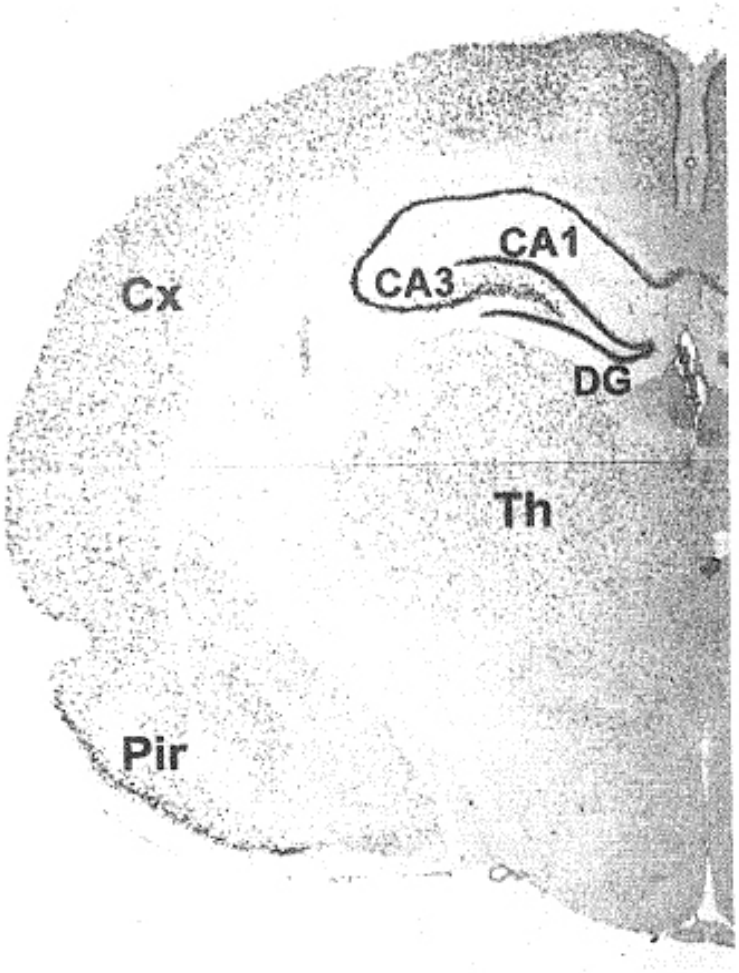

Figure 15. ***In situ hybridization of RhoA mRNA in adult rat brain.*** *Coronal sections of rat forebrain hybridized with a DIG-labelled cRNA probe for RhoA.. Cs, cerebral cortex; Th, thalamus; Pir, piriform cortex; DG, dentate gyrus. (taken from Olenik et al., 1997)*

Even though *in vitro* studies have showed that Rho GTPases are important in neuronal development, it has not been actually shown that Rho GTPases are involved in axonal and dendritic outgrowth in the mouse *in vivo*.

1.10 Rho GTPases and formation of cortex

The generation and migration of cortical neuron needs to be tightly regulated for proper lamina formation in cortex. The adult neocortex consists of six layers serving different roles. Major sensory and motor areas can be distinguished by their architecture of neurons and neuropil. How cortical areas differentiate during development and the involvement of neural activity in this process are still under intense investigation (Katz and Shatz, 1996).

The somatosensory pathways bring sensory information from the periphery into the brain. For example, information from the whisker pad goes by the trigeminal nerve that projects to

the trigeminal complex in the brainstem, which in turn sends projections to the medial ventral posterior nucleus of the thalamus (VPm). The final connection from VPm to the primary somatosensory cortex is the synaptic connection.

The primary somatosensory cortex of mammals has a typical cytoarchitecture in layer IV of the cortex, called barrels, which represent each individual whisker vibrissae. Barrels are made up of groups of stellate cortical neurons with cell bodies arranged in a ring and dendrites filling the hole in the center of the barrel, known as the barrel hollow. Barrel formation occurs over the first two days after birth, and it depends on sensory input from the relevant whisker vibrissae. Barrels show experience-dependent plasticity; if a whisker is cut during this formation period, the corresponding cortical barrel is not formed but is combined with the neighboring barrel. As thalamic axons grow through the lower layers of the cortex within the first days after birth, they make bundles to form a barrel-like pattern (reviewed by O'Leary *et al.*, 1994; Agmon *et al.*, 1995). Subsequently, this segregated group of axons reaches layer IV. Most neurons become dislocated to form the barrel walls, and readjust their dendrites into the barrel hollows, where they receive synaptic input from their particular distinguished bundle of thalamic afferents from the ventroposterior complex of the thalamus. The remaining few cortical neurons in the barrel hollow maintain symmetrically distributed dendrites (Greenoug and Chang, 1988).

The morphological reorganization and differentiation of cortical neurons to form barrels are partially due to signals delivered by thalamic axons. For instance, it has been shown that barrels were formed in the primordial visual cortex transplanted into the neonatal somatosensory cortex when invaded by axons from ventroposterior (VP) thalamus nucleus (Schlaggar and O'Leary, 1991). Interfering with the VP axons totally disorders barrel differentiation (Welker *et al.*, 1996; Abdel-Majid *et al.*, 1998; Cases *et al.*, 1996). Mice deficient in the monoamine oxidase A (MAOA) gene show decreased serotonin levels, and a failure of ingrowing thalamic axons to separate to form the primordial barrel pattern and of the rearrangement of cortical neurons (Case *et al.*, 1996). However, the exact mechanism of the rearrangement of neurons in layer IV responding to the pre-formed pattern of thalamic axons needs to be further addressed.

In $p75^{NTR}$ deficient mice, fewer filopodia on subplate growth cones was observed. There is a reduced thalamic innervation of visual cortex in $p75^{NTR}$ deficient mice, but normal innervation of auditory and somatosensory cortex (McQuillen *et al.*, 2002). A function of subplate neurons and $p75^{NTR}$ in area-specific innervation of neocortex has been suggested in that despite the fact that $p75^{NTR}$ deficient mice cause a morphological defect with random ectopic

projections in subplate axons, most of the subplate axons arrive at the internal capsule as they do in wild-type mice.

It has also been shown that BDNF is involved in neuronal laminar destination in the developing mouse cerebral cortex; BDNF changed the location and projections of neurons in layer IV to the deeper layers V and VI (Fukumitsu *et al.*, 2006). It has also been shown that the progenitor neurons in layer IV, but not in layer II/III, have been altered to become neurons in layer V and VI by BDNF treatment (Ohmiya *et al.*, 2001). There may be a link to alter the migratory machinery between the Rho GTPases and BDNF.

During postnatal brain development, experience-dependent synaptic rearrangement is important to optimize neuronal network circuitry to meet environmental demands. The Rho GTPases have been suggested to be involved in neurological diseases such as X-linked mental retardation (MR) (reviewed by Ramakers, 2002; Neghishi and Katoh, 2002) as well as Alzheimer's disease (Cordle *et al.*, 2005), and thereby the importance of Rho GTPases in the development, maintenance and function of the nervous system have been demonstrated in humans. It is unclear, however what the exact roles of Rho GTPases are in layer formation in the cortex.

1.11 Project aims utilizing the RhoA transgenic mice

RhoA, RhoB, and RhoC have been shown to interact with $p75^{NTR}$ through Rho-GDIs and inhibit neurite extension of neurons *in vitro*. RhoA, RhoB, and RhoC are known to be expressed in developing rat DRG and spinal cord (Erschbamer *et al.*, 2005) and RhoA and RhoB are expressed in developing chick DRG at E6.5, which is equivalent to mouse 12.5 d.p.c. (Malosio *et al.*, 1997). RhoA, RhoB, and RhoC have shown gene-specific patterns of expression in the sensorimotor cortex, DRG, and spinal cord in the adult, suggesting different roles for the Rho GTPases family members (Erschbamer *et al.*, 2005) and RhoA has been shown to be expressed in adult rat brain (Figure 15; Olenik *et al.*, 1997). Considering all the preliminary data shown previously that Rho GTPases can play an important role in the development of the nervous system, we were interested in using transgenic RhoA mice to answer the question, do RhoA, RhoB, and RhoC guide developmental outgrowth of peripheral nerves?

Our primary hypotheses for the early development of the RhoA transgenic mice were:

1) Expression of a dominant negative RhoA (N19-RhoA) or the RhoA inhibitor C3 transferase may interfere with growth inhibitory signals such as those provided by Sema3A because RhoA activation has been shown in Sema3A signalling, and thus axons from the DRG neurons may grow out into normally non-permissive areas.

2) Overexpression of constitutively active RhoA (V14-RhoA) may reduce or abrogate nerve extension, similar to that seen in the *p75* mutant mouse where GTP-bound Rho could activate signaling proteins such as Rho kinase (ROCK) which resulted in no growth or induced retraction through growth cone collapse (Dickson, 2001).

However, since the protein expression of dominant negative N19-RhoA after crossing with Cre mice was detectable only at the postnatal stage, I decided to look at the consequence of the dominant negative RhoA expression in the brain at the postnatal stage.

In this thesis, I report the construction and analysis of mutant-variant RhoA transgenic mice, focusing upon the N19-RhoA mouse line at postnatal stage.

2 METHODS

2.1 Construction of targeting vectors

2.1.1 HA-tagged dominant negative RhoA (N19-RhoA)

2.1.2 HA-tagged constitutively active RhoA (V14-RhoA)

2.1.3 EGFP fusion-C3 transferase

Additional details are given in the Appendix chapter, where I also briefly review the background techniques.

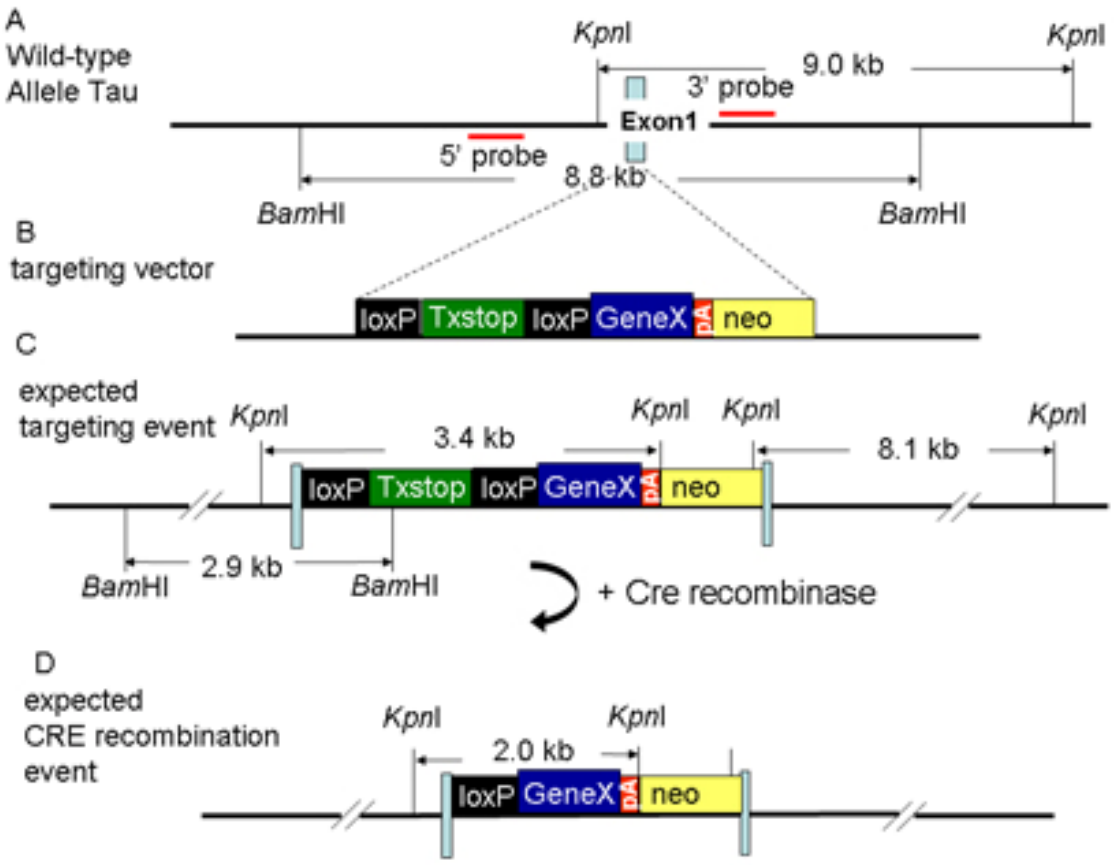

Figure 16. ***Tau targeting construct and strategy*** *Homologous recombination strategy for exon 1 of mouse N19-RhoA, V14-RhoA, or EGFP-C3 gene.* ***A****, wild-type allele of tau gene.* ***B****, targeting vector.* ***C****, expected homologous recombination event.* ***D****, predicted structure of the tau allele after crossing with the Cre deletor mouse. Exon 1, light blue; loxP sites, black box; cDNAs of interest, GeneX in a blue box. Red bars indicate the hybridization probes and arrows indicate the expected size of restriction fragments for Southern analysis.*

The tau targeting vector backbone, termed pSilvia, and a *stop cassette* construct LSL/pGEM were gifts from Dr. Silvia Arber. The plasmid pSilvia was generated to target to the tau locus and cDNAs can be inserted in Exon 1 (Figure 16A and B). cDNAs of interest lie downstream of a *stop cassette* flanked by loxP sites. The plasmid LSL/pGEM contains a *stop cassette* which consist of a transcriptional termination signal and a neomycin resistance gene cassette as a positive selection marker for embryonic stem (ES) cell culture. After insertion of the polylinker site of PWL512p into the *Sal*I site of the LSL/pGEM plasmid, termed pPWL512/LSL/pGEM, each interested cDNA could be inserted into the unique *Eco*RI site of the pPWL512/LSL/pGEM plasmid. Each plasmid in pPWL512/LSL/pGEM was finally subcloned into the pSilvia with the unique *Asc*I site. The orientation of all insertions was verified by complete DNA sequencing. The functionality of the loxP sites was confirmed by transforming the targeting vector into *E. Coli* cells expressing Cre recombinase and subsequent PCR analysis using a specific pair of primers to amplify the fragments containing a *stop cassette* gene floxed by two loxP showed a complete removal of a *stop cassette* (Figure 17).

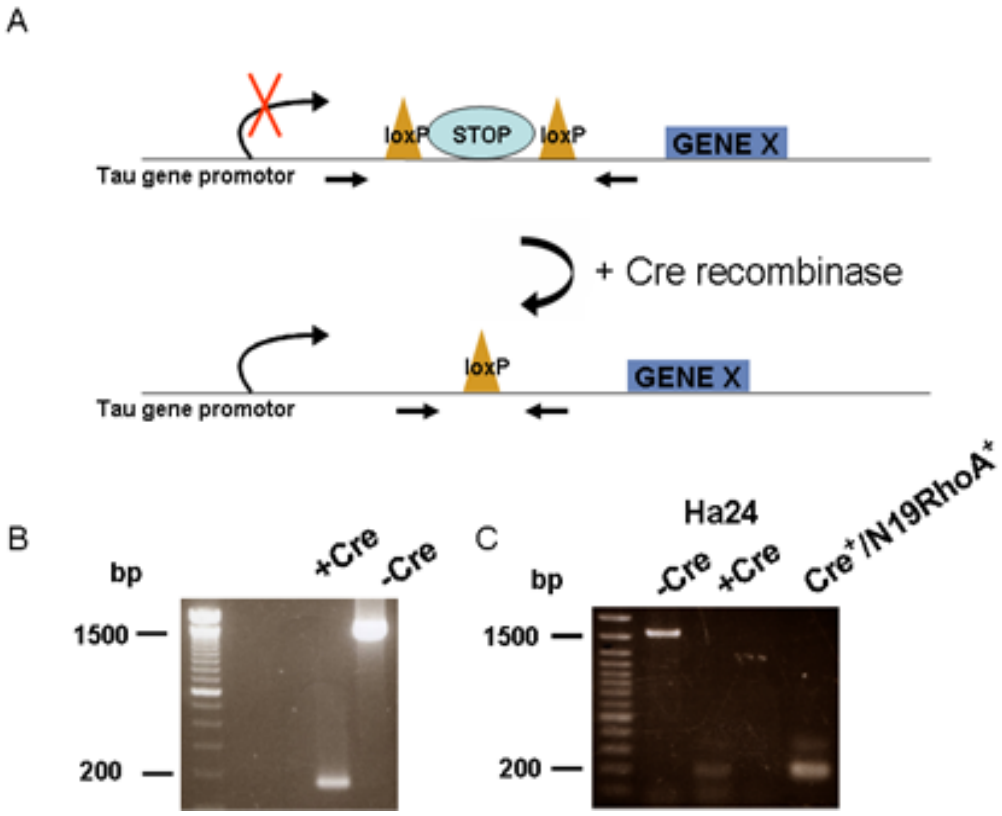

Figure 17. ***Schematic strategy and efficiency of the removal of a stop cassette by Cre recombinase***

A *Schematic representation for the removal of the stop cassette by Cre recombinase. The fragment containing a floxed stop cassette was amplified by PCR.* ***B*** *PCR analysis on DNA from transfected targeting plasmid into Cre-expressing bacteria.* ***C*** *PCR analysis on DNA from the targeted ES cells after the electroporation of a Cre plasmid p (+Cre) and the genomic DNA from the cerebellar granule cells of Cre^{+}/$N19RhoA^{+}$ mouse*

The targeting vector was linearized with *Pme*I and 30 µg were electroporated into mouse embryonic stem (ES) cells (strain J1 for N19-RhoA and EGFP-C3 and strain V6.5 for V14-RhoA). After 36 hours of culture, the cells were grown in G418 (380 µg/ml) on top of a layer of mitotically-inactivated embryonic mouse fibroblast cells (see the Appendix 5.7 "Mouse embryonic stem cell culture"). Individual resistant colonies were picked up 6-8 days after G418 selection and split into 24-well plates (on top of a layer of mitotically-inactivated embryonic mouse fibroblast cells) and 24-well plates (coated with 0.1 % gelatin) for expansion. After 2-3 days, the clones cultured in 24-well feeder plates were frozen in ES cell medium containing 10% DMSO and 25% FCS at -80 °C and then stored in liquid nitrogen. The clones cultured on gelatin plates were expanded for genomic DNA isolation.

ES cell colonies were screened by Southern blots; genomic DNA was digested with *Bam*HI for a Tau specific 5' external probe and with *Kpn*I for a Tau specific 3' external probe. The same Southern blot technique was employed to establish targeting of the tau locus with all three targeting vectors. For the N19-RhoA and V14-RhoA constructs, the *Bam*HI fragment resulted in an 8.8-kb band for the wild-type allele and a 2.9-kb band for the targeted allele, and *Kpn*I fragment results in a 9.0-kb band for the wild type allele and a 8.1-kb band for the targeted allele.

For the N19-RhoA construct, 49 neomycin-resistant clones were picked, of which 28 colonies were analyzed by Southern blots. First electroporation for N19-RhoA construct, of the first 11 colonies in total screened, five were positive with the 5' external probe (*Bam*HI digestion) and, of 28 colonies screened, five were positive with the 3' external probe (*Kpn*I digestion) (Figure 18).

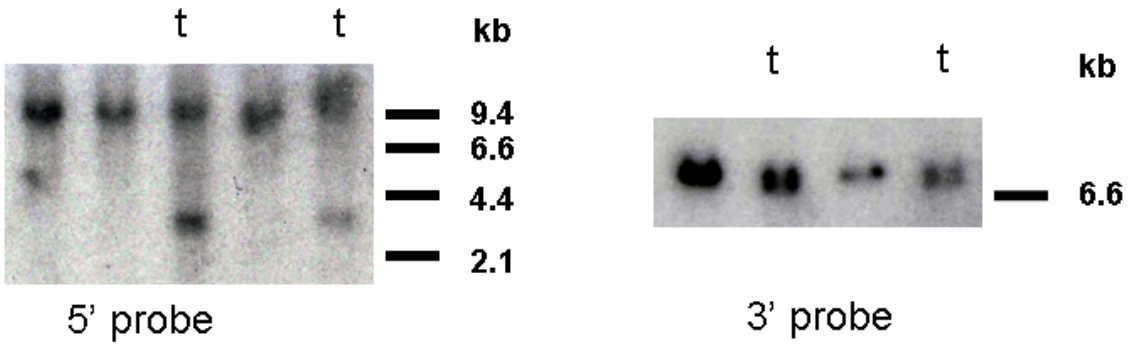

Figure 18. ***Southern blots of ES cell clones (HA2 and HA24) after the electroporation of N19-RhoA targeting construct.*** *(Left) a 8.8-kb BamHI band for the targeted allele and a wild-type 2.9-kb when probing with the 5' external probe. (Right) KpnI digested DNA of clones revealed a 8.1-kb band for the targeted allele and a 9.0-kb for the wild- type allele when probing with the 3' external probe. t: targeted clone.*

For the V14-RhoA construct, 48 neomycin-resistant clones were picked and were analyzed by Southern blots. Of 34 colonies screened, four were positive with the 5' external probe (*Bam*HI digestion) and of 24 colonies screened, three were positive with the 3' external probe (*Kpn*I digestion) (Figure 19).

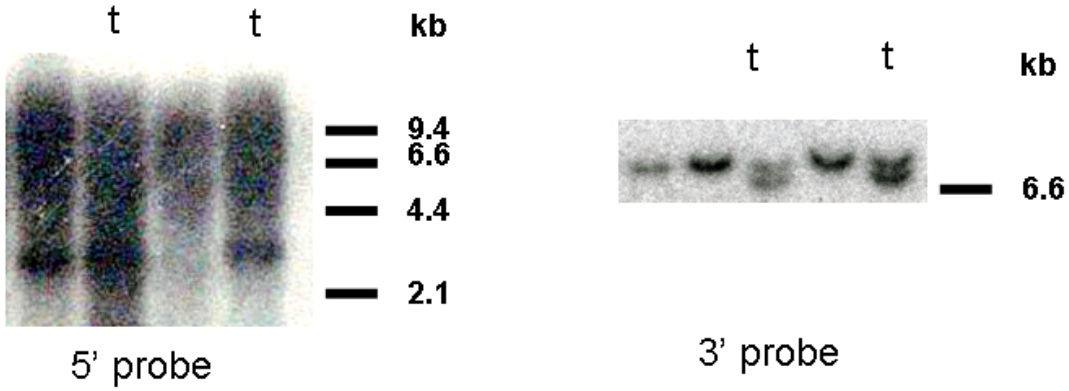

Figure 19. ***Southern blots of ES cell clones (HB60 and HB62) after the electroporation of V14-RhoA targeting construct.*** *(Left) 8.8-kb BamHI band for the targeted allele and a wild-type 2.9-kb when probing with the 5' external probe. (Right) KpnI digested DNA of clones revealed a 8.1-kb band for the targeted allele and a 9.0-kb for the wild type allele when probing with the 3' external probe. t: targeted clone..*

For the EGFP-C3 construct, 118 neomycin-resistant clones were picked, and analyzed by Southern blots. Of 65 colonies screened, two were positive with the 5'external probe (*Bam*HI digestion), and of 8 colonies screened, two were positive with the 3' external probe (*Kpn*I digestion) (Figure 20).

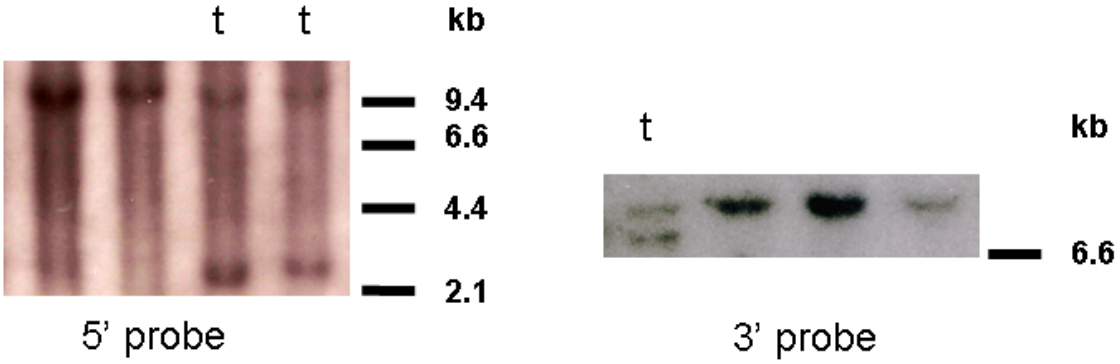

Figure 20. ***Southern blots of ES cell clones (C3-60 and C3-62) after the electroporation of EGFP-C3 targeting construct.*** *(Left) a 8.8 kb BamHI band for the targeted allele and a wild-type 2.9 kb when probing with the 5' external probe. (Right) long running gel of KpnI digested DNA of clones 2 and 3 revealed a 8.1 kb band for the targeted allele and a 9.0 kb for the wild type allele when probing with the 3' external probe. t: targeted clone.*

Targeted ES Cells (Ha2 and Ha24 for N19-RhoA, V14-17 and V14-20 for V14-RhoA, and C3-60 and C3-62 for EGFP-C3) were injected by F. Zimmermann at the Interfakultaere Biomedizinische Forschungseinrichtung, University of Heidelberg into the blastocysts of mice of the inbred strain C57/BL6 for the N19-RhoA and EGFP-C3 constructs and of mice of the inbred strain FVB/N for the V14-RhoA constructs. Of 5 chimeras obtained, 2 high density male chimeras were bred with C57/BL6 wild-type mice to generate the N19-RhoA mouse line. The germline transmission of the targeted N19-RhoA allele was confirmed by Southern blots of mouse tail DNA digested with *Bam*HI and *Kpn*I hybridized with the 5' external probe and the 3' external probe, respectively. All mice were handled according to the guidelines of the University of Heidelberg animal facility and the State of Baden-Wuerttemberg.

The subsequent generations of N19-RhoA and EGFP-C3 have been maintained on a C57/BL6 background. The generations of V14-RhoA have been maintained on an FVB/N or a C57/BL6 background. N19-RhoA and V14-RhoA mice were analyzed by PCR with primers amplifying a specific HA-tagged RhoA (Figure 38).

2.2 Proof of the functionality of the loxP sites in targeted ES cells

The targeted ES cell line Ha24 was electoroporated with the linearized plasmids pCAGGS-CRE (a gift from Prof. Dr. Junichi Miyazaki, Kyoto, Japan) and pPgk-PURO. After 36 hours of electroporation, the cells were grown in puromycin (2 µg/ml) on top of a layer feeder fibroblast cells (feeder fibroblast cells were not puromycin resistant). Individual resistant colonies were picked up 6-8 days after puromycin selection and split into 24-well plates (coated with 0.1 %

gelatin) for expansion. After 2-3 days, the clones cultured in 24-well plates were frozen in ES cell medium containing 10 % DMSO and 25 % FCS at -80 °C and then stored in liquid nitrogen. The clones cultured on gelatin plates were expanded for genomic DNA isolation and analyzed by PCR for deletion of a stop cassette.

2.3 Breeding with Cre mice to remove a *floxed stop cassette*

To remove a *floxed stop cassette* from the tau locus we crossed the N19-RhoA mice with two lines of mice that express Cre recombinase. Offspring were genotyped by PCR for both HA-tagged RhoA and Cre. The Cre mice we used were EIIa::CRE (Lakso *et al.*, 1996) and Nestin::CRE (Kurihara *et al.*, 2000), which were gifts from Prof. Dr. S. Offermanns' lab. The EIIa::CRE mouse line expresses CRE recombinase under the control of the adenovirus EIIa promoter. Expression of CRE recombinase starts from the zygote stage and recombination of a floxed allele occurs in all cell types. The nestin::CRE mouse targets expression of CRE recombinase from the nestin promoter and nervous system enhancer, and therefore this is a specific promoter for proliferating glial and neuronal precursors.

2.4.1 Cloning of N19-RhoA and V14-RhoA cDNA

The two mutant forms of the RhoA proteins that we used are 1) a dominant-negative mutant made by mutating threonine (T) at amino acids 19 to asparagine (N), termed N19-RhoA and 2) a constitutively-active form made by mutating glycine at amino acid 14 for RhoA to valine (V), termed V14-RhoA. HA tagged N19-RhoA or V14-RhoA cDNAs subcloned into a targeting vector that would allow integration at the ROSA locus (plasmids courtesy of Dr. U. Mueller, Scripps Research Institute, La Jolla, CA, U.S.A.) were amplified by PCR using the primers described (see the Appendix section 5.9.1 "Primers used for targeting vector construction" for more details). The PCR primers introduced a Kozak sequence including *Bam*HI that facilitated cloning.

The coding region of HA-tagged N19-RhoA or V14-RhoA was amplified from human cDNA using AccuPrime *Pfx* DNA polymerase (Invitrogen). The mouse and human RhoA genes are both 582 bp in size and they share 93.6% nucleotide identity and 99.5% identical at amino acids level. PCR primers were designed from the predicted human cDNA sequence (NCBI accession number: NM_001664) tagged with an HA peptide.: forward primer RhoA1 5'-AAT GTC GAC GGC ACC ATG GCC tac ccc tac g-3' and reverse primer RhoA2 5'- TAT GCG GCC GCT CAC AAG ACA AGG CAA CC -3' (19 cycles at 95 °C for 30 sec, 65 °C (+/- 7

°C gradient PCR) for 30 sec, 72 °C for 30 sec, 100 ng of cDNA). Lower case letters indicate a part of an HA peptide sequences and a *Sal*I site was underlined in the forward primer, and a *Not*I site was underlined in the reverse primer The PCR fragment was gel-purified with QIAEX II gel extraction kit (Qiagen) and subcloned into the ZERO blunt TOPO cloning vector (PCR-blunt Amp Cloning Kit, Invitrogen). The insert was then excised with *EcoR*I and subcloned into the PWL512/LSL/pGEM vector (gift of Dr. Silvia Arber, see 2.1 "Construction of targeting vectors"), and termed N19RhoA/PWL512/LSL/pGEM or V14RhoA/PWL512/LSL/pGEM. They were inserted into the unique *Asc*I site of pSilvia and linearized with *Pme*I. Each amplified fragment was verified by complete sequencing (see Appendix section 5.9.2 "Sequencing primers used for N19-RhoA and V14-RhoA cDNA"). The final targeting construct was termed N19RhoA/PWL512/LSL//pGEM/pSilvia for the N19-RhoA construct or V14RhoA/PWL512/LSL//pGEM/pSilvia for the V14-RhoA construct.

2.4.2 Cloning of EGFP fusion C3

A cDNA encoding the C3 transferase from the Gram-positive bacteria *Clostridium limosum* was a kind gift from Prof. Dr. Klaus Aktories of the University of Freiburg, Germany. In order to subclone the C3 cDNA into the pEGFP-C1 vector (Clontech), the *Bgl*II site of EGFP-C1 was changed toa *Bam*HI site. 1 µg of pEGFP-C1 plasmid was linearized with *Bgl*II in 20 µl reaction mixture for 1 hour at 37 °C and added *EcoR*I afterwards. The C3 fragment digested with *Bam*HI and *Eco*RI was ligated into the pEGFP-C1 vector digested with *Bgl*II and *Eco*RI and transformed into DH5α *E. coli* cells.

PCR primers to amplify GFP fused C3 transferase cDNAs were designed from the published *Clostridium limosum* C3 transferase sequence (NCBI accession No. X87215) and GFP sequence; forward primer 5'-CGG TTT AAA CCG CCA CCA TGG TGA GGT GAG CAA GGG C-3' (*Pme*I site is underlined) and reverse primer 5'-TAT GCG GCC GCC TAT CTT TTT AAT AAT CCT G-3' (*Not*I site is underlined) (25 cycles at 95 °C for 30 sec, 65 °C (+/- 7 °C gradient PCR) for 30 sec, 72 °C for 30 sec, 100 ng of cDNA). The PCR fragment was gel purified and subcloned into pCR II-TOPO vector (Invitrogen) with sites. The insert was then excised with *Eco*RI and subcloned into the PWL512/LSL/pGEM vector (gift of Dr. Silvia Arber, see 2.1 "Construction of targeting vectors"), and termed EGFP-C3/PWL512/LSL/pGEM. A fragment from this plasmid was finally inserted into the unique *Asc*I site of pSilvia. In order to linearize this plasmid with *Pme*I, digestion was carried out with EtBr to optimize the linealized condition because there were two *Pme*I sites in the final construct. Each amplified fragment was

verified by complete sequencing (see Appendix section 5.9.2 "Sequencing primers used for EGFP-C3 cDNA"). The final targeting construct was termed EGFP-C3/PWL512/LSL/pGEM/pSilvia.

2.5 Substitution in N19RhoA/cDNA3.1(+) to wtRhoA/cDNA3.1(+)

We purchased the wild type RhoA cDNAs from Deutsches Ressourcenzentrum for Genomforschung GmbH (RZPD):(RZPD clone ID is IRALp962A174Q). The wild type RhoA plasmid with CMV promoter was used in the cotransfection of the wild type RhoA with N19-RhoA or EGFP-C3 transferase cDNA to see the efficiency of inhibition of Rho GTPases activity by expression of N19-RhoA or C3 transferase (see 2.7 "Rhotekin pulldown assay"). In order to clone the wild type RhoA, a 100 bp fragment containing the V14 amino acid of V14-RhoA was substituted with the fragment from wild type RhoA. V14RhoA/cDNA3.1(+) was double digested with *Bsp*EI and *Eco*RV, and then used as a vector. The wild type RhoA was also digested with *Bsp*EI and *Eco*RV, and the expected fragment size of 100 bp was gel purified to subclone in the vector from V14RhoA/cDNA3.1(+) above. Complete sequencing verified the wild type RhoA sequence.

2.6 Recombinant expression of mouse N19-RhoA and V14-RhoA cDNAs in different cells

3 µg of N19RhoA/cDNA3.1(+) or V14RhoA/cDNA3.1(+) expression vectors were transfected into HEK293 cells, HN10 cells, and Swiss 3T3 cells in 35-mm plates each using Lipofectamine (Invitrogen). 2 days after the transfection, cells were lysed in 300 µl of RIPA buffer in each plate and protein expression was analyzed by Western blots.

2.7 Rhotekin pulldown assay

HEK293 cells in 6-cm dishes were cotransfected with wild type RhoA (6 µg) and different amounts of N19RhoA or EGFP-C3 using TransFectin Lipid Reagent (BioRad) and cultured with serum starved medium, because LPA in serum is known to activate endogenous Rho. After 2 days of transfection, transfected cells were trypsinized with 1x Trypsin (5 mg/ml), placed into a 2 ml eppendorf tube, and pelleted at 3000 rpm at 4 °C. The cells were resuspended in 320 µl of lysis buffer (50 mM Tris-HCl pH 7.4, 150 mM NaCl, 5 mM $MgCl_2$) with 10 µg/ml Aprotinin (Roche), 10 µg/ml Leupepetin (Roche), and 10 µg/ml PMSF (ROTH) (protease inhibitors are all added into lysis buffer right before sonicating) and sonicated three times for 15 sec. 20 µl out of 320 µl was kept as a lysis control and stored at -80 °C. With the remaining 300 µl, 100 µl Rhotekin beads (prepared by Julia Hoffmann, see the Appendix 5.1 "Rhotekin beads

preparation") were added and incubated upon the rotator for 45 min. The cells were centrifuged at 4 °C for 15 min at 2900 rpm and the supernatant was discarded. After 1 ml of wash buffer (50 mM Tris-HCl, pH 7.5, 0.5 % TritonX-100, 150 mM NaCl, 5 mM $MgCl_2$) with 10 µg/ml Aprotinin, 10 µg/ml Leupepetin (Roche), and 10 µg/ml PMSF (protease inhibitors are all added in wash buffer right before use) was added, the beads were resuspended and washed for 5 min with rotating. The supernatant was discarded. After washing three times, the pellet was resuspended in 15 µl of 2x sample buffer (see the Appendix 5.6 3 "6x Sample Buffer") and analyzed by Western blots.

2.8 Metaphase spreads for Karyotype analysis

ES cells that were free of MEFs by several passages were passaged onto gelatin-coated 6-cm plates. In the next morning, the medium was changed and 15 µl of colcemid (10 µg /ml) was added. After 6 hours of incubation, the cells were washed with 1x PBS, trypsinized with 0.1 % trypsin for 3 min at 37 °C in the incubator, and received ES medium to stop the trypsinization. The cells were pelleted at 900 rpm for 5 min and the pelleted cells were resuspended after the supernatant was removed. Cells were transferred to 2 ml eppendorf tube and were pelleted at 2000 rpm for 2 min. Cells were carefully resuspended in 1 ml 0.075 M (0.56 %) KCl and were vortexed at a very low speed while KCl was added dropwise, and then incubated for 10 min at RT. The cells were centrifuged at 2,000 rpm at RT and supernatant was carefully removed with a pipette tip. The pellet was resuspended slowly and carefully in 1 ml of cold and freshly made MeOH + acetic acid (3:1) solution, and this step was repeated one more time. The cells sat overnight at 4 °C, and were then centrifuged at 2000 rpm for 2 min and resuspended in MeOH/ acetic acid solution. The slides were cleaned with EtOH and dipped briefly in water. The cells were immediately dropped onto the slides, which were held at a slight angle on the ground using a siliconized pasteur pipette from 2-3 meter height. The slides were put in a tray in 37 °C water bath and air dried. The cells were stained with 3 % Giemsa in GuRR buffer for 20 min at RT. Giemsa and GuRR were purchased from Invitrogen. The slides were dipped into water briefly and coverslipped in Entallen Neu (Merck). Karyotypes were analyzed under the microscope.

2.9 Hybridization probes

The same 5' external and 3' external probes for all three targeting vectors were prepared for Southern blot with the analysis of targeting of the EGFP cDNA to the tau locus (Tucker *et al.*, 2001). 8 µg of pTAU-SRI 5'sonde was digested with *Sma*I and followed by *Eco*RI which

produced an approximately 500-bp genomic fragment and used as the 5' external probe which is located 2.8-kb upstream of exon 1. 8 µg of pTAU KHBRI 3'sonde was double digested with *Bam*HI and *Eco*RI yielding a 600-bp genomic fragment for the 3' external probe. 25 ng of each probe was used for each Southern blot hybridization.

For the analysis of Cre recombinase efficiency for the removal of a *stop cassette*, an approximately 600-bp N19-RhoA cDNA fragment, amplified by PCR (using a forward primer RhoA1 and a reverse primer RhoA2) was used as a probe for Southern blot analysis.

2.10.1 Southern blots

Digested genomic DNA fragments were separated by electrophoresis on 0.7% agarose gels (containing 0.5 µg/ml ethidium bromide) in 1 x TAE buffer (800 mM Tris-HCl, 400 mM NaOAc, 40 mM EDTA, pH 8.3 adjusted with acetic acid). After electrophoresis, the gel was incubated 30 min in denaturing solution (0.5 M NaOH, 1.5 M NaCl) to denature the DNA, and neutralized with neutralization solution (1 M Tris pH 7.4, 1.5 M NaCl). Blotting was performed by a standard capillary Southern transfer set up using 10 x SSC (0.4 M NaOH) onto a positively charged nylon Hybond N^+ (Amersham) membrane (the denatured DNA binds covalently to the membrane). After transferring the membrane overnight, the membrane was UV-crosslinked and prehybridized at 65 °C overnight in Church buffer (7% SDS, 0.5 M Na_2HPO_4, 1 mM EDTA, 1% BSA).

2.10.2 Southern blot membrane hybridization

The Southern blots were hybridized with specific DNA probes labelled with α^{32}P-dCTP (Hartman Analytic GmbH) by using Ready-To-Go DNA Labelling Beads (Amersham) (the technique for radiolabelling DNA restriction endonuclease fragments was introduced by Feinberg and Vogelstein, 1983). Unincorporated labeled nucleotides from the DNA-labeling reaction were removed using ProbeQuant G-50 Micro Columns (Amersham). Hybridization was performed overnight at 65 °C in Church buffer. After hybridization, the membrane was washed twice in 1 x SSC/0.1% SDS at 65 °C for 15 min and twice with 1 x SSC/0.1% SDS at 65 °C for 20 min. The membrane was then exposed to an X-ray film (Kodak) at -80 °C in cassette with scintillation screens.

2.11 Western blots

Embryos (13.5 d.p.c. and 17.5 d.p.c.) or pups (P3, P6, P10, and P20) were killed and subsequently their brains were removed and homogenized on ice in RIPA buffer (50 mM Tris, pH 8.0, 150 mM NaCl, 1 mM EDTA, 1% Triton X-100, 0.5% NaDOC, 0.1% SDS) containing 1 tablet of protease inhibitor (Roche), freshly added protease inhibitors 1 mM PMSF, and 2 μg/ml E64. The homogenate was centrifuged 20 min at 12000 rpm at 4 °C. The obtained supernant proteins were aliquoted and stored at -80 °C. The protein concentration of the samples was determined using a Bradford protein assay reagent (Bio-Rad).

The protein samples were separated by SDS-PAGE in a discontinuous system (5% acrylamide-containing stacking gel and 13% acrylamide-containing resolving gel) and then transferred to Immobilon-P transfer membrane (Millipore). The membranes were incubated in 5% skimmed milk in TBST (0.1% Tween20 in TBS（25 mM Tris Base, 125 mM NaCl, pH 8.0)) at least one hour at 4 °C. The membranes were then incubated with the affinity purified mouse anti-RhoA antibody (Santa Cruz Biotechnology product number sc-418) (1:1,000) or rabbit anti-HA antibody (Santa Cruz Biotechnology, product number sc-805) (1:1,000) for overnight at 4 °C and washed with TBST 3 times for 10 min at RT. The membranes were next incubated with anti-rabbit IgG or anti-mouse IgG, horseradish peroxidase linked antibody (Santa Cruz) (1:10,000) for 1 hour at RT and then washed three times with TBST at RT. All membranes were visualized using ECL plus Western Blotting Detection System (Amersham Biosciences) and exposure to ECL Hyperfilm (Amersham Biosciences).

2.12 Insoluble protein immunoblot analysis

The pellets obtained were dissolved in 4x sample buffer (125 mM Tris-HCl, pH 6.8, 4% SDS, and 25% glycerol) and further sonicated four times for 10 sec each. The solubilized protein solutions after sonication were used for immunoblot analysis.

2.13 Neurofilament whole mount staining

Neurofilament 165 kDa was stained to analyze the outgrowth of embryo nervous system at 10.5-13.5 d.p.c. Embryos were removed from uterus in successive baths of cold 1x PBS on ice. Cleaned embryos were transferred into MeOH:DMSO 4:1 solution and fixed overnight at 4 °C. After washing out fixative with 100% MeOH 5 times for 10 min each, embryos were bleached by agitating in 6% H_2O_2 at 4 °C for at least 4 hours. Embryos were rehydrated by successive steps 30 min each in 90%, 70%, 50%, 30%, 0% MeOH in PBS/0.1% TritonX-100, and then

incubated for 2 hrs at RT in 80% FCS:20% DMSO for blocking. Embryos were incubated by gently rocking with 2H3 anti-neurofilament monoclonal mouse antibody (1:400) at 4 °C at least 24 hours for embryos up to 11.5 d.p.c. and 48-96 hours for later-stage embryos in blocking solution, and then washed at least 10 times in PBS/ 0.1% Triton X-100 at RT for 6 hours. Embryos were then incubated with the monoclonal mouse antibody (1:400) for at least 24 hours for small embryos up to 11.5 d.p.c. and 36 hours for the later stage embryos in blocking solution at 4 °C and washed with PBS/ 0.1% Triton X-100 at least 10 times for 6 hours at RT. The embryos were rocked in a 0.5 mg/ml DAB in 1x PBS in small glass beakers with wide mouths for 30 min, and 4 µl of 0.3% H_2O_2 was added per 5 ml of DAB solution while the staining process was monitored under the microscope. The development process was carried out in the dark. The coloring reaction was stopped by switching to 1 x PBS, washing several times in 1x PBS/0.1% NaN_3, and washed overnight. For longer storage, embryos were dehydrated by successive steps 30 min each in 30, 50, 70, 100% MeOH in PBS/ 0.1% TritonX-100, and then cleared in benzyl alcohol:benzyl benzoate 1:2 in glass containers.

2.14 Cerebellar granular cells culture

The original protocol for cerebellar granule cells culture was supplied by Dr. Haruhiko Bito (Bito *et al.*, 2000) and was modified after optimizing the culture condition. Details for all mediums used for cell cultures can be found in the Appendix 5.5 "Cerebellar granular cell culture Medium". 5-day old pups were sacrificed by decapitation, the skull was removed, and the brains were taken out and placed into 1 x HBSS (+1% HEPES, 1% p/s). The pia mater was removed carefully as much as possible, the cerebellum placed into a 300 µl digestion solution (10 mg trypsin in 1 ml of 1 x HBSS) in a 1.5 ml eppendorf tube, and incubated at 37 °C for 10 min. The digested cerebellum was gently triturated using pipet tips until no clumps and aggregates were visually detected, and 300 ml of 20% FBS/HANKS(-) was added to stop the reaction. After filtering the cells, another 10 ml of 20% FBS/HANKS(-) was added into the filter to make sure that all cells were filtered. The pellet was centrifuged at 1,000 rpm for 5 min and resuspended in 20% FBS/HANKS(-). I plated out 70,000 cells per each coverslips of a 24-well plate which had been precoated with 100 µg/ml Poly-L-lysine (Sigma). The cells were plated in the 500 ml pre-equilibrated 10% FBS/MEM or MEM without FBS to starve the cell to eliminate the possibility to activate Rho by LPA in serum at 37 °C per well and settled down for 30 min at room temperature. Then the cells were placed into the CO_2 incubator.

2.15 Immunocytochemistry

Cultured neurons were fixed for 5 min at RT with 4% PFA and washed three times with PBS. Cells were incubated in a blocking buffer (5% NGS, 0.5% Triton X-100, 1% BSA in PBS) for 1 hr at RT. Then, cultures were incubated with monoclonal antibody to Tuj1 (1:2000) for 4 hours at RT and washed sequentially three times with 1x PBS, followed by a Cy3-labeled anti-mouse monoclonal antibody for 1 hr. DAPI (100 nM) and phalloidin (1:100) were used to stain the nucleus and F-actin, respectively.

2.16 Immunohistochemistry

Mice were perfused transcardially with physiological saline (0.9% NaCl, 2% polyvidon25 (Merck), freshly added 0.2% procainhydrochlorid (Merck)) and then with cold 4% PFA in final concentration of 0.1 M $NaH_2PO_4*H_2O$ and $Na_2HPO_4*2H_2O$ with 2% polyvidon25, pH 7.6 (pH was adjusted by using only 0.2 M $NaH_2PO_4*H_2O$ and 0.2 M $Na_2HPO_4*2H_2O$). The brains were removed and preserved at 4°C in PBS (154 mM NaCl, 13 mM $NaH_2PO_4*H_2O$, 60 mM $Na_2HPO_4*2H_2O$, pH 7.4). The brains were washed 3 times in PBS at RT, and placed in 10% Sucrose/PBS for 1 hour, 20% Sucrose/PBS for 1 hour, and 30% Sucrose/PBS for overnight at 4 °C. Brains were embedded in Jung tissue freezing medium (Leica microsystem) on dry ice and stored in -20 °C. Brain sections were cut at 25 µm using the cryostats (LEICA CM3050S) and stored in PBS at 4 °C.

2.17 Hematoxylin and Eosin staining

Hematoxylin (catalog number 5B535) and Eosin Y (catalog number 1B425) were purchased from Chroma. After frozen brain sections were dipped in distilled water for 5 min, they were stained in Mayer's Hematoxylin solution for 3 min. Then sections were washed with distilled water twice and followed by tap water for more than 20 min. Then, the sections were stained in 0.1% Eosin solution for 3 min, and washed with distilled water for 5 min twice. Sections were mounted in Aqua-Poly/Mount coverslipping medium (Polysciences, Inc) and analyzed under the microscope.

2.18 NeuN staining

NeuN staining was done by Dorge Komljenovic. Free floating brain sections were washed in PBS for 30 min, rinsed in 2% H_2O_2 in 10% methanol for 20 min to block endogenous peroxidase, then washed again in PBS for 30 min. Sections were then rinsed in PBS containing

0.4% TritonX-100 for 1 hour at RT, followed by an incubation in PBS/0,1% Triton X-100/1.5% horse serum/1%BSA for 1 hour at RT. Overnight incubation with mouse anti-NeuN monoclonal antibody (1:1000; Chemicon MAB377) in PBS/0.1% TritonX-100/1% BSA at 4°C was followed by 30 min washing in PBS. Biotinylated secondary antibody and peroxidase-labeled avidin-biotin complex were applied according to the instructions of the manufacturer (Vectastain Elite ABC, Vector Laboratories, Burlingame, UK). Sections were washed in PBS for 30 min and processed in 0.05% DAB (Sigma) and 0.006% H_2O_2. Sections were washed again in PBS for 10 min and mounted and coverslipped using Aquatex mounting medium.

3 RESULTS

3.1 Transient Expression of N19-RhoA, V14-RhoA, and C3 genes

Before I started making a targeting construct, I checked the protein expression of HA-tagged dominant negative RhoA (N19-RhoA), HA-tagged constitutively active RhoA (V14-RhoA), and EGFP-C3, all three driven by the CMV promoter by transient transfecton of HN10, Swiss 3T3, and HEK293 cells. The fragment of N19-RhoA or V14-RhoA which were fused at the N-terminus with an HA (YPYDVPDYA) epitope tag was inserted into the cDNA3.1(+) vector with the CMV promoter. An antibody directed against Rho or HA detected the proper size of proteins of dominant-negative RhoA and constitutively active RhoA from transfected HN10 and HEK293 cells (Figure 21A and 21B), but not from Swiss 3T3 transfected cells (Figure 21C). Therefore, HA-tagged N19-RhoA and HA-tagged V14-RhoA were used for further experiments.

I decided to make an EGFP fusion protein of C3 at its N-terminus because when C3 was tagged with an HA peptide, as with the N19-RhoA or V14-RhoA constructs, protein expression of C3 trasnferase was not detectable for unknown reasons. The exoenzyme from *Clostridium limosum* (gift from Prof. Dr. Klaus Aktorius), homologous to the C3 transferase from *Clostridium botulinum*, was fused at its N-terminus with the EGFP cDNA by using an expression vector pEGFP-C1 (Clontech) which is driven by the CMV promoter, and this plasmid was termed EGFP-C3. The transient transfected EGFP-C3 protein expression was detected in HEK293 cells (Figure 21D). Therefore, the EGFP fusion protein of C3 transferase was used for further experiments to generate targeting constucts.

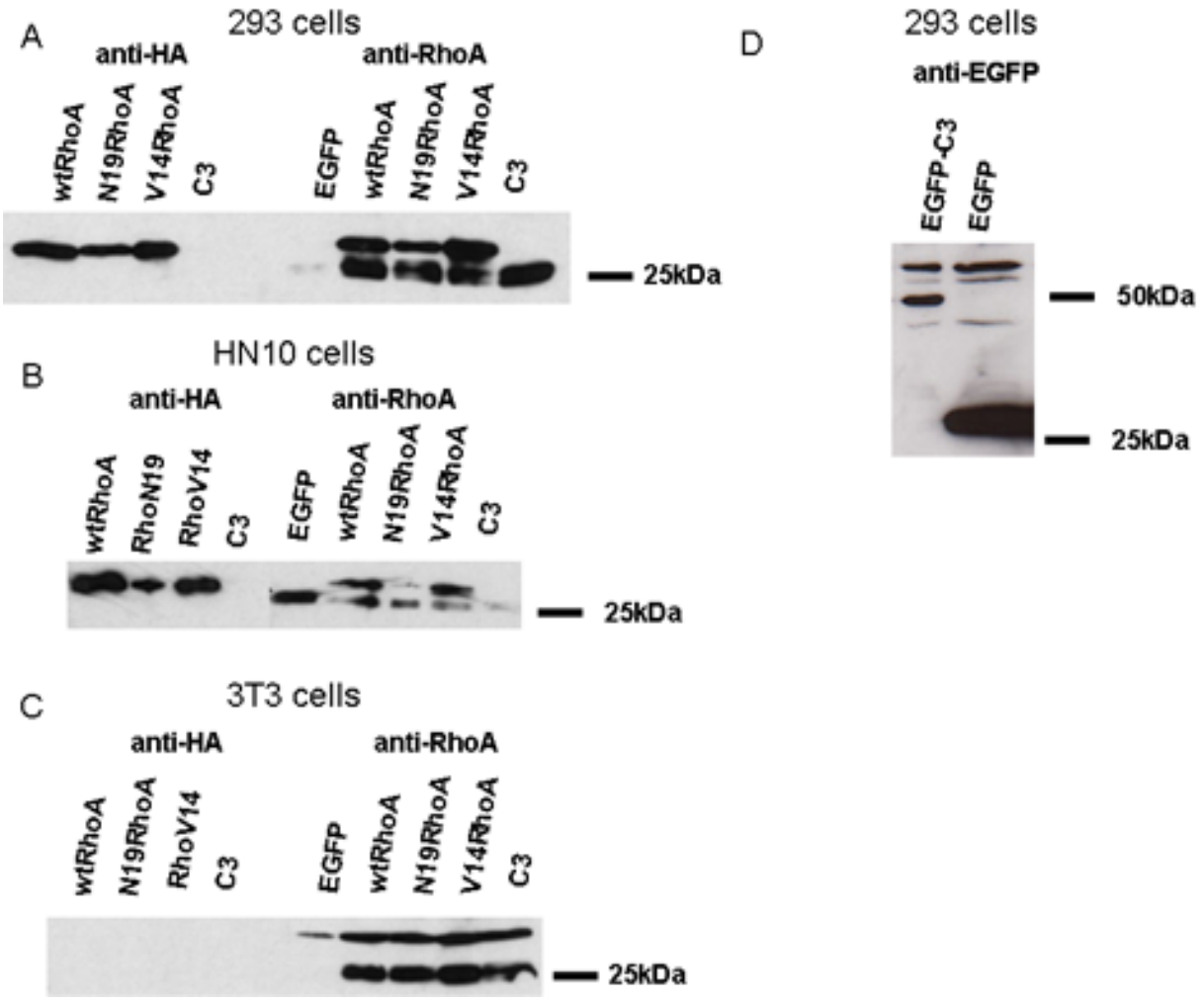

Figure 21. ***Transient expression of the CMB promoter HA-tagged N19-RhoA, HA-tagged V14-RhoA, and EGFP fusion C3 by Western blot analysis.*** ***A.*** *HEK293 cells,* ***B.*** *HN10 cells,* ***C.*** *3T3 cells*
RhoA was detected using anti-HA antibody and anti-Rho antibody. Endogenous RhoA is 24 kDa and recombinant RhoA is 28 kDa. EGFP fusion C3 was detected using anti-EGFP antibody. EGFP is 27 kDa and C3-EGFP is an approximately 54 kDa.

3.2 Inhibition of Rho activity by N19-RhoA or C3 transferase gene

To see the efficiency of inhibition of Rho activation, we employed a method to precipitate GTP-bound Rho using the Rho-binding domain (RBD) of a downstream effector protein Rhotekin (Ren *et al.*, 1999) because RBD interacts only with GTP-bound Rho. HEK293 cells co-transfected with wild-type RhoA and either N19-RhoA or EGFP-C3 were serum starved so that LPA in serum does not activate endogenous Rho. This Rhotekin pulldown assay showed that transfection of 1/4 μg of C3 transferase plasmid completely abolished the Rho activity of GTP binding (Figure 22A), whereas transfection of 2 μg of N19-RhoA plasmid was required to inactivate Rho (Figure 22B). Even though this is not a comparison of the protein amount

between N19-RhoA and C3 transferase, the size of their nucleotides is close and we expected that they produce the similar amount of the protein. Thereby, N19-RhoA may not be as effective in inhibiting Rho function as the C3 transferase, but this result showed that both dominant negative N19-RhoA and C3 transferase genes are able to inhibit Rho activity. These results suggested that the degrees of Rho GTPases inhibition may be controlled genetically comparing with N19-RhoA and C3 transferase expression. Also, its ability to inhibit wild-type Rho activity when co-expressed in HEK293 cells showed that an HA tag or EGFP protein did not change the function of the constructs.

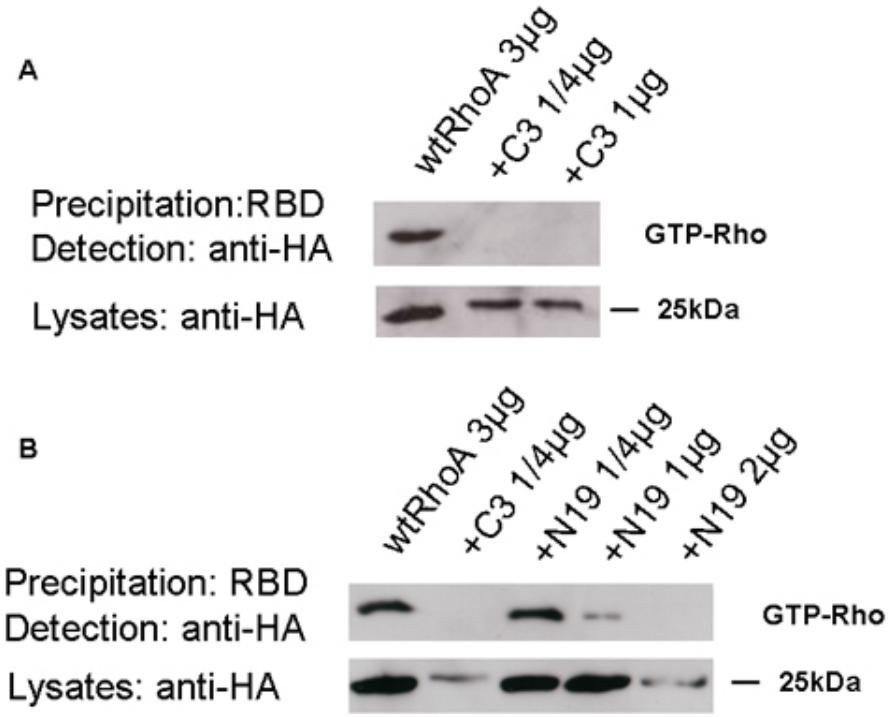

Figure 22. ***Inhibition of Rho with transient transfection of C3 transferase and N19-RhoA detected by Rhotekin pulldown assay.*** *HEK293 cells were co-transfected with wtRhoA and either EGFP-C3 or HA tagged N19-RhoA. Only GTP-bound Rho was pulled down with Rhotekin binding sites. Lysates were used as a control.*

3.3 N19-RhoA, V14-RhoA, and EGFP-C3 gene targeting strategy

A cDNA encoding HA-tagged N19-RhoA, HA-tagged V14-RhoA, or EGFP-fused C3 was targeted to the tau locus. We constructed a targeting vector by placing the HA-tagged N19-RhoA, HA-tagged V14-RhoA, and EGFP-fused C3 into Exon 1 of the tau gene (Figure 16). This inserts lie downstream of a tranclscriptional *stop cassette* flanked by two *loxP* sites (gift from Dr. Silvia Arber) (Figure 23A). Because of this *floxed stop cassette*, expression of the endogenous tau promoter at the altered locus will produce a truncated, non protein-coding heterologous

transcript, and the introduced cDNAs will not be transcribed (Figure 23). Southern blot analysis of targeted ES cell clones following *Bam*HI or *Kpn*I digestion and hybridization with 5' or 3' external probes respectively, showed that targeting N19-RhoA or V14-RhoA yielded a 2.9- or 8.1-kb band, and the untargeted allele remains at 8.8-and 9.0-kb, respectively (Figure 18 and 19).

The ability of the loxP sites to undergo recombination by Cre recombinase in targeted ES cells was confirmed by electroporation of a plasmid expressing Cre recombinase into ES cells. PCR analysis using genomic DNA from the targeted ES cell (Ha24) amplified the fragments containing a *stop cassette* gene floxed by LoxP sites with a specific pair of primers, yielding a 1558 bp fragment before and a 187 bp fragment after removal of the *stop cassette*. Therefore, PCR analysis showed a proper reduction of size, indicating a complete removal of the *stop cassette* (Figure 17B). More importantly, PCR analysis using the genomic DNAs of cerebellar granular neurons (CGN) from Cre^{+}/ $N19RhoA^{+}$ (positive for Cre and N19-RhoA genes by PCR) double transgenic mouse also showed the corresponding reduction of size (Figure. 17C), and later, Southern blot analysis confirmed this PCR result, indicating the removal of the *stop cassette* after mating with Cre-expressing mice (Figure 24). Offspring were genotyped by PCR for both HA-tagged RhoA and Cre.

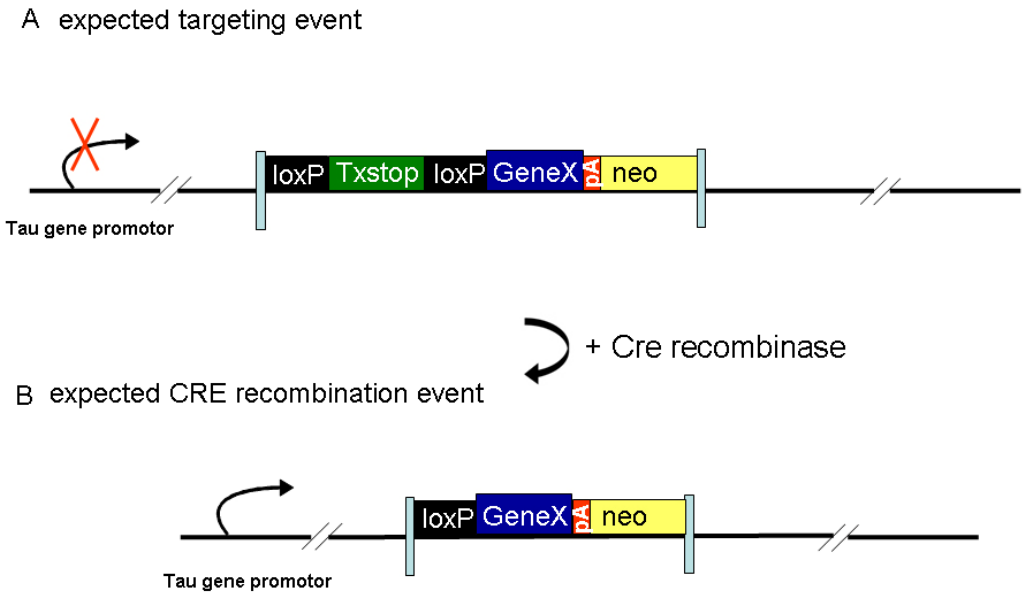

Figure 23. ***Experimental strategy to flox the stop cassette.*** *RhoA transgenic mice were crossed with EIIa-Cre or Nestin-Cre mice to remove a termination transcription stop cassette.* ***A****, Expected targeting event.* ***B****, Expected CRE homologous recombination event. An approximately 1-kb fragment (Txstop: a termination transcription stop cassette) is removed by CRE recombinase exposure.*

3.4 Generation of N19-RhoA trasngenic mice

By homologous recombination in ES cells, we generated mice expressing N19-RhoA gene fused to a *stop cassette* flanked by two *loxP* sites targeted at tau locus. Targeting efficiency of ES cells in total analysis was 16%. Targeted ES cells were injected into blastocysts by Frank Zimmermann at the Interfakultaere Biomedizinische Forschungseinrichtung, University of Heidelberg and 7 chimeric males were born. The heterozygous and homozygous N19-RhoA mice are healthy, and breed normally; mutants are obtained in the expected Mendelian ratio. I analyzed germ line-transmitted progeny of chimeras generated from two independent clones. These mice were mated with the EIIa::Cre and Nestin::Cre mice to obtain double-transgenic mice (Cre^+/ $N19RhoA^+$) to remove a floxed *stop cassette* from the tau locus.

Tail DNAs from heterozygous transgenic offspring were genotyped by *Bam*HI or *Kpn*I digestion and hybridized with the 5' external probe: a 2.9-kb band was produced together with the 8.8-kb wild-type allele (data not shown) or with the 3' external probe: a 8.1-kb together with a 9.0-kb band for the wild-type allele (data not shown). These data show that the N19-RhoA construct has passed through the germline of chimeric males and at the same time the conditions for PCR reaction was also established to genotype both Cre and RhoA mice (see the Appendix 5.7.3. "PCR genotyping of mice"). Further genotyping of the transgenic mice was done by PCR.

To assess the expression of the dominant-negative forms by Cre-*loxP* recombination, we performed Southern blot analysis upon genomic DNA from cerebellar granular cultures prepared from 17.5 d.p.c. embryos and P3 mice on Cre^+/ $N19RhoA^+$ by *Kpn*I digestion and hybridized with the RhoA specific probe: a 2-kb band was produced together with the 7-kb wild-type allele. Cre-loxP recombination had occurred in Cre^+/ $N19RhoA^+$ mice showing the shorter fragment of 2,010 bp while Cre^-/ $N19RhoA^+$ mice showed 3,381 bp with a *stop cassette*. The proper DNA size reduction of an approximately 1.4-kb after removing a *stop cassette* by Cre recombinase exposure was detected in corresponding double-transgenic mice (Figure 24), indicating that the *stop cassette* was properly removed after being exposed to Cre recombinase, allowing expression of the gene, in agreement with the PCR result. Also, recombination occurs with 100% efficiency in cerebellar granule neurons, because Southern blot analysis showed only one fragment corresponding with the expected size of 2-kb. The other, higher molecular weight fragment is probably from endogenous RhoA.

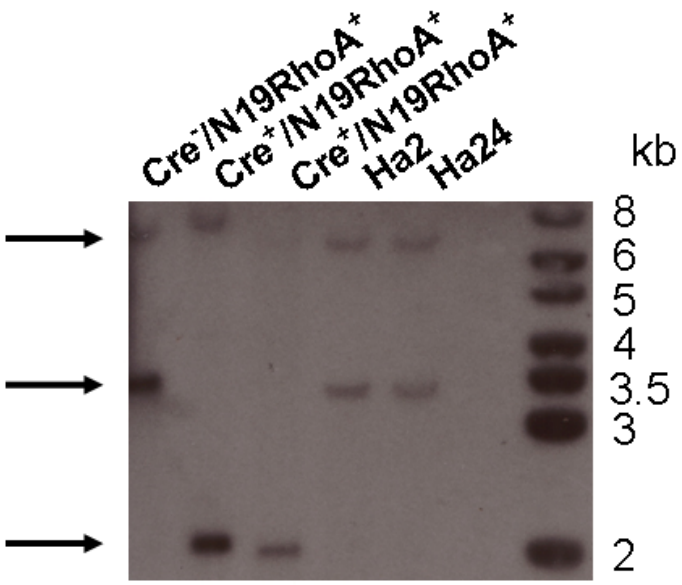

Figure 24. ***Cre recombination in heterozygote offspring after crossing of HA-N19RhoA with Cre.*** *Southern blot analysis of offsprings with RhoA specific probe revealed the 2.0-kb band which is corresponding to the recombination event (the lowest band). Genomic DNA was prepared from cerebellar granular neurons culture. The 3.4-kb band is corresponding to the fragment with a stop cassette before Cre exposure (the middle band). The higher molecular weight band is presumably an endogenous RhoA (the upper band). The corresponding genotypes of the mice are indicated above the lanes. Cre^+: positive for a Cre gene, $N19RhoA^+$: positive for a dominant negative RhoA.gene. Cre^-/ $N19RhoA^+$ as wild-type mice and Cre^+/ $N19RhoA^+$ as double transgenic mice. HA2 and HA24 indicate genomic DNAs from the N19-RhoA targeted ES cells.*

3.5 Expression of HA-N19RhoA protein by Western blotting

I checked the protein expression from whole brain lysates from a litter of both EIIa-Cre^+/ $N19RhoA^+$ and Nestin-Cre^+/ $N19RhoA^+$ double transgenic mice. A proper-sized HA-tagged N19-RhoA protein was detected (Figure 25 and 26) with expression detectable at P3 onwards. The level of protein expression at P3, P6, P10 and P20 also was not different among the four time points, which suggested that the N19-RhoA protein expression level had already reached its highest level during this postnatal period. The level of protein expression in mice brain did not show any differences between the cross with EIIa-Cre and Nestin-Cre. However, the recombinant protein expression level of HA-tagged N19-RhoA was relatively lower than endogenous RhoA. Western blots using a dilution of different amount of protein revealed that endogenous RhoA protein is about 10-fold higher than recombinant protein in the whole brain lysate (Figure 27). Unexpectedly, I could not detect the HA-tagged N19-RhoA protein from embryos (Figure 28) or from neonates before P3, which was a surprise given that high expression of EGFP targeted at tau locus begins at 9.0 d.p.c. It is still possible that the recombinant protein is expressed at very low, undetectable levels in embryos, especially as there

were some background bands detected from the embryos' brain lysate near the expected recombinant proteins. Nevertheless, the inhibitory effects caused by such a low expression of N19-RhoA would not necessarily cause any effects in the development of the nervous system of embryos. Therefore, the recombinant protein was expressed but detected only after P3. This protein expression pattern motivated me to look at the effects of N19-RhoA in the nervous system at postnatal stages, although there was much less recombinant dominant negative RhoA than endogenous RhoA.

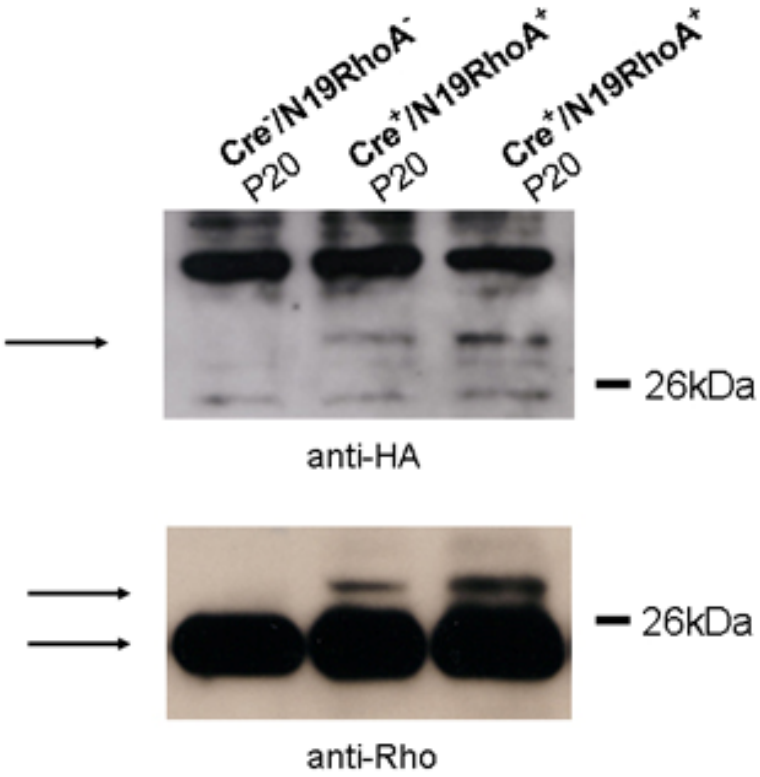

Figure 25. ***Protein expression analysis of whole brain lysate at postnatal day 20 (P20) using the anti-HA antibody and anti-RhoA antibody.*** *Western blots on membranes incubated with anti-HA antibody (1:1000) and with anti-RhoA antibody (1:500) overnight at 4℃. 20 µg proteins were loaded in each lane. The corresponding genotypes of the mice used for whole brain protein extraction are indicated above the lanes. Arrow in the blot of anti-HA antibody indicates the recombinant protein. Upper arrow indicates the recombinant RhoA and lower arrow indicates the endogenous RhoA in the blot of anti-Rho antibody. Cre^+: positive for a Cre gene; Cre^-: negativeve for a Cre gene; $N19RhoA^+$: positive for a dominant negative RhoA.gene.*

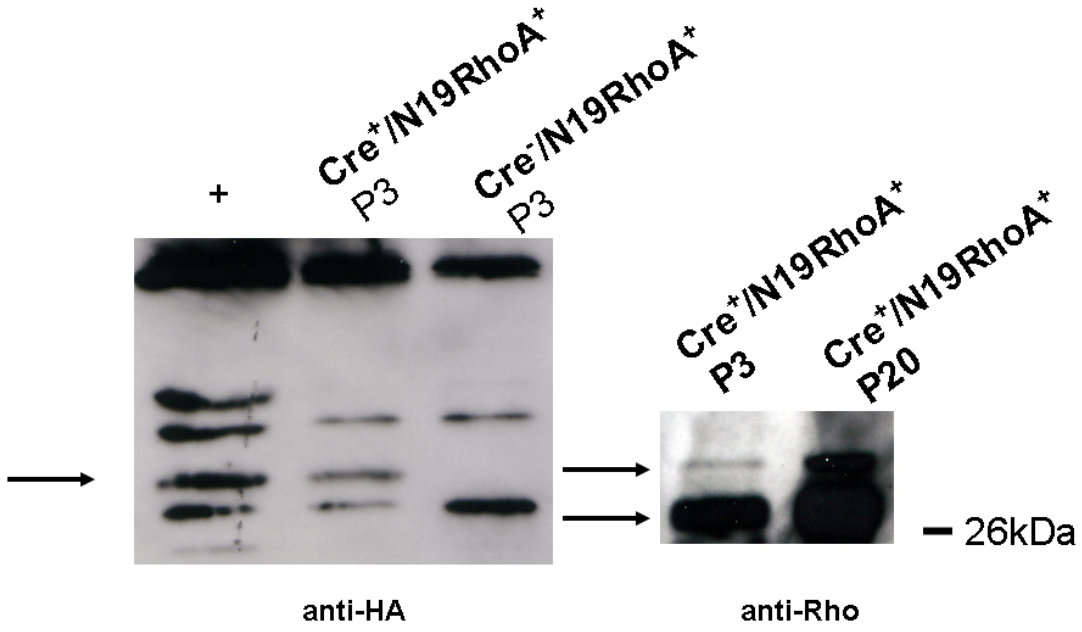

Figure 26. ***Protein expression analysis of whole brain lysate at postnatal day 3 (P3) using the anti-HA antibody and anti-RhoA antibody***. *The corresponding genotypes of the mice are indicated above the lanes. Arrow in the blot of anti-HA antibody indicates the recombinant protein. Upper arrow indicates the recombinant RhoA and lower arrow indicates the endogenous RhoA in the blot of anti-Rho antibody. Cre^+: positive for a Cre gene, $N19RhoA^+$; Cre^-: negativeve for a Cre gene, $N19RhoA^+$; positive for a dominant negative RhoA.gene.* ***+:*** *Protein lysate from Cre^+/ $N19RhoA^+$ at P20 same as in Figure 25.*

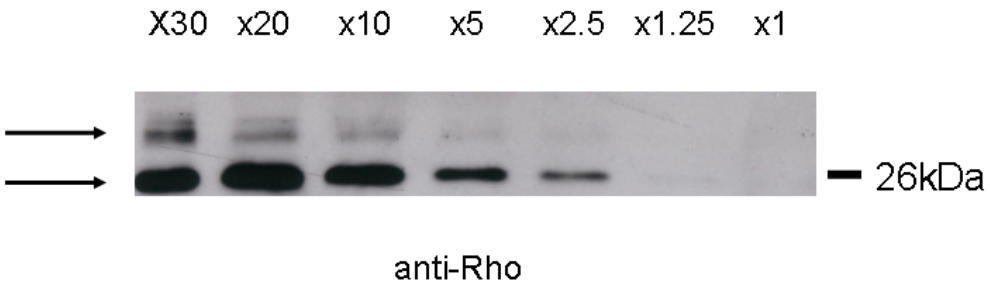

Figure 27. ***Dilution of Protein expression analysis of whole brain lysate from postnatal mice using the anti-RhoA antibody.*** *All protein lysate is from whole brain of Cre^+/ $N19RhoA^+$ at P20 same as in Figure 25. Upper arrow indicates the recombinant RhoA and lower arrow indicates the endogenous RhoA..*

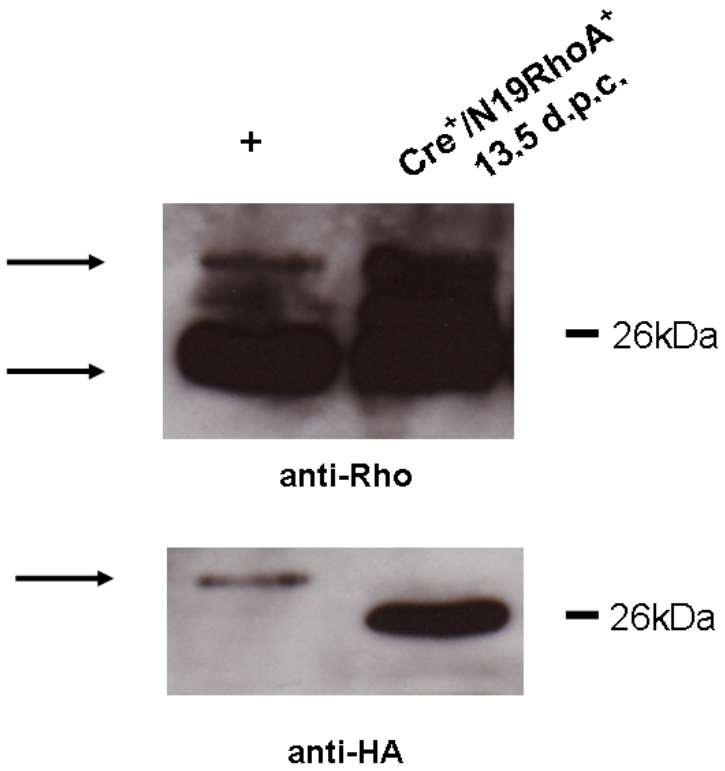

Figure 28. ***Protein expression analysis of whole brain lysate at 13.5 d.p.c. using the anti-HA antibody and anti-RhoA antibody***. *The corresponding genotype of the mouse is indicated above the lane. Arrow in the blot of anti-HA antibody indicates the recombinant protein. Upper arrow indicates the recombinant RhoA and lower arrow indicates the endogenous RhoA in the blot of anti-Rho antibody. Cre^+: positive for a Cre gene, $N19RhoA^+$; $N19RhoA^+$; positive for a dominant negative RhoA.gene.* **+:** *Protein lysate from Cre^+/ $N19RhoA^+$ at P20 same as in Figure 25.*

I checked if N19-RhoA became an insoluble protein by sonicating the pellets from the brains of P0 mice. Semaphorin3A (Sema3A) was hardly detected in the soluble fraction of protein extracts from P0 mice brain but was detected as an insoluble protein in these brain lysates, even though Sema3A were detected as soluble protein at the later stages (Morita *et al.*, 2006). However, there was no obvious N19-RhoA protein expression detected even in insoluble protein lysates, which indicated that there was no insoluble N19-RhoA protein expression at this stage either (Figure 29).

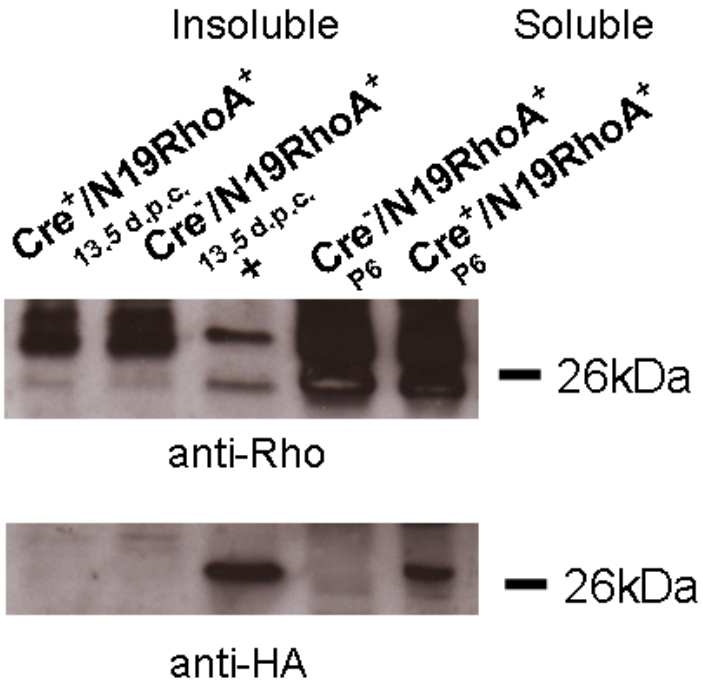

Figure 29. *Protein expression analysis of whole brain lysate in insoluble (at 13.5 d.p.c.) and soluble (P6) protein using the anti-RhoA and anti-HA antibody. The corresponding genotypes of the mice are indicated above the lanes. Cre$^+$: positive for a Cre gene, N19RhoA$^+$; Cre$^-$: negativeve for a Cre gene, N19RhoA$^+$; positive for a dominant negative RhoA.gene. +: HA-N19-RhoA expressed in HN10 cells.*

This result of the low protein expression together with the result of the 100% Cre recombinase efficiency suggests that the tau promoter is not as strong in its expression of the recombinant RhoA protein as the endogenous RhoA promoter in its expression of RhoA.

3.6 Peripheral nervous system in N19-RhoA mice

Even though we did not detect visible protein expression during embryogenesis, we initially analyzed initial nerve development in the central and peripheral nervous system using EIIa-Cre$^+$/ N19RhoA$^+$ double transgenic embryos, compared to either Cre$^-$/ N19RhoA$^+$, Cre$^+$/ N19RhoA$^-$, or Cre$^-$/ N19RhoA$^-$ embryos as a wild-type control by whole-mount staining using an anti-Neurofilament 165 kDa antibody (clone 2H3) which labels outgrowing nerves in the peripheral and central nervous system (Figure 30). We did not observe any major differences in the embryos at 12.0 d.p.c. in terms of outgrowth of peripheral neurons, suggesting that N19-RhoA seemed not to disturb the growth inhibitory signals such as secreted by Sema3A to cause the abnormality in the axonal projection pattern. It is possible that such a low expression or no expression of N19-RhoA protein in embryos did not cause any effects on the outgrowing nerves during the development of embryogenesis. Therefore, it is still possible that if there were much

more of N19-RhoA protein expressed in neurons, it may cause effects on the outgrowth of neurons.

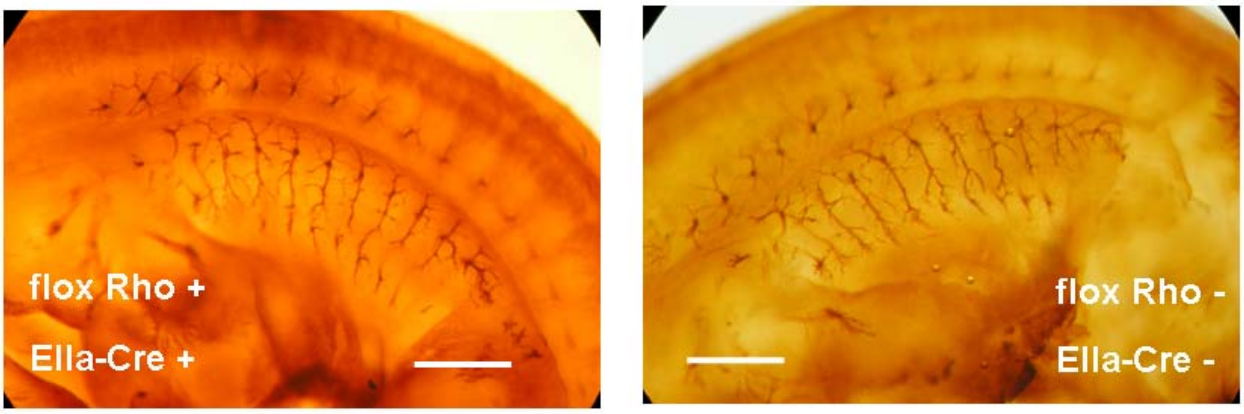

Figure 30. ***Whole-mount immunostainings of embryos at 11.5 d.p.c. using the 2H3 antibody, which recognized the neuronal specific protein β tubulin III.*** *Littermates of the same somite number were compared. Cre^{+}/ N19RhoA^{+} (right), Cre^{-}/ N19RhoA^{-} (left). Rostal is to the left, and dorsal is at the top of all panels. Scale bar, 1 mm.*

3.7 Axonal outgrowth in the cerebellar granular neurons from N19-RhoA mice

Cerebellar granule cells were prepared for culture from litters of EIIa-Cre^{+}/ N19RhoA^{+} double transgenic and Cre^{-}/ N19RhoA^{+} or Cre^{+}/ N19RhoA^{-} as wild-type mice at P5 and fixed with 4 % PFA at different time points to see the effects on the axonal outgrowth stained with TuJ1 antibody. Culture of cerebellar neurons of EIIa-Cre^{+}/ N19RhoA^{+} double transgenic mice showed no difference in axonal outgrowth or cell survival compared to of Cre^{+}/ N19RhoA^{-} or Cre^{+}/ N19RhoA^{-} mice (Figure 31).

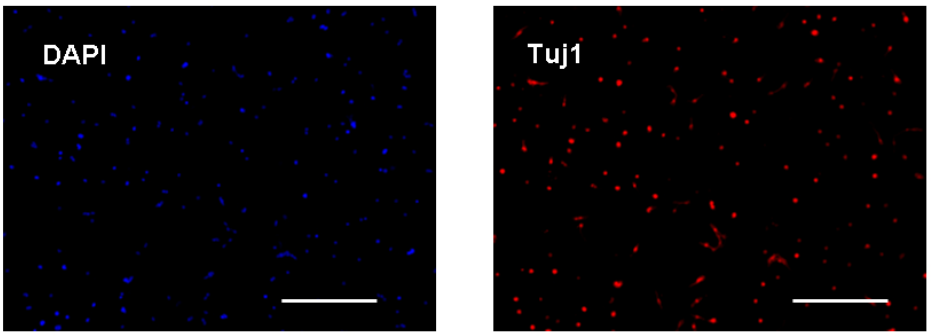

Cre+/N19RhoA-

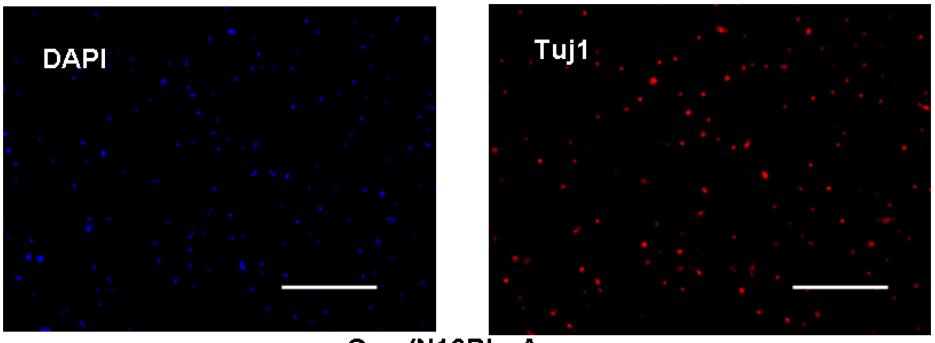

Cre+/N19RhoA+

24 hrs

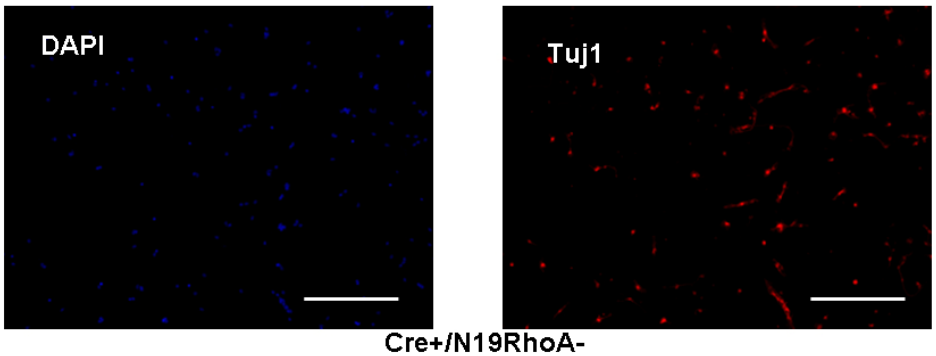

Cre+/N19RhoA-

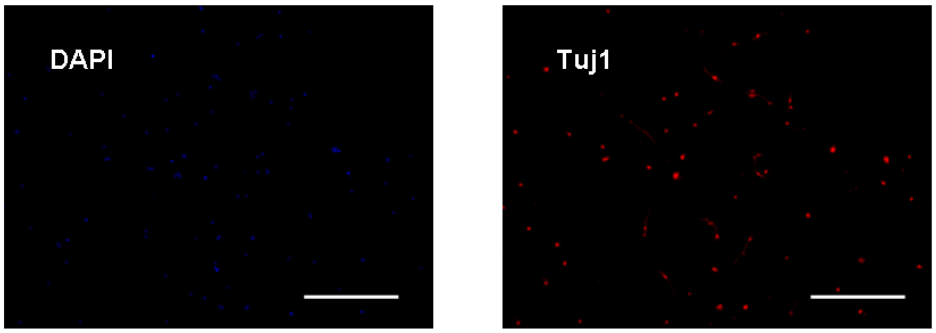

Cre+/N19RhoA+

48 hrs

Figure 31. ***Immunocytochemistry of CGN culture prepared from cerebellum of P5 mice.*** *They were fixed at 24 hrs (top 4 panels) and 48 hrs (bottom 4 panels) after plating. DAPI staining (left) and Tuj1 staining (right). Each corresponding genotype is indicated under the panels. Scale bar, 200 μm.*

The expression of recombinant N19-RhoA in the relatively pure cerebellar granular neuron cultures was also very low (data not shown). When I checked the protein expression of the whole brain without cerebellum, the protein expression levels did not differ between the one with cerebellum and without; this suggested that the expression of a dominant negative RhoA protein in cerebellum is not that high. This suggests that expression of dominant negative RhoA is higher in specific parts of the brain, and this prompted me to investigate the entire postnatal brain for potential defects.

3.8 Analysis of the brain in N19-RhoA mice

To investigate the significance of Rho regulation in postnatal brain, brains from postnatal mice were fixed and processed for frozen sectioning. We decided to examine the stages P21, P60 and P65 staining because of the recombinant protein expression detected at the postnatal stages before these stages. Hematoxylin stained nuclei blue with some metachromasia. Any major difference in the total number of cells was not observed in the brain section of Hematoxylin staining at P21, P60 and P65.

In order to avoid the possibility of sex differences, only female animals were compared for the brain analysis. The brain weight of the transgenic mice that have expressed a dominant negative RhoA (Cre^+/ $N19RhoA^+$) was about 11% smaller on average than the wild-type (Cre^+/ $N19RhoA^-$) (Figure 32). Even though there was no significant change in organization of cortex layer, the packing density of the cells varies between the transgenic mice that have expressed a dominant negative RhoA and the wild-type mice.

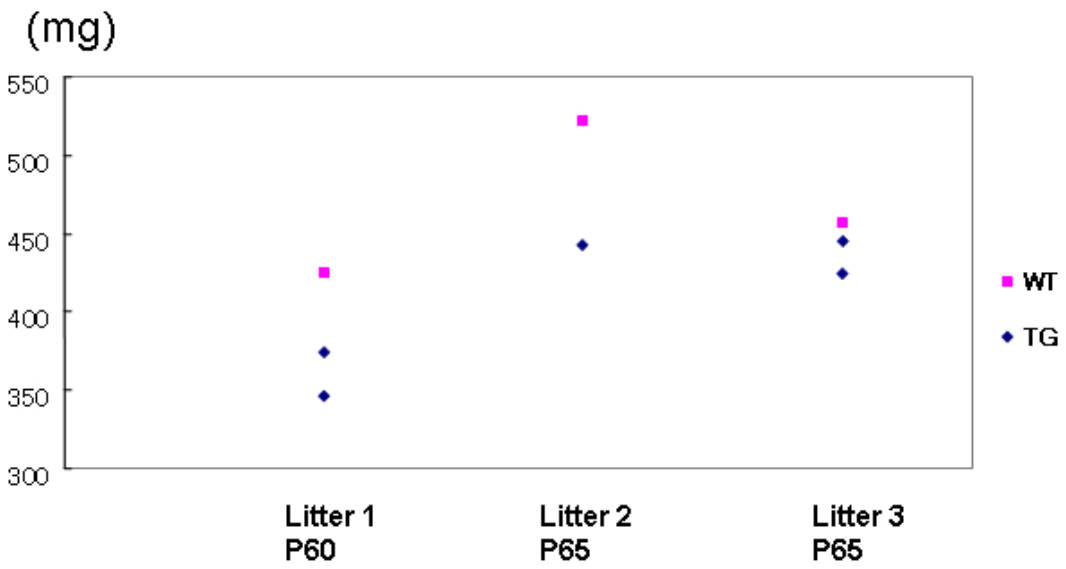

Figure 32. ***Brain weight of P60 and P65 mice.*** *Brain weight of the transgenic mice (TG) was smaller than the wild-type mice (WT). Brain weight was compared in the same litter.*

At P60 and P65, moreover, there are more severe involutions of the cells in specific area of layer IV in somatosensory cortex in the brain and clumping rather than a uniform distribution was seen in layer V (lamina ganglionaris) (Figure 33c). The involutions seem to be corresponding to the barrels in barrel cortex. The morphology of this barrel-like discontinuous pattern looks like a normal barrel but this pattern was observed continuously toward the posterior part of the brain only in double transgenic Cre^{+}/ $N19RhoA^{+}$ mouse. A barrel-like discontinuous pattern was observed from the anterior part of the brain at the very beginning of the hippocampus as also seen in wild-type mouse (Cre^{+}/ $N19RhoA^{-}$) but these structures continued to the posterior part of the hippocampus only in the double transgenic Cre^{+}/ $N19RhoA^{+}$ mouse brain. This observation indicated that there is an alternation in the layer IV, especially in the barrel cortex and implied that the barrels were extended toward the posterior part of the brain cortex.

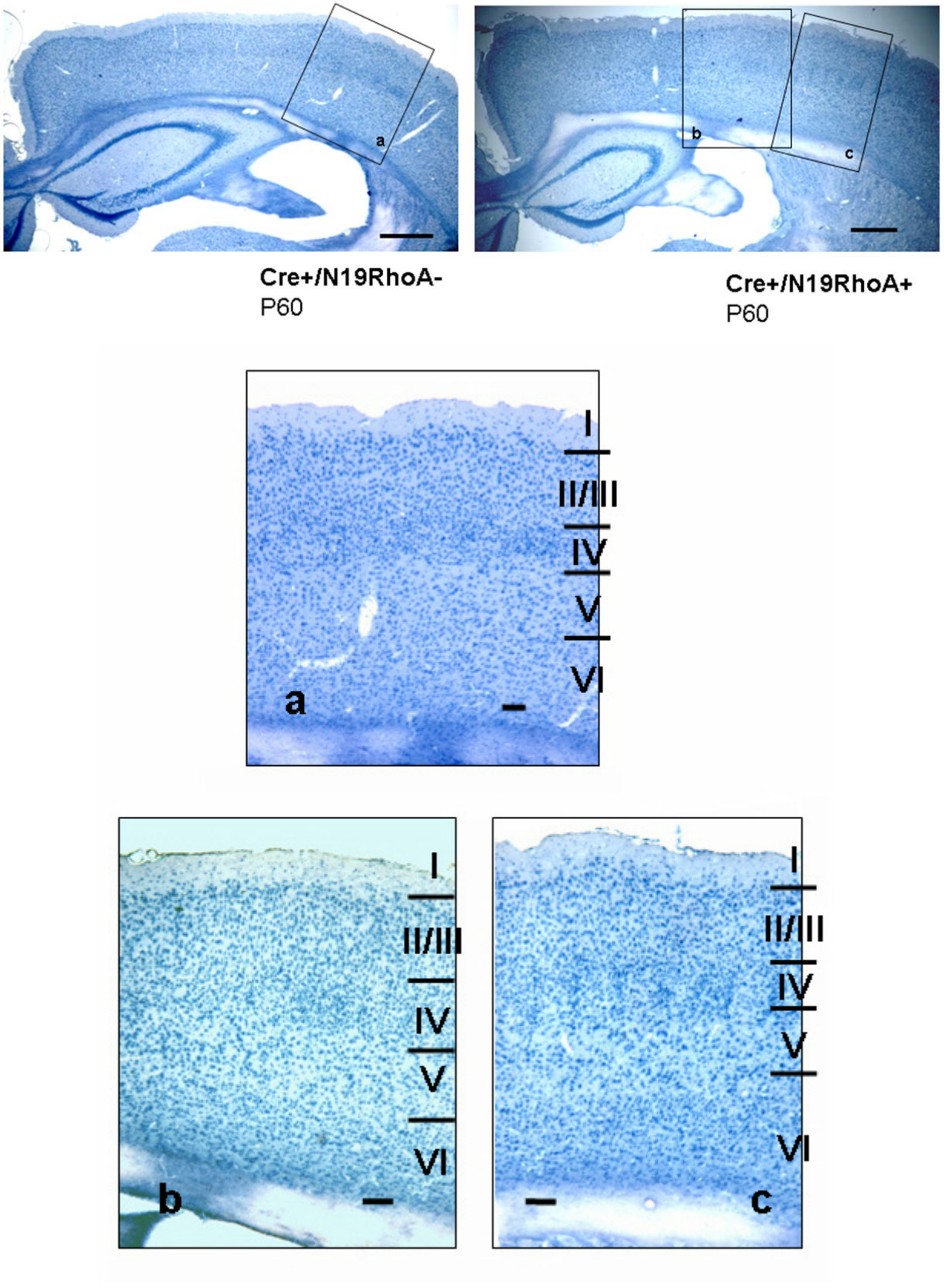

Figure 33. *Hematoxylin staining in coronal sections at the level of somatosensory cortex of wild-type (Cre^+/ $N19RhoA^-$) (left on the top panel) and transgenic (Cre^+/ $N19RhoA^+$) (right on the top panel) mice brain at P60. The*

bottom panels show the higher magnification of corresponding area of a, b, and c in each top panel. Scale bars, 0.5 mm (top two panels), 0.1 mm (bottom three panels)

In order to see if these phenotypes were reflective of a change in the number and distribution of neurons, we stained brain sections with an antibody that specifically recognizes neurons, anti-NeuN. Brain sections stained with the anti-NeuN antibody showed that there is a significant difference between layer IV and V of the cortex (Figure 34). Average number of neurons in layer IV was 14.9 neurons/ 100 μm^2 in double transgenic mouse and 9.6 neurons/100 μm^2 in wild-type mouse and in layer V was 5.5 neurons/ 100 μm^2 in double transgenic mouse and 8.2 neurons/ 100 μm^2 in wild-type (Figure 35A). The density of neuron in layer IV, the density was increased about 35.6% in double transgenic mouse than in wild-type mouse while in layer V and the density was decreased about 32.4% in double transgenic mouse than in wild-type (Figure 34 and 35B).

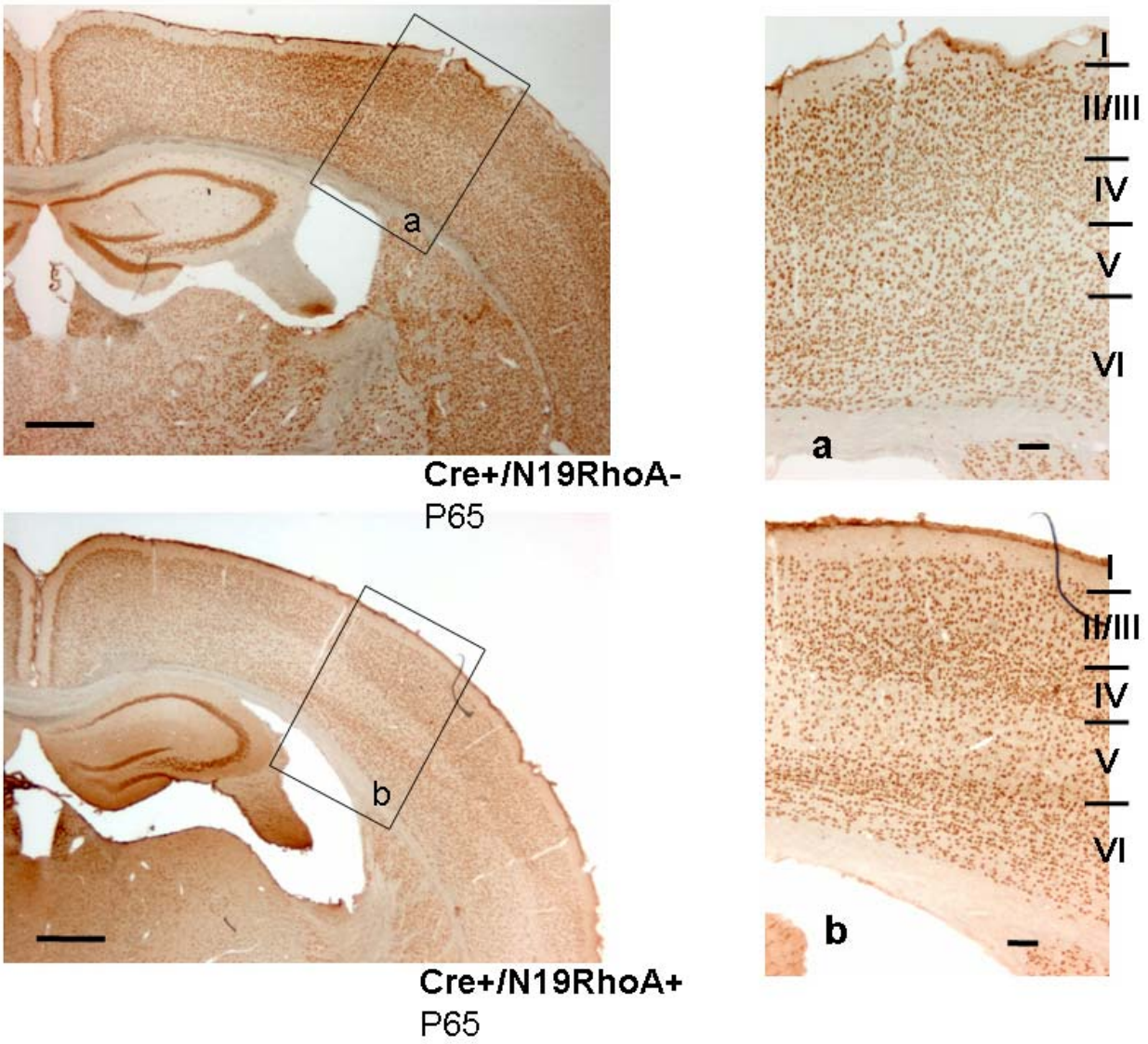

Figure 34. *NeuN immunohistochemistry in coronal sections at the level of somatosensory cortex of wild-type (Cre^{+}/ $N19RhoA^{-}$) (top) and transgenic (Cre^{+}/ $N19RhoA^{+}$) (bottom) mice brain at P65. The right panels show the higher magnification of corresponding area of a and b in each right panel. Scale bars, 0.5 mm (left panels), 0.1 mm (right panels).*

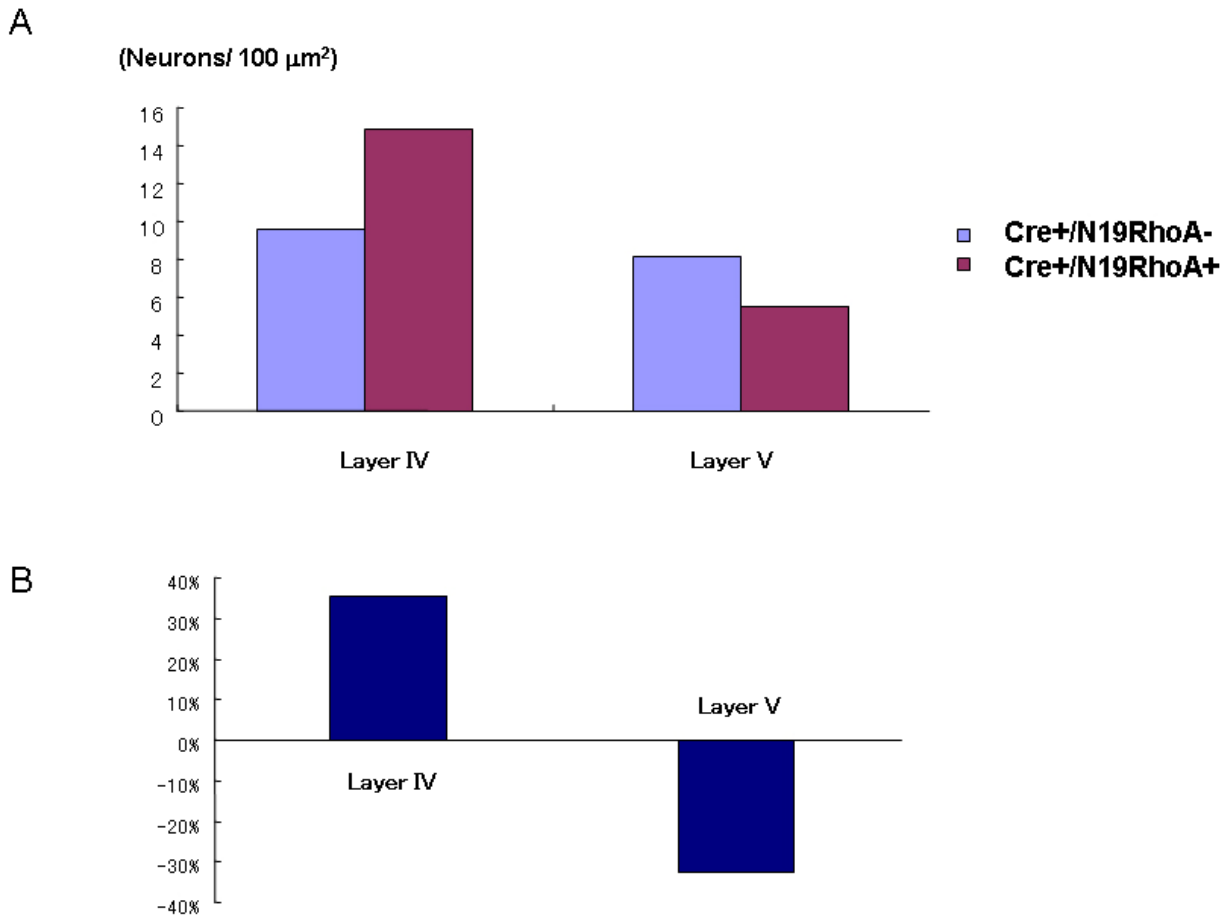

Figure 35. *Quantification of the number of neurons in layer IV and V from NeuN immunohistochemistry in coronal sections at the level of somatosensory cortex of wild-type (Cre^+/ $N19RhoA^-$) and transgenic (Cre^+/ $N19RhoA^+$) mice brain at P65.* **A.** *The average number of neurons per 100 μm^2. Average number of neurons in layer IV was 14.9 neurons/ 100 μm^2 in double transgenic mouse and 9.6 neurons/ 100 μm^2 in wild-type mouse. In layer V, 5.5 neurons/ 100 μm^2 in double transgenic mouse and 8.2 neurons/ 100 μm^2 in wild-type mouse.* **B.** *The relative percentages of the number of neurons in transgenic mouse compared to the one in wild-type mouse. In layer IV, the number of neurons in transgenic mice was increased in 35.6% and in layer V, the number of neurons in transgenic mouse was decreased in 32.4% compared to the wild-type mouse.*

3.9 Generation of EGFP fusion C3 transferase transgenic mice

By homologous recombination in embryonic stem (ES) cells, we generated mice expressing an EGFP-C3 gene fusion protein downstream of a *stop cassette* flanked by two *loxP* sites targeted at the tau locus. The targeting frequency of ES cells in total analysis was 25%. The targeted ES cells were injected into the blastocysts by Frank Zimmermann at the Interfakultaere Biomedizinische Forschungseinrichtung, University of Heidelberg and 8 chimeric males were born. Tail DNAs from heterozygous transgenic offspring were genotyped by *Bam*HI digestion and hybridized with the 5' external probe: a 2.9-kb band was produced together with the 8.8-kb

wild-type (Figure 36). Thereby, the EGFP-C3 construct has passed through the germline of chimeric males. The chimeric EGFP-C3 male mice are healthy, and breed normally; mutants are obtained in the expected Mendelian ratio.

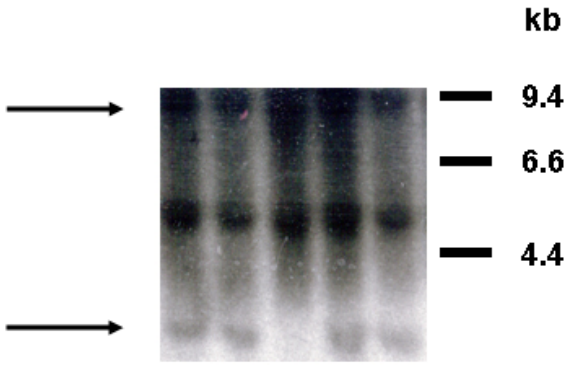

Figure 36. *Southern blot analysis of genomic DNAs from EGFP-C3 transgenic mice following BamHI digestion and hybridization with the 5' external probes. Wild-type displays a 8.8-kb allele. Targeting of EGFP-C3 yielded a 2.9-kb band.*

3.10 Generation of V14-RhoA transgenic mice

By homologous recombination in embryonic stem (ES) cells, we generated mice expressing a V14-RhoA variant downstream of a *stop cassette* flanked by two *loxP* sites targeted at tau locus. Targeting frequency of ES cells in total analysis was 12%. Targeted ES cells were injected into the blastocysto by Frank Zimmermann at the Interfakultaere Biomedizinische Forschungseinrichtung, University of Heidelberg and 3 chimeric males were born. The chimeric V14-RhoA male mice are healthy, but did not breed well. My first Southern blot analysis showed that V14-RhoA contruct did not go germ line even though PCR analysis showed the positive result (data not shown).

4 DISCUSSION

4.1 Generation of N19-RhoA mouse

We were concerned that the long-term expression of Rho variants in all neurons of the mouse could cause serious toxic effects and make the transgenic mouse infertile or inviable if we simply inserted the Rho variants directly into the tau locus, as had been done before with EGFP. Therefore, I decided to place the transcriptional *stop cassette* upstream of each gene that I wanted to express. This construct was then inserted into Exon 1 of the tau locus. In the resulting mouse line, transcription from the endogenous tau promoter was prematurely terminated by the transcriptional *stop cassette*. After crossing the transgenic mouse to a Cre-expressing mouse line, the *stop cassette* was removed, and this then allowed for the neuron-specific expression of the construct of interest. Southern blot analysis using genomic DNA from cerebellar granular neurons confirmed that the transcriptional *stop cassette* was properly removed with 100% efficiency by Cre recombinase. However, HA-tagged N19-RhoA recombinant protein expression was observed only at very low levels and only in postnatal mice. This low protein expression was unexpected because tau is known to be highly expressed in neurons (Binder *et al.*, 1995). Also, very strong EGFP expression was seen in neurons when inserted into the tau locus (Tucker *et al*., 1999) and the mouse line Tau-MeCP2, in which the *Mecp2* cDNA was placed under the control of the endogenous promoter of Tau, where the tau-MeCP2 transcript was expressed at a level 2- to 4-times higher than endogenous MeCP2 (Luikenhuis *et al.*, 2004). Cre recombinase completely removed the transcriptional stop cassette with 100% efficiency so that the gene can get expressed; therefore the Tau gene promoter was not strong enough to express high levels of the dominant negative N19-RhoA, when compared to endogenous levels of RhoA expression. There are many non-neuronal cell types in the brain that are expected to only express endogenous Rho and not the N19-RhoA construct, and therefore Western blot examination of whole brain lysates should underestimate the amount of N19-Rho being expressed in neurons, compared to endogenous Rho. Nevertheless, examination of a pure neuronal population (isolated cerebellar granule neurons) did not reveal a higher level of N19-RhoA expression compared to endogenous RhoA. It could be the case that this cell type does not express high levels of tau either, but this is still unclear. In any case, the presence of a phenotype in the cortex suggests that certain neuronal cell types either express a higher level of

the N19-RhoA construct, or a lower level of endogenous Rho transcripts. This remains to be investigated.

4.2 Peripheral nervous system in Cre$^+$/ N19RhoA$^+$ mice

Members of the Rho family of small GTPases are involved in cytoskeletal rearrangements in axons: Cdc42 and Rac1 play a role in filopodia and lamellipodia formation in growth cones and RhoA in growth cone collapse and neurite retraction (Gallo and Letourneau, 2004). Therefore, we expected to see effects upon the peripheral nervous system in Cre$^+$/ N19RhoA$^+$ mice during embryogenesis. However, we did not observe any phenotypic changes in the growth cone in the cerebellar granular neurons culture and in nerve outgrowth in double transgenic embryos by expression of dominant negative RhoA. Because of such a low protein expression of N19-RhoA, it is quite possible that the recombinant protein was located only in the soma without diffusion of the protein to the growth cone.

The neurofilament whole-mount staining of Cre$^+$/ N19RhoA$^+$ embryos 10.5-13.5 d.p.c. did not show any significant alternations in the developing peripheral nervous system when compared with the wild-type embryos. We initially expected that outgrowth would be more diverse and extensive due to the inhibition of the Sema3A repulsive signal by inhibiting Rho GTPase activity. Sema3A, a secreted guidance cue, primarily repels axons from inappropriate targets, and has been suggested to cause growth cone collapse. In DRG neurons, growth cone collapse in response to Sema3A requires the RhoA effector ROCK, which suggested RhoA activation in Sema3A signalling (Dontchev and Letourneau, 2002), and Sema3A deficient mice show severe axonal projection patterns in the peripheral nervous system during embryogenesis, including in the trigeminal, facial vagus, accessory, and glossopharyngeal nerves (Taniguchi *et al.*, 1997). Thereby, inhibition of Rho activity by expressing N19-RhoA in mouse embryos was expected to trigger axons from the DRG to grow out into non-permissive areas because of the inhibition of the Rho-based effect signalled by Sema3A. At this point, there are two possible reasons why no phenotype was observed in the whole-mount staining during nerve outgrowth. One possibility is that inhibition of Rho activity may not play an important role in the peripheral nervous development of embryos because of other compensatory molecules. Another reason is that undetectable protein expression levels of dominant negative RhoA, as revealed by Western blot analysis, did not affect the nervous system. Knowing the role of Rho GTPases in axonal outgrowth previously shown *in vitro*, it is most likely that the very low expression of N19-RhoA did not cause severe changes in the early peripheral nervous system in embryos.

4.3 Axonal outgrowth of cerebellar granular neurons in Cre^{+}/ $N19RhoA^{+}$ mice

As I did not see any effects upon peripheral nerve outgrowth in embryos, and as I could detect N19-RhoA protein expression in postnatal animals, I checked if there is any effect on the axonal outgrowth in cerebellar granular cultures prepared from N19-RhoA expressing mice at postnatal day 5 (P5). Because the recombinant protein N19-RhoA is expressed in brain at P5, the cerebellar granular culture was prepared from the cerebellum at P5. However, no significant effects upon the neurite outgrowth from Cre^{+}/ $N19RhoA^{+}$ mice were seen compared to neurons prepared from the Cre^{-}/ $N19RhoA^{+}$ or Cre^{+}/ $N19RhoA^{-}$ mice (Figure 31). I speculate that a low protein expression of dominant negative RhoA, which was confirmed by a Western blot upon protein lysates made from the cerebellar granule neurons, did not bring a high inhibition of Rho activity to modulate neurite outgrowth. Much higher inhibition of Rho activity is probably required to augment axonal processes.

4.4 Apoptosis in N19-RhoA mice

A previously-published analysis using mice expressing a dominant-negative form for RhoA showed an increase of apoptosis in spinal motor neurons during embryogenesis (Kobayashi *et al.*, 2004). However, because there was no detectable protein expression of dominant negative form of RhoA in embryos, it was probable that the recombinant RhoA did not affect the cell survival in the peripheral nervous system in embryos that were our double transgenic Cre^{+}/ $N19RhoA^{+}$. Since inhibition of Rho, Rac, and Cdc42 by *Clostridium difficile* toxin B induced cerebellar granular neuron apoptosis *in vitro* by c-Jun phosphorylation (Linseman *et al.*, 2001), I checked the number of granule neurons in cerebellum in culture. However, the total number of neurons in cerebellar granular neurons did not show any significant change, suggesting that there was no cell death or apoptosis caused by such a low expression of dominant negative RhoA. However, RhoA-based apoptosis may play a role in the cortex, as discussed in the next section.

4.5 Preliminary observation on alternations in cortex of N19-RhoA mice

Because of the protein expression of a dominant negative RhoA in postnatal stages in brain, I analyzed the long-term effects of dominant negative RhoA expression in the cortex. I first noticed that there are more severe involutions in specific areas of somatosensory cortex in brain at P60 as well as at P65 when they are stained with Hematoxylin. Further, NeuN staining showed that there is a 35.6 % reduction of neurons in layer V and a 32.4 % increase of neurons in layer IV in the mouse brain expressing a dominant negative RhoA. One possible reason for the reduction of the neurons in layer V is that there is an increase in cell death in neurons of layer

V, since N19-RhoA expression in mice has been shown to cause apoptosis in motor neurons in spinal cord during early embryonic development (Kobayashi *et al.*, 2004). However, if the apoptosis occurs in neurons in layer V, one might expect that it occurs in all neurons, not only in neurons in a selective area of cortex. The difference in the density of neurons could also come from defects in the migration process, in that the stop signals to form the proper layers are somehow misinterpreted during migration, in that neurons that are supposed to stop in layer V, which is formed before layer IV during cortical development, continue to migrate and stop in layer IV. The same could hold true for neurons destined for layer II or III, which form after layer IV. In this scenario, neurons destined for layer II and/or III would stop prematurely in layer IV. However, I did not find any significant reduction in the number of neurons in these two layers, though a subtle reduction may be hard to see. In order to resolve these two possibilities, it would be useful to examine layer IV with markers specific for neurons of layer II/III and layer V.

Another possible reason is that cortical interneurons do not properly migrate to layers IV and V, as cortical interneurons are known to proceed along tangential migratory paths to reach the cortex during development (Nadarajah *et al.*, 2003). If the interneurons do not migrate properly from layer IV to layer V, the accumulation of neurons in layer IV could be seen.

Furthermore, a barrel-like discontinuous pattern is more extended toward the posterior part of the cortex in the mice expressing a dominant negative RhoA. Therefore, the formation of barrel cortex may also be affected. The aberrant accumulation of neurons in layer IV could in turn cause defects during the formation of barrels.

Preliminary measurements also indicate that transgenic mice expressing a dominant negative RhoA have smaller brains than wild-type littermates. However, I did not observe any major architectural changes in the cortex. The reduction of the brain size may be related to the alterations in the numbers of neurons in the cortex and possibly other brain areas that remain to be investigated.

In the reeler mouse mutant, despite the alteration in the positioning of cortical neurons in that the cortical plate developed under the subplate, therefore preventing the normal “inside-out” cell migration (reviewed by Olson and Walsh, 2002), the neuronal roles are proper to each corresponding layer (Polleux *et al.*, 1998; Tarabykin *et al.*, 2001). The positioning of neurons in each layer in our double transgenic mice were normal, consisting of six layers, and the functional role may not be altered by the inhibition of Rho activity. However, it will be interesting to investigate the functional outcome of the increase of the neurons in layer IV and the reduction of the neurons in layer V.

The preliminary data observed in the cortex of our double transgenic mice need to be confirmed. Inhibition of Rho activity by expressing a dominant negative RhoA is possibly involved in the formation of cortical layers, migration of neurons in the cortex, innervation of axons from the thalamus, formation and organization of barrels, and / or apoptosis of neurons in cortex.

4.6 Generation of EGFP-C3 and V14-RhoA mice

From the Rhotekin pulldown assay, it was assumed that C3 is more effective than N19-RhoA in inhibiting Rho GTPase activity. From my first Southern blot analysis using tail genomic DNAs from EGFP-C3 mice, I have shown that EGFP-C3 line has gone through the germline. However, the PCR conditions for genotyping have not yet been established for the EGFP-C3 line. On the other hand, my first Southern blot analysis using the tail genomic DNAs from V14-RhoA mice show that the V14-RhoA construct has not passed through the germline of chimeric males, even though the PCR analysis for genotyping showed a positive result. The germline transmission of both the EGFP-C3 and the V14-RhoA mouse lines needs to be confirmed with Southern blot analysis.

4.7 Summary and future plans

I have generated two different transgenic mice lines, N19-RhoA and EGFP-C3, whose expression can be induced using the Cre-loxP recombination system. This Cre-loxP system can elucidate the *in vivo* role of the Rho signaling pathways in the development of neurons and this system will provide a useful experimental tool to study the functions of Rho GTPases in mice development, physiology, and pathology. But this system needs to be improved to have higher protein expression of variant of Rho by either generating homozygous Cre^{+}/ $N19RhoA^{+}$ mice or employing a tau promoter expression vector, in which even higher levels of expression can be observed.

Rho GTPases are involved in a wide variety of process in different cell types and without question in growth cone regulation. However, it also seems obvious that Rho GTPases function as a common denominator in many pathways, similar to a Ras or a MAP kinase. Also, the activity balance between the GEFs and GAPs is important in the regulation of Rho GTPases suggesting therefore a role for them in axonal outgrowth and in neuronal development. Therefore, what is determinant for the phenotype is probably the other upstream or downstream effectors. Rho GTPases are the central signals, but it is the other signal proteins like Sema3A,

Rho kinase, or neurotrophins that determine how that signal is interpreted in each cell type context.

Since the protein expression level was not detectable during embryogenesis driven by the endogenous tau promoter in our transgenic mice, the analysis of the neurite outgrowth in embryo in our mice did not show any phenotypic changes. Even though our initial plan was to look at the neuronal outgrowth and growth cone direction caused by modifiers of Rho GTPase activity, we decided to look at the consequence of the long-term inhibition of Rho in adult brain. Our first observation of abnormality in the brain expressing N19-RhoA suggested that a low expression of dominant negative RhoA affected neuronal development in cortex. There is an increase of neurons in layer IV and a decrease in layer V of cortex in double transgenic mice. The barrel formation and/or the positioning of barrels in cortex may also be altered. The alteration of barrel formation and / or the positioning of barrels could be due to the alteration of migratory mechanism in cortex. The total protein expression levels of the brain between without and with cerebellum did not differ between them, suggesting that the dominant negative RhoA expression in cerebellum was not high. It is also important to define the specific regions of brain where the N19-RhoA most expresses in brain.

My first southern blot analysis for EGFP-C3 line showed that they have passed through the germline. However, I have not established the PCR genotyping condition for the EGFP-C3 line. On the other hand, a constitutively active RhoA (V14-RhoA), mouse line showed positive results by PCR analysis that they contain V14-RhoA. However, Southern blot analysis has not shown that the V14-RhoA has been passed through germline. These contradictory results of V14-RhoA line need to be clarified by Southern blot analysis to confirm germline transmission.

Since the C3 transferase is more effective in inhibiting Rho GTPase activity than dominant negative RhoA, it is possible that EGFP-C3 mice could show stronger effects and phenotypes on axonal outgrowth or in brain cortex than dominant negative RhoA (N19-RhoA) mice. From the low protein expression of N19-RhoA driven by tau endogenous promoter, I expect that the protein expression of EGFP-C3 driven by tau endogenous promoter will be very low. Therefore, it would be necessary to analyze the long-term inhibition of Rho activity by C3 transferase in adult mice. It will be interesting to compare the phenotypes in brain between a dominant negative RhoA and C3 transferase.

By the same reasoning, protein expression of a constitutively active RhoA (V14-RhoA) driven by the tau promoter would be also low, and it would be necessary to analyze the long-term effects in the brain. However, a constitutively active RhoA may cause stronger phenotypes because it activates the downstream of Rho, for instance ROCK or mDia. Overexpression of

constitutively active RhoA (V14-RhoA) may reduce or abrogate nerve extension, and/or perhaps impair neuronal migration cortex formation.

My preliminary observation in a dominant negative RhoA mice brain showed that RhoA may play an important role during formation of the cortex layer, possibly in the barrel formation in layer IV and the neurons in layer V. This is the first time that RhoA has been shown to play a role in the formation of cortical layers and/or migration of neurons in the cortex *in vivo*. However, there are a lot of questions that need to be answered. What is the consequence of having a smaller brain in the transgenic mice, if any? Why does the inhibition of Rho activity make the brain smaller even though the architecture of brain is reserved? What are the mechanisms for the difference in neuron number in each layer of cortex? Are Rho GTPases involved in the migratory mechanism? What is the functional role of Rho GTPases in barrel formation? How was the change of the barrels affected from the whisker? When do these phenotypes occur? Are these phenotypes causes by apoptosis? Is it possible to rescue these phenotypes by crossing to V14-RhoA? Or how does this affect the function in brain? Not only in cortex, there are probably other areas in the brain that might be affected by the inhibition of Rho activity, for example in the hippocampus or thalamus.

5 APPENDIX

The Appendix contains supplementary material on methods and probes relating to gene targeting/homologous recombination.

5.1 Rhotekin beads preparation

The Rhotekin-beads used for the Rhotekin pulldown assay were prepared by Julia Hoffmann in our laboratory. Rhotekin expressing bacteria were harvested in 20 ml LB media with Ampicillin (100 μg/ml) and Chloramphenical (34 μg/ml) on a shaker at 37 °C overnight. The following day, 2-4 ml of overnight culture was added in 4 x 500 ml LB media with Ampicillin and Chloramphenicol on a shaker at 37 °C and induced with 500 μl of 0.5 M IPTG until the OD_{600} became between 0.7 and 0.8, followed by 3 hrs incubation at 30 °C on shaker. The bacterial cultures were placed in 500 ml tubes, centrifuged for 10 min at 4000 rpm, and the pellets were washed twice with 200 ml of cold 1x PBS. The pellets were resuspended and centrifuged for 10 min at 4000 rpm at 4 °C, and the pellets were resuspended in 20 ml lysis buffer and 5 ml was placed in four 15 ml Falcon-tubes. The cells were sonicated for 15 sec six times approximately at 130 W, 500 μl of 10 % Triton X-100 was added per tube to make the final concentration of 1 % Triton X-100, and incubated for 15 min on ice, rocking. Lysates were decanted in 8 Ultracentrifuge tubes on ice and centrifuged for 12 min at 27,000 rpm (UZ, g100ATS-0112 in Hitachi himacCS 100fx). 1.3 ml of the beads (Glutathione Sepharose 4B, Amersham) for 2 L of medium was washed in 50 ml tube twice with 15 ml of 1x PBS at 4 °C. Beads were centrifuged at 1,000 rpm at 2 °C for 1 min. Rhotekin lysates were added to the beads and incubated for 45 min, shaking horizontally to avoid making bubbles. The beads were washed with 20 ml of cold wash buffer (see the Appendix 5.6.2 “Wash buffer for Rhotekin assay”) for 1 min at 1,000 rpm at 2 °C and then the supernatant was removed. Beads were resolved in 20 ml wash buffer + 10 % Glycerol and aliquot beads were kept at -80 °C. 200 μl or 400 μl of Rhotekin beads was used for each incubation in the pulldown assay.

5.2 Further details on construction of the N19-RhoA, V14-RhoA, and EGFP-C3 targeting vectors

The tau targeting vector backbone, termed pSilvia (Figure 37-4), and a *stop cassette* construct LSL/pGEM (Figure 37-3) were gifts from Dr. Silvia Arber. The plasmid pSilvia was generated to target to the tau locus, such that any given cDNA can be inserted into Exon 1. cDNAs of interest lie downstream of a *stop cassette* flanked by loxP sites. The plasmid pLSL/pGEM contains a *stop cassette*, which consists of a transcriptional termination signal and a neomycin resistance gene cassette as a positive selection marker for embryonic stem (ES) cell culture. After insertion of the polylinker site of PWL512p into the *Sal*I site of the LSL/pGEM plasmid, termed pPWL512/LSL/pGEM (Figure 37-1), each cDNA of interest could be inserted into the unique *Eco*RI site of the pPWL512/LSL/pGEM plasmid (Figure 37-2). Each plasmid in pPWL512/LSL/pGEM was finally subcloned into pSilvia using a unique *Asc*I site The insert was then excised with *EcoR*I and subcloned into the PWL512/LSL/pGEM vector (Figure 37-3). They were inserted into the unique *Asc*I site of pSilvia and linearized with *Pme*I (Figure 37-4).

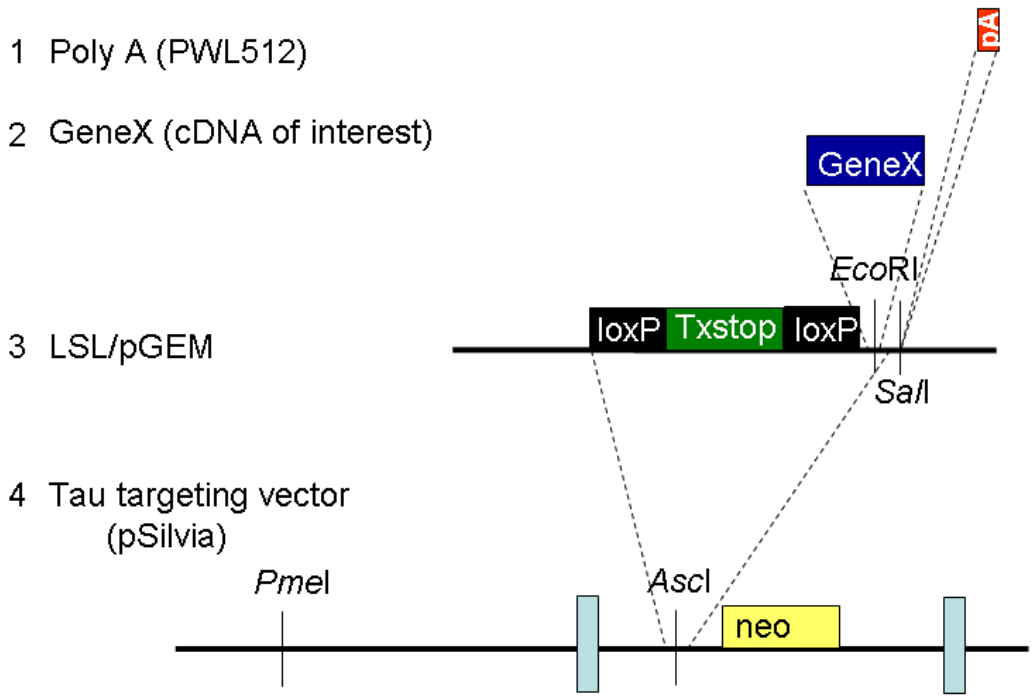

Figure 37. ***Cloning strategy of targeting construct:*** *1. poly adenylation site and 2. cDNA of interest were inserted into* a *stop cassette construct LSL/pGEM vector. 4. Each plasmid in pPWL512/LSL/pGEM was finally subcloned into the tau targeting vector backbone, pSilvia.*

The homologous recombination technique was invented by Cappechi and Smithies independently; (reviewed by Capecchi, 2005; Smithies, 2005). The basic protocol is still the same as the original techniques and was merged with the embryonic stem cell biology discovered by Martin Evans (Evans and Kaufman, 1981). The total technology includes

making the targeting vector by subcloning relevant fragments, inserting a removable transcriptional *stop cassette* and gene expression, and characterizing hybridization probes to detect homologous gene targeting by Southern blot analysis. Once the targeting vectors were constructed, the targeting vectors were transfected into ES cells and screening undertaken for homologous events.

5.3 Probes for Southern blot analysis

5.3.1 5' and 3' external Tau genomic probe

The 5' external probe is a 420 bp fragment located immediately upstream of the 5' end of the 8 Kb *Eco*RI-*Eco*RI fragment used for the construction of the tau targeting vector.

5.3.2 RhoA probe

The RhoA probe consists of an approximately 600 bp fragment obtained by double digestion with *Not*I and *Sal*I of N19-RhoA in Topo vector plasmid and purified by gel extraction.

5.4 Mouse embryonic stem cell culture

Electroporated cells were cultured on mouse fibroblasts inactivated with mitomycin C (Sigma) in ES cell Medium (See the Appendix 5.5 "Medium for cell cultures"). Electroporated cells were grown in ES cell medium supplemented with G418 (380 μg/ml) for selection. Individual resistant colonies were picked 6-8 days after electroporation and split into 96 well feeder plates and 24-well plates (coated with 0.1% gelatine) for expansion. After 2-3 days, the clones cultured in 24-well MEF plates were frozen in ES cell medium containing 10% DMSO and 25% FCS and stored in liquid nitrogen. The clones cultured on gelatine plates were expanded for genomic DNA isolation.

5.5 Medium for cell cultures

MEF medium

DMEM Glutamax, High Glucose (Invitrogen)
10% NCS (newborn calf serum)
2 mM L-Glutamate (Invitrogen)

ES Medium

DMEM Glutamax, High Glucose (Invitrogen)

2 mM L-Glutamine (Invitrogen)
0.15 mM ß-mercaptoethanol (Sigma)
0.1 mM non essential amino acids (Invitrogen)
10% FBS (fetal bovine serum)
1000 U/ml leukaemia inhibitory factor (LIF) (Invitrogen)
50 µg/ml P/S (penicillin/streptomycin) (Invitrogen)

1x PBS for cell culture
140 mM NaCl
3 mM KCl
10 mM $NaHPO_4$*(H_2O)
2mM KH_2PO_4

Cerebellar granular cell culture Medium (1-8)

Protocol given from Dr. Haruhiko Bito (Bito *et al.*, 2000) was modified after optimizing the culture condition

1. MEM-GT

For each 500 ml of MEM (Life Technologies)
add 2.5 g Glucose, 100 mg $NaHCO_3$, 50 mg Transferrin (Calbiochem #616420)

2. HANK's salt solution (HANKS(-))

HANKS Balanced Salt Solution (Sigma, no biocarbonate, no calcium, no magnesium), add 350 mg/L $NaHCO_3$, pH. 7.4.

3. Digestion solution

137 mM NaCl, 5 mM KCl, 7 mM Na_2HPO_4, 25 mM HEPES, pH. 7.2

4. Dissociation solution

HANK's salt solution + 12 mM $MgSO_4$*($7H_20$)

5. 20% FCS/HANKS(-)

6. 10% FCS/MEM

10% FCS, 2 mM Glutamine, 25 µg/ml of insulin, 1x B-27 supplement in MEM-GT

7. 5% FCS/MEM + Ara-C

5% FCS, 0.5 mM Glutamine, 25 µg/ml insulin, 1x B-27 supplement, 4 µM Cytosine arabinoside (Ara-C) (Sigma) in MEM-GT

8. 5% FCS/MEM - Ara C

5% FCS, 0.5 mM Glutamine, 25 µg/ml insulin stock, 1x B-27 supplement in MEM-GT

5.6 Buffers

5.6.1 Lysis buffer for Rhotekin beads preparation and Rhotekin pulldown assay

50 mM Tris-HCl, pH 7.4
150 mM NaCl
5 mM $MgCl_2$
1 mM DTT
*10µg/ml Aprotinin
*10µg/ml Leupeptin
*10µg/ml PMSF
* freshly added just prior to use

5.6.2 Wash buffer for Rhotekin beads preparation and Rhotekin pulldown assay

50 mM Tris-HCl, pH7.5
0.5 % Triton X-100
150 mM NaCl
5 mM $MgCl_2$
*10µg/ml Aprotinin
*10µg/ml Leupeptin
*10µg/ml PMSF
* freshly added just prior to use

5.6.3 6x Sample buffer for western blots

30% glycerol
10% SDS
0.6 M DTT
0.012% bromphenol blue
7 ml/ 10 ml 0.5 M Tris*Cl containing 0.4% SDS

5.7. Genotyping of mice

5.7.1 Preparation of mouse tail DNA

Tail biopsies were digested with proteinase K (500 µg/ml) (Roche) overnight at 55 °C in 500 µl Lysis buffer (10 mM Tris pH 8, 100 mM EDTA, 0.5% SDS). The DNA from the supernatant was precipitated with 500 µl 100% isopropanol, washed with 70% ethanol, air dried and dissolved in 50 µl TE.

5.7.2 Mouse tail DNA digestion by restriction enzyme for Southern blotting

The tail biopsy DNA was digested overnight at the appropriate temperature in 25 µl reaction mixture containing 10 µl DNA, 2.5 µl 10X restriction endonuclease buffer, 10.5 µl H_2O and 2 µl restriction endonuclease (10 U/µl). All the digestion volume was loaded for electrophoresis.

5.7.3 PCR genotyping of mice

0.3 µl of the tail DNA, 2µl 10X PCR buffer (NEB), 0.4µl 10mM dNTPs, 0.4µl 10µM sense primer, 0.4 µl 10 µM antisense primer, 16.1 µl H_2O and 0.1 µl Taq polymerase to the PCR reaction.

For genotyping the N19-RhoA mice, two primers flanking the 5' loxP site were used: HaRhoA-S-2 and HaRhoA-AS-2 (see Appendix section 5.9.4 "Primers used for targeting vector construction"), giving a 220 bp wild type band (Figure 38). PCR reactions were done for 46 cycles at 94 °C for 45 sec, 70 °C for 45 sec, 72 °C for 30 sec.

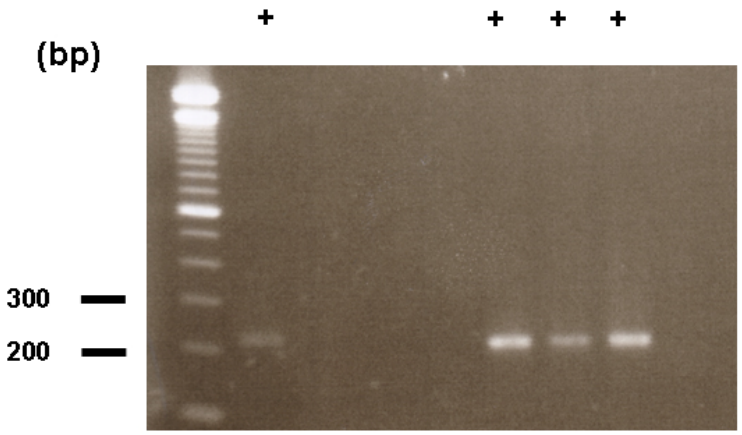

Figure 38. ***Genotyping of N19-RhoA mice***. *Genotyping of HA-N19RhoA mice by PCR using primers HaRhoA-A-2 and HaRhoA-AS-2. Expected PCR product size is 220 bp. +: positive PCR product.*

During crossing of N19-RhoA mice with the mice, we detected the Cre-positive mice by PCR using primers CRE(+) and CRE(-) (see Appendix section 5.9.4 "Primers for genotyping") that give a 486 bp amplicon (Figure 39). PCR conditions were 45 cycles at 95 °C for 30 sec, 55 °C for 30 sec and 72 ° for 30 sec.

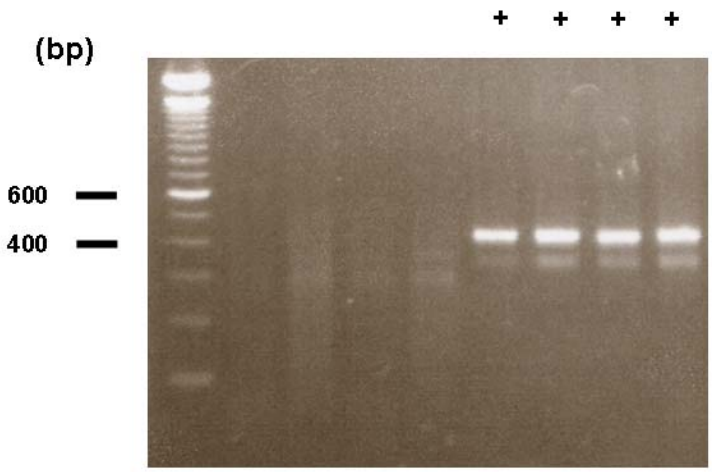

Figure 39. ***Genotyping of Cre mice.*** Genotyping strategy of Cre mice by PCR using primers Cre(+) and Cre(-). *Expected PCR product size is 486 bp. +: positive PCR product.*

5.8. Removal of the stop cassette insertion from the N19RhoA line

Crossing mice heterozygous or homozygous for N19-RhoA with a Cre-expressing resulted in the removal of a *floxed stop cassette*. After Cre recombination, the N19-RhoA cassette is activated and expressed. The two Cre-expressing lines EIIa::Cre or Nestin::Cre have been used for all my analysis of the N19-RhoA mice.

5.9 List of primers

5.9.1 Primers used for targeting vector construction

RhoA1:	5'-AATGTCGACGGCACCATGGCCTACCCCTACG- 3' (sense)
RhoA2:	5'-TATGCGGCCGCTCACAAGACAAGGCAACC-3' (antisense)
C3int1:	5'-AATGGATCCATGCCTTATGCGGATTCTTTTAAGG-3' (sense)
C3int2:	5'-TATGCGGCCGCCTATCTTTTTAATAATGCTG-3' (antisense)
MTfor1:	5'-CGGTTTAAACCGCCACCATGGTGAGCAAGGGC-3' (sense)

5.9.2 Sequencing primers

HSRho2:	5'-CCCAGAAAAGTGGTCCCCAG-3'
HSRho3:	5'-GCACGTTGGGACAGAAATGC-3'
C3-KA-2:	5'-GGTGCTACTTCTAGGAAGCAAC-3'
C3-KA-3:	5'-GATGAAGCAAGGGCATGGGG-3'
TAUTKII5'-2:	5'-GGCAGATGACAGGAGACAG-3'
TAUTKII3':	5'-GTATGTCCACCCCACTGACC-3'

TauTKII3'-upS: 5'-GGTCAGTGGGGTGGACATAC-3'
TauTKII3'-dwS: 5'-CAGAGTCCAGATGGCCAGG-3'
TauTKII3'dwS-2: 5'-GCGGATTTCTGAGTTCAAGGC-3'
TAUTKII5'-2upS: 5'-CTGTCTCCTGTCATCTGCC-3'
TAUTKII5'-3upS: 5'-GACAGCACCAAAGAGGTAC-3'
PWL512pA-dwS: 5'-CCATCAGAAGCTGGTCGAC-3'
TKNEO5'-1: 5'-GCGGATTTCTGAGTTCAAGGC-3'
SilviaT7-upS: 5'-GGTCAACAGAGTGAGTTCCG-3'
SilviaT3-dwS: 5'-GTCCAACCACGTAGGATGG-3'
TAUTKII3'-dwS-3: 5'-CAGTGGCTAAGAGCACTCG-3'
TKNEO-gap-pA: 5'-GCTTGCCGAATATCATGGTGG-3'
TauTK-Exon1-3'upS: 5'-GGACTGCTGTAGAACTGAG-3'

5.9.3 Standard primers

pBluescript II SK (+) sequencing primers

T3: 5'-AATTAACCCTCACTAAAGGG-3'
T7: 5'-TAATACGACTCACTATAGGG-3'
SP6: 5'- CGATTTAGGTGACACTATAG-3'

5.9.4 Primers for genotyping

HA-RhoA primers

HaRhoA-S-2: 5'-TACGACGTGCCCGACTAC-3' (sense)
HaRhoA-AS-2: 5'-GCTGTGTCCCACAAAGCC-3' (antisense)

EGFP-C3 primers

C3-KA-4: 5'-GATCCTGGATATTTAGGACCGG-3' (sense)
C3-KA-2: 5'-GGTGCTACTTCTAGGAAGCAAC-3' (antisense)

CRE primers

CRE(+): 5'-GCCGAAATTGCCAGGATCAG-3' (sense)
CRE(-): 5'-AGCCACCAGCTTGCATGATC-3' (antisense)

6 ABBREVIATIONS

α^{32}P-dCTP	Deoxcytosine triphosphate labeled with ^{32}P in alpha position
Ara-C	Cytosine arabinoside
ATP	Adenosine triphosphate
β	Beta
BDNF	Brain-derived neurotrophic factor
bp	Base pair
BSA	Bovine serum albumin
C	Celsius
cDNA	Complementary DNA
CGC	Cerebellar granule cells
CNS	Central Nervous System
COOH-terminal	Carboxyl terminal
Cre	Cre recombinase
EtBr	Ethidium bromide
DAB	3,3'-diaminobenzidine
DNA	Deoxyribonucleic acid
DMEM	"Dulbecco's Modified Eagle Medium"
DMSO	Dimethylsulfoxid
dNTP	Deoxyribonucleotide triphosphate
d.p.c.	days *post coitum*
DRG	Dorsal root ganglian
DTT	Dithiothreitol
E. coli	*Escherichia coli*
EGFP	Enhanced green fluorescent protein
et al.	et alii
EDTA	Ethylenediamine tetraacetic acid
ES	Embryonic Stem
FCS	Fetal calf serum
γ	Gamma
G	Glycine

G proteins	signal transducing GTP-binding proteins
G418	Geneticin
GAPs	GTPase-activating proteins
GDI	guanine dissociation inhibitor
GEFs	guanine nucleotide exchange factors
HA	Hemagglutinin
HEK	Human embryonic kidney
HEPES	N-(2-Hydroxyethyl)piperazine-N'-ethanesulfonic acid
hr(s)	hour(s)
HRP	Horse radish peroxide
IgG	Immunoglobulin G
IPTG	Isopropylthiogalaktoside
JNK	c-jun N-terminal kinase
kb	Kilobase
kD	Kilodalton
lacZ	β-galactosidase
LB	Luria Broth
LoxP	Locus of crossing over (for) phage P
LPA	lysophosphatidic acid
µ	Micro
M	Milli
m	Meter
M	Molar
MAG	Myelin-associated glycoprotein
MAPK	MAP kinase
MEF	Mouse embryonic fibroblast
MeCP2	methyl-CpG binding protein 2
Min	Minute
mRNA	Messenger RNA
MW	Molecular weight
NCS	Newborn Calf Serum
N	Asparagine
Neo	Neomycin resistance gene

NGF	nerve growth factor
NgR	Nogo receptor
N-terminus	Amino-terminus
OD	Optical Density
PAGE	Polyacrylamide gel electrophoresis
PBS	Phosphate-buffered saline
PCR	Polymerase chain reaction
PFA	Paraformaldehyde
PNS	Peripheral nervous system
PMSF	Phenylmethylsulfonylfluorid
P/S	penicillin/streptomycin
RT	Room temperature
RT-PCR	Reverse transcription coupled to polymerase chain reaction
RTT	Rett syndrome
Puro	Puromycin resistance gene
PVP	Polyvinylpyrollidone
RNA	Ribonucleic acid
RNase	Ribonuclease
ROK/ROCK	Rho kinase
rpm	Rounds per minute
S	Serine
Sec	Second
Sema3A	Semaphorin3A
SDS	Sodium-dodecyl-sulfat
T	Threonine
TAE	Tris-acetate-EDTA
TE	Tris/EDTA buffer
TEMED	N, N, N, N-Tetramethylethylendiamin
Tris	Tris(hydroxymethyl)aminomethane
Tris-HCl	Tris(hydroxymethyl)aminomethane-hydrochloride
TRITC	Tetramethyl-Rhodaminisothiocyanat
U	Unit
V	Valine

V	Volt
VP	Ventroposterior
mVP	medial ventral posterior nucleus of the thalamus
Wt	Wild-type

7 REFERENCES

Abdel-Majid, R.M., Leong, W.L., Schalkwyk, L.C., Smallman, D.S., Wong, S.T., Storm, D.R., Fine, A., Dobson, M.J., Guernsey, D.L. and Neumann, P.E. (1998) Loss of adenylyl cyclase I activity disrupts patterning of mouse somatosensory cortex. Nat Genet, 19, 289-291.

Abo, A., Boyhan, A., West, I., Thrasher, A.J. and Segal, A.W. (1992) Reconstitution of neutrophil NADPH oxidase activity in the cell-free system by four components: p67-phox, p47-phox, p21rac1, and cytochrome b-245. J Biol Chem, 267, 16767-16770.

Adamson, P., Marshall, C.J., Hall, A. and Tilbrook, P.A. (1992) Post-translational modifications of p21rho proteins. J Biol Chem, 267, 20033-20038.

Agmon, A., Yang, L.T., Jones, E.G. and O'Dowd, D.K. (1995) Topological precision in the thalamic projection to neonatal mouse barrel cortex. J Neurosci, 15, 549-561.

Aktories, K. and Frevert, J. (1987) ADP-ribosylation of a 21-24 kDa eukaryotic protein(s) by C3, a novel botulinum ADP-ribosyltransferase, is regulated by guanine nucleotide. Biochem J, 247, 363-368.

Alsina, B., Vu, T. and Cohen-Cory, S. (2001) Visualizing synapse formation in arborizing optic axons in vivo: dynamics and modulation by BDNF. Nat Neurosci, 4, 1093-1101.

Aspenstrom, P. (1999a) The Rho GTPases have multiple effects on the actin cytoskeleton. Exp Cell Res, 246, 20-25.

Aspenstrom, P. (1999b) Effectors for the Rho GTPases. Curr Opin Cell Biol, 11, 95-102.

Avraham, H. and Weinberg, R.A. (1989) Characterization and expression of the human rhoH12 gene product. Mol Cell Biol, 9, 2058-2066.

Awasaki, T., Saito, M., Sone, M., Suzuki, E., Sakai, R., Ito, K. and Hama, C. (2000) The Drosophila trio plays an essential role in patterning of axons by regulating their directional extension. Neuron, 26, 119-131.

Bamji, S.X., Majdan, M., Pozniak, C.D., Belliveau, D.J., Aloyz, R., Kohn, J., Causing, C.G. and Miller, F.D. (1998) The p75 neurotrophin receptor mediates neuronal apoptosis and is essential for naturally occurring sympathetic neuron death. J Cell Biol, 140, 911-923.

Barbacid, M. (1993) Nerve growth factor: a tale of two receptors. Oncogene, 8, 2033-2042.

Barrette, B.A., Srivatsa, P.J., Cliby, W.A., Keeney, G.L., Suman, V.J., Podratz, K.C. and Roche, P.C. (1997) Overexpression of p34cdc2 protein kinase in epithelial ovarian carcinoma. Mayo Clin Proc, 72, 925-929.

Bateman, J., Shu, H. and Van Vactor, D. (2000) The guanine nucleotide exchange factor trio mediates axonal development in the Drosophila embryo. Neuron, 26, 93-106.

Bernards, A. and Settleman, J. (2005) GAPs in growth factor signalling. Growth Factors, 23, 143-149.

Bibel, M. and Barde, Y.A. (2000) Neurotrophins: key regulators of cell fate and cell shape in the vertebrate nervous system. Genes Dev, 14, 2919-2937.

Binder, L.I., Frankfurter, A. and Rebhun, L.I. (1985) The distribution of tau in the mammalian central nervous system. J Cell Biol, 101, 1371-1378.

Bishop, A.L. and Hall, A. (2000) Rho GTPases and their effector proteins. Biochem J, 348 Pt 2, 241-255.

Bito, H., Furuyashiki, T., Ishihara, H., Shibasaki, Y., Ohashi, K., Mizuno, K., Maekawa, M., Ishizaki, T. and

Narumiya, S. (2000) A critical role for a Rho-associated kinase, p160ROCK, in determining axon outgrowth in mammalian CNS neurons. Neuron, 26, 431-441.

Bobak, D., Moorman, J., Guanzon, A., Gilmer, L. and Hahn, C. (1997) Inactivation of the small GTPase Rho disrupts cellular attachment and induces adhesion-dependent and adhesion-independent apoptosis. Oncogene, 15, 2179-2189.

Bothwell, M. (1995) Functional interactions of neurotrophins and neurotrophin receptors. Annu Rev Neurosci, 18, 223-253.

Brann, A.B., Scott, R., Neuberger, Y., Abulafia, D., Boldin, S., Fainzilber, M. and Futerman, A.H. (1999) Ceramide signaling downstream of the p75 neurotrophin receptor mediates the effects of nerve growth factor on outgrowth of cultured hippocampal neurons. J Neurosci, 19, 8199-8206.

Brennan, C., Rivas-Plata, K. and Landis, S.C. (1999) The p75 neurotrophin receptor influences NT-3 responsiveness of sympathetic neurons in vivo. Nat Neurosci, 2, 699-705.

Capecchi, M.R. (2005) Gene targeting in mice: functional analysis of the mammalian genome for the twenty-first century. Nat Rev Genet, 6, 507-512.

Carroll, P., Lewin, G.R., Koltzenburg, M., Toyka, K.V. and Thoenen, H. (1998) A role for BDNF in mechanosensation. Nat Neurosci, 1, 42-46.

Cases, O., Vitalis, T., Seif, I., De Maeyer, E., Sotelo, C. and Gaspar, P. (1996) Lack of barrels in the somatosensory cortex of monoamine oxidase A-deficient mice: role of a serotonin excess during the critical period. Neuron, 16, 297-307.

Cerione, R.A. and Zheng, Y. (1996) The Dbl family of oncogenes. Curr Opin Cell Biol, 8, 216-222.

Chang, Q., Khare, G., Dani, V., Nelson, S. and Jaenisch, R. (2006) The disease progression of Mecp2 mutant mice is affected by the level of BDNF expression. Neuron, 49, 341-348.

Chardin, P., Boquet, P., Madaule, P., Popoff, M.R., Rubin, E.J. and Gill, D.M. (1989) The mammalian G protein rhoC is ADP-ribosylated by Clostridium botulinum exoenzyme C3 and affects actin microfilaments in Vero cells. Embo J, 8, 1087-1092.

Chen, W.G., Chang, Q., Lin, Y., Meissner, A., West, A.E., Griffith, E.C., Jaenisch, R. and Greenberg, M.E. (2003) Derepression of BDNF transcription involves calcium-dependent phosphorylation of MeCP2. Science, 302, 885-889.

Chuang, T.H., Xu, X., Knaus, U.G., Hart, M.J. and Bokoch, G.M. (1993) GDP dissociation inhibitor prevents intrinsic and GTPase activating protein-stimulated GTP hydrolysis by the Rac GTP-binding protein. J Biol Chem, 268, 775-778.

Cohen-Cory, S. and Fraser, S.E. (1995) Effects of brain-derived neurotrophic factor on optic axon branching and remodelling in vivo. Nature, 378, 192-196.

Cordle, A., Koenigsknecht-Talboo, J., Wilkinson, B., Limpert, A. and Landreth, G. (2005) Mechanisms of statin-mediated inhibition of small G-protein function. J Biol Chem, 280, 34202-34209.

Coumans, J.V., Lin, T.T., Dai, H.N., MacArthur, L., McAtee, M., Nash, C. and Bregman, B.S. (2001) Axonal regeneration and functional recovery after complete spinal cord transection in rats by delayed treatment with transplants and neurotrophins. J Neurosci, 21, 9334-9344.

Crowley, C., Spencer, S.D., Nishimura, M.C., Chen, K.S., Pitts-Meek, S., Armanini, M.P., Ling, L.H., McMahon, S.B., Shelton, D.L., Levinson, A.D. and et al. (1994) Mice lacking nerve growth factor display perinatal loss of sensory and sympathetic neurons yet develop basal forebrain cholinergic neurons. Cell, 76,

1001-1011.

Dechant, G. and Barde, Y.A. (1997) Signalling through the neurotrophin receptor p75NTR. Curr Opin Neurobiol, 7, 413-418.

Dechant, G. and Barde, Y.A. (2002) The neurotrophin receptor p75(NTR): novel functions and implications for diseases of the nervous system. Nat Neurosci, 5, 1131-1136.

DeFeo-Jones, D., Scolnick, E.M., Koller, R. and Dhar, R. (1983) ras-Related gene sequences identified and isolated from Saccharomyces cerevisiae. Nature, 306, 707-709.

DerMardirossian, C. and Bokoch, G.M. (2005) GDIs: central regulatory molecules in Rho GTPase activation. Trends Cell Biol, 15, 356-363.

Dickson, B.J. (2001) Rho GTPases in growth cone guidance. Curr Opin Neurobiol, 11, 103-110.

Dontchev, V.D. and Letourneau, P.C. (2002) Nerve growth factor and semaphorin 3A signaling pathways interact in regulating sensory neuronal growth cone motility. J Neurosci, 22, 6659-6669.

Engert, F. and Bonhoeffer, T. (1999) Dendritic spine changes associated with hippocampal long-term synaptic plasticity. Nature, 399, 66-70.

Ernfors, P., Lee, K.F., Kucera, J. and Jaenisch, R. (1994) Lack of neurotrophin-3 leads to deficiencies in the peripheral nervous system and loss of limb proprioceptive afferents. Cell, 77, 503-512.

Erschbamer, M.K., Hofstetter, C.P. and Olson, L. (2005) RhoA, RhoB, RhoC, Rac1, Cdc42, and Tc10 mRNA levels in spinal cord, sensory ganglia, and corticospinal tract neurons and long-lasting specific changes following spinal cord injury. J Comp Neurol, 484, 224-233.

Etienne-Manneville, S. and Hall, A. (2002) Rho GTPases in cell biology. Nature, 420, 629-635.

Evans, M.J. and Kaufman, M.H. (1981) Establishment in culture of pluripotential cells from mouse embryos. Nature, 292, 154-156.

Farnsworth, C.L. and Feig, L.A. (1991) Dominant inhibitory mutations in the Mg(2+)-binding site of RasH prevent its activation by GTP. Mol Cell Biol, 11, 4822-4829.

Feig, L.A. (1994) Guanine-nucleotide exchange factors: a family of positive regulators of Ras and related GTPases. Curr Opin Cell Biol, 6, 204-211.

Fenstermaker, V., Chen, Y., Ghosh, A. and Yuste, R. (2004) Regulation of dendritic length and branching by semaphorin 3A. J Neurobiol, 58, 403-412.

Frost, D.O. (2001) BDNF/trkB signaling in the developmental sculpting of visual connections. Prog Brain Res, 134, 35-49.

Fukui, Y. and Kaziro, Y. (1985) Molecular cloning and sequence analysis of a ras gene from Schizosaccharomyces pombe. Embo J, 4, 687-691.

Fukumitsu, H., Ohtsuka, M., Murai, R., Nakamura, H., Itoh, K. and Furukawa, S. (2006) Brain-derived neurotrophic factor participates in determination of neuronal laminar fate in the developing mouse cerebral cortex. J Neurosci, 26, 13218-13230.

Gallo, G., Lefcort, F.B. and Letourneau, P.C. (1997) The trkA receptor mediates growth cone turning toward a localized source of nerve growth factor. J Neurosci, 17, 5445-5454.

Gallo, G. and Letourneau, P.C. (1998a) Axon guidance: GTPases help axons reach their targets. Curr Biol, 8,

R80-82.

Gallo, G. and Letourneau, P.C. (1998b) Localized sources of neurotrophins initiate axon collateral sprouting. J Neurosci, 18, 5403-5414.

Gallo, G. and Letourneau, P.C. (2000) Neurotrophins and the dynamic regulation of the neuronal cytoskeleton. J Neurobiol, 44, 159-173.

Gallo, G. and Letourneau, P.C. (2004) Regulation of growth cone actin filaments by guidance cues. J Neurobiol, 58, 92-102.

Garrett, M.D., Self, A.J., van Oers, C. and Hall, A. (1989) Identification of distinct cytoplasmic targets for ras/R-ras and rho regulatory proteins. J Biol Chem, 264, 10-13.

Gehler, S., Gallo, G., Veien, E. and Letourneau, P.C. (2004) p75 neurotrophin receptor signaling regulates growth cone filopodial dynamics through modulating RhoA activity. J Neurosci, 24, 4363-4372.

Goldberg, J.L., Espinosa, J.S., Xu, Y., Davidson, N., Kovacs, G.T. and Barres, B.A. (2002) Retinal ganglion cells do not extend axons by default: promotion by neurotrophic signaling and electrical activity. Neuron, 33, 689-702.

Greenough, W.T. and Chang, F.L. (1988) Dendritic pattern formation involves both oriented regression and oriented growth in the barrels of mouse somatosensory cortex. Brain Res, 471, 148-152.

Gu, H., Zou, Y.R. and Rajewsky, K. (1993) Independent control of immunoglobulin switch recombination at individual switch regions evidenced through Cre-loxP-mediated gene targeting. Cell, 73, 1155-1164.

Gundersen, R.W. and Barrett, J.N. (1979) Neuronal chemotaxis: chick dorsal-root axons turn toward high concentrations of nerve growth factor. Science, 206, 1079-1080.

Hakeda-Suzuki, S., Ng, J., Tzu, J., Dietzl, G., Sun, Y., Harms, M., Nardine, T., Luo, L. and Dickson, B.J. (2002) Rac function and regulation during Drosophila development. Nature, 416, 438-442.

Hancock, J.F. and Hall, A. (1993) A novel role for RhoGDI as an inhibitor of GAP proteins. Embo J, 12, 1915-1921.

Harrington, A.W., Kim, J.Y. and Yoon, S.O. (2002) Activation of Rac GTPase by p75 is necessary for c-jun N-terminal kinase-mediated apoptosis. J Neurosci, 22, 156-166.

Hart, M.J., Maru, Y., Leonard, D., Witte, O.N., Evans, T. and Cerione, R.A. (1992) A GDP dissociation inhibitor that serves as a GTPase inhibitor for the Ras-like protein CDC42Hs. Science, 258, 812-815.

Hengst, U., Cox, L.J., Macosko, E.Z. and Jaffrey, S.R. (2006) Functional and selective RNA interference in developing axons and growth cones. J Neurosci, 26, 5727-5732.

Henning, S.W., Galandrini, R., Hall, A. and Cantrell, D.A. (1997) The GTPase Rho has a critical regulatory role in thymus development. Embo J, 16, 2397-2407.

Hippenmeyer, S., Vrieseling, E., Sigrist, M., Portmann, T., Laengle, C., Ladle, D.R. and Arber, S. (2005) A developmental switch in the response of DRG neurons to ETS transcription factor signaling. PLoS Biol, 3, e159.

Hirsch, E., Pozzato, M., Vercelli, A., Barberis, L., Azzolino, O., Russo, C., Vanni, C., Silengo, L., Eva, A. and Altruda, F. (2002) Defective dendrite elongation but normal fertility in mice lacking the Rho-like GTPase activator Dbl. Mol Cell Biol, 22, 3140-3148.

Hori, Y., Kikuchi, A., Isomura, M., Katayama, M., Miura, Y., Fujioka, H., Kaibuchi, K. and Takai, Y. (1991)

Post-translational modifications of the C-terminal region of the rho protein are important for its interaction with membranes and the stimulatory and inhibitory GDP/GTP exchange proteins. Oncogene, 6, 515-522.

Ihara, K., Muraguchi, S., Kato, M., Shimizu, T., Shirakawa, M., Kuroda, S., Kaibuchi, K. and Hakoshima, T. (1998) Crystal structure of human RhoA in a dominantly active form complexed with a GTP analogue. J Biol Chem, 273, 9656-9666.

Jalink, K. and Moolenaar, W.H. (1992) Thrombin receptor activation causes rapid neural cell rounding and neurite retraction independent of classic second messengers. J Cell Biol, 118, 411-419.

Jalink, K., van Corven, E.J., Hengeveld, T., Morii, N., Narumiya, S. and Moolenaar, W.H. (1994) Inhibition of lysophosphatidate- and thrombin-induced neurite retraction and neuronal cell rounding by ADP ribosylation of the small GTP-binding protein Rho. J Cell Biol, 126, 801-810.

Jin, Z. and Strittmatter, S.M. (1997) Rac1 mediates collapsin-1-induced growth cone collapse. J Neurosci, 17, 6256-6263.

Just, I., Schallehn, G. and Aktories, K. (1992) ADP-ribosylation of small GTP-binding proteins by Bacillus cereus. Biochem Biophys Res Commun, 183, 931-936.

Just, I., Selzer, J., Jung, M., van Damme, J., Vandekerckhove, J. and Aktories, K. (1995) Rho-ADP-ribosylating exoenzyme from Bacillus cereus. Purification, characterization, and identification of the NAD-binding site. Biochemistry, 34, 334-340.

Kagoshima, M. and Ito, T. (2001) Diverse gene expression and function of semaphorins in developing lung: positive and negative regulatory roles of semaphorins in lung branching morphogenesis. Genes Cells, 6, 559-571.

Kaibuchi, K., Kuroda, S. and Amano, M. (1999) Regulation of the cytoskeleton and cell adhesion by the Rho family GTPases in mammalian cells. Annu Rev Biochem, 68, 459-486.

Kaplan, D.R. and Miller, F.D. (2003) Axon growth inhibition: signals from the p75 neurotrophin receptor. Nat Neurosci, 6, 435-436.

Katz, L.C. and Shatz, C.J. (1996) Synaptic activity and the construction of cortical circuits. Science, 274, 1133-1138.

Kobayashi, K., Takahashi, M., Matsushita, N., Miyazaki, J., Koike, M., Yaginuma, H., Osumi, N. and Kaibuchi, K. (2004) Survival of developing motor neurons mediated by Rho GTPase signaling pathway through Rho-kinase. J Neurosci, 24, 3480-3488.

Kohn, J., Aloyz, R.S., Toma, J.G., Haak-Frendscho, M. and Miller, F.D. (1999) Functionally antagonistic interactions between the TrkA and p75 neurotrophin receptors regulate sympathetic neuron growth and target innervation. J Neurosci, 19, 5393-5408.

Kozma, R., Ahmed, S., Best, A. and Lim, L. (1995) The Ras-related protein Cdc42Hs and bradykinin promote formation of peripheral actin microspikes and filopodia in Swiss 3T3 fibroblasts. Mol Cell Biol, 15, 1942-1952.

Kozma, R., Sarner, S., Ahmed, S. and Lim, L. (1997) Rho family GTPases and neuronal growth cone remodelling: relationship between increased complexity induced by Cdc42Hs, Rac1, and acetylcholine and collapse induced by RhoA and lysophosphatidic acid. Mol Cell Biol, 17, 1201-1211.

Kuhn, T.B., Brown, M.D., Wilcox, C.L., Raper, J.A. and Bamburg, J.R. (1999) Myelin and collapsin-1 induce motor neuron growth cone collapse through different pathways: inhibition of collapse by opposing mutants of rac1. J Neurosci, 19, 1965-1975.

Kuhn, T.B., Meberg, P.J., Brown, M.D., Bernstein, B.W., Minamide, L.S., Jensen, J.R., Okada, K., Soda, E.A.

and Bamburg, J.R. (2000) Regulating actin dynamics in neuronal growth cones by ADF/cofilin and rho family GTPases. J Neurobiol, 44, 126-144.

Kurihara, H., Zama, A., Tamura, M., Takeda, J., Sasaki, T. and Takeuchi, T. (2000) Glioma/glioblastoma-specific adenoviral gene expression using the nestin gene regulator. Gene Ther, 7, 686-693.

Lakso, M., Pichel, J.G., Gorman, J.R., Sauer, B., Okamoto, Y., Lee, E., Alt, F.W. and Westphal, H. (1996) Efficient in vivo manipulation of mouse genomic sequences at the zygote stage. Proc Natl Acad Sci U S A, 93, 5860-5865.

Lamoureux, P., Altun-Gultekin, Z.F., Lin, C., Wagner, J.A. and Heidemann, S.R. (1997) Rac is required for growth cone function but not neurite assembly. J Cell Sci, 110 (Pt 5), 635-641.

Lee, K.F., Li, E., Huber, L.J., Landis, S.C., Sharpe, A.H., Chao, M.V. and Jaenisch, R. (1992) Targeted mutation of the gene encoding the low affinity NGF receptor p75 leads to deficits in the peripheral sensory nervous system. Cell, 69, 737-749.

Lee, K.F., Bachman, K., Landis, S. and Jaenisch, R. (1994) Dependence on p75 for innervation of some sympathetic targets. Science, 263, 1447-1449.

Lentz, S.I., Knudson, C.M., Korsmeyer, S.J. and Snider, W.D. (1999) Neurotrophins support the development of diverse sensory axon morphologies. J Neurosci, 19, 1038-1048.

Leonard, D., Hart, M.J., Platko, J.V., Eva, A., Henzel, W., Evans, T. and Cerione, R.A. (1992) The identification and characterization of a GDP-dissociation inhibitor (GDI) for the CDC42Hs protein. J Biol Chem, 267, 22860-22868.

Li, Z., Van Aelst, L. and Cline, H.T. (2000) Rho GTPases regulate distinct aspects of dendritic arbor growth in Xenopus central neurons in vivo. Nat Neurosci, 3, 217-225.

Liebl, E.C., Forsthoefel, D.J., Franco, L.S., Sample, S.H., Hess, J.E., Cowger, J.A., Chandler, M.P., Shupert, A.M. and Seeger, M.A. (2000) Dosage-sensitive, reciprocal genetic interactions between the Abl tyrosine kinase and the putative GEF trio reveal trio's role in axon pathfinding. Neuron, 26, 107-118.

Linseman, D.A., Laessig, T., Meintzer, M.K., McClure, M., Barth, H., Aktories, K. and Heidenreich, K.A. (2001) An essential role for Rac/Cdc42 GTPases in cerebellar granule neuron survival. J Biol Chem, 276, 39123-39131.

Lom, B. and Cohen-Cory, S. (1999) Brain-derived neurotrophic factor differentially regulates retinal ganglion cell dendritic and axonal arborization in vivo. J Neurosci, 19, 9928-9938.

Luikenhuis, S., Giacometti, E., Beard, C.F. and Jaenisch, R. (2004) Expression of MeCP2 in postmitotic neurons rescues Rett syndrome in mice. Proc Natl Acad Sci U S A, 101, 6033-6038.

Luo, L., Hensch, T.K., Ackerman, L., Barbel, S., Jan, L.Y. and Jan, Y.N. (1996) Differential effects of the Rac GTPase on Purkinje cell axons and dendritic trunks and spines. Nature, 379, 837-840.

Luo, L., Jan, L.Y. and Jan, Y.N. (1997) Rho family GTP-binding proteins in growth cone signalling. Curr Opin Neurobiol, 7, 81-86.

Luo, L. (2000) Rho GTPases in neuronal morphogenesis. Nat Rev Neurosci, 1, 173-180.
Machesky, L.M. and Hall, A. (1996) Rho: a connection between membrane receptor signalling and the cytoskeleton. Trends Cell Biol, 6, 304-310.

Madaule, P. and Axel, R. (1985) A novel ras-related gene family. Cell, 41, 31-40.

Maddala, R., Deng, P.F., Costello, J.M., Wawrousek, E.F., Zigler, J.S. and Rao, V.P. (2004) Impaired

cytoskeletal organization and membrane integrity in lens fibers of a Rho GTPase functional knockout transgenic mouse. Lab Invest, 84, 679-692.

Maletic-Savatic, M., Malinow, R. and Svoboda, K. (1999) Rapid dendritic morphogenesis in CA1 hippocampal dendrites induced by synaptic activity. Science, 283, 1923-1927.

Malosio, M.L., Gilardelli, D., Paris, S., Albertinazzi, C. and de Curtis, I. (1997) Differential expression of distinct members of Rho family GTP-binding proteins during neuronal development: identification of Rac1B, a new neural-specific member of the family. J Neurosci, 17, 6717-6728.

Mandelkow, E. and Mandelkow, E.M. (1995) Microtubules and microtubule-associated proteins. Curr Opin Cell Biol, 7, 72-81.

Markus, A., Patel, T.D. and Snider, W.D. (2002) Neurotrophic factors and axonal growth. Curr Opin Neurobiol, 12, 523-531.

Martinowich, K., Hattori, D., Wu, H., Fouse, S., He, F., Hu, Y., Fan, G. and Sun, Y.E. (2003) DNA methylation-related chromatin remodeling in activity-dependent BDNF gene regulation. Science, 302, 890-893.

McAllister, A.K., Katz, L.C. and Lo, D.C. (1999) Neurotrophins and synaptic plasticity. Annu Rev Neurosci, 22, 295-318.

McQuillen, P.S., DeFreitas, M.F., Zada, G. and Shatz, C.J. (2002) A novel role for p75NTR in subplate growth cone complexity and visual thalamocortical innervation. J Neurosci, 22, 3580-3593.

Menesini Chen, M.G., Chen, J.S. and Levi-Montalcini, R. (1978) Sympathetic nerve fibers ingrowth in the central nervous system of neonatal rodent upon intracerebral NGF injections. Arch Ital Biol, 116, 53-84.

Ming, G., Song, H., Berninger, B., Inagaki, N., Tessier-Lavigne, M. and Poo, M. (1999) Phospholipase C-gamma and phosphoinositide 3-kinase mediate cytoplasmic signaling in nerve growth cone guidance. Neuron, 23, 139-148.

Moorman, J.P., Bobak, D.A. and Hahn, C.S. (1996) Inactivation of the small GTP binding protein Rho induces multinucleate cell formation and apoptosis in murine T lymphoma EL4. J Immunol, 156, 4146-4153.

Moorman, J.P., Luu, D., Wickham, J., Bobak, D.A. and Hahn, C.S. (1999) A balance of signaling by Rho family small GTPases RhoA, Rac1 and Cdc42 coordinates cytoskeletal morphology but not cell survival. Oncogene, 18, 47-57.

Morii, N., Kawano, K., Sekine, A., Yamada, T. and Narumiya, S. (1991) Purification of GTPase-activating protein specific for the rho gene products. J Biol Chem, 266, 7646-7650.

Morita, A., Yamashita, N., Sasaki, Y., Uchida, Y., Nakajima, O., Nakamura, F., Yagi, T., Taniguchi, M., Usui, H., Katoh-Semba, R., Takei, K. and Goshima, Y. (2006) Regulation of dendritic branching and spine maturation by semaphorin3A-Fyn signaling. J Neurosci, 26, 2971-2980.

Mozer, B., Marlor, R., Parkhurst, S. and Corces, V. (1985) Characterization and developmental expression of a Drosophila ras oncogene. Mol Cell Biol, 5, 885-889.

Mueller, B.K. (1999) Growth cone guidance: first steps towards a deeper understanding. Annu Rev Neurosci, 22, 351-388.

Nadarajah, B., Alifragis, P., Wong, R.O. and Parnavelas, J.G. (2003) Neuronal migration in the developing cerebral cortex: observations based on real-time imaging. Cereb Cortex, 13, 607-611.

Nakayama, A.Y., Harms, M.B. and Luo, L. (2000) Small GTPases Rac and Rho in the maintenance of dendritic spines and branches in hippocampal pyramidal neurons. J Neurosci, 20, 5329-5338.

Nakazawa, T., Watabe, A.M., Tezuka, T., Yoshida, Y., Yokoyama, K., Umemori, H., Inoue, A., Okabe, S., Manabe, T. and Yamamoto, T. (2003) p250GAP, a novel brain-enriched GTPase-activating protein for Rho family GTPases, is involved in the N-methyl-d-aspartate receptor signaling. Mol Biol Cell, 14, 2921-2934.

Negishi, M. and Katoh, H. (2005) Rho family GTPases and dendrite plasticity. Neuroscientist, 11, 187-191.

Newsome, T.P., Schmidt, S., Dietzl, G., Keleman, K., Asling, B., Debant, A. and Dickson, B.J. (2000) Trio combines with dock to regulate Pak activity during photoreceptor axon pathfinding in Drosophila. Cell, 101, 283-294.

Ng, J., Nardine, T., Harms, M., Tzu, J., Goldstein, A., Sun, Y., Dietzl, G., Dickson, B.J. and Luo, L. (2002) Rac GTPases control axon growth, guidance and branching. Nature, 416, 442-447.

Nishiki, T., Narumiya, S., Morii, N., Yamamoto, M., Fujiwara, M., Kamata, Y., Sakaguchi, G. and Kozaki, S. (1990) ADP-ribosylation of the rho/rac proteins induces growth inhibition, neurite outgrowth and acetylcholine esterase in cultured PC-12 cells. Biochem Biophys Res Commun, 167, 265-272.

Nobes, C.D. and Hall, A. (1995) Rho, rac, and cdc42 GTPases regulate the assembly of multimolecular focal complexes associated with actin stress fibers, lamellipodia, and filopodia. Cell, 81, 53-62.

Nobes, C.D., Hawkins, P., Stephens, L. and Hall, A. (1995) Activation of the small GTP-binding proteins rho and rac by growth factor receptors. J Cell Sci, 108 (Pt 1), 225-233.

O'Leary, D.D., Ruff, N.L. and Dyck, R.H. (1994) Development, critical period plasticity, and adult reorganizations of mammalian somatosensory systems. Curr Opin Neurobiol, 4, 535-544.

Ohmiya, M., Shudai, T., Nitta, A., Nomoto, H., Furukawa, Y. and Furukawa, S. (2002) Brain-derived neurotrophic factor alters cell migration of particular progenitors in the developing mouse cerebral cortex. Neurosci Lett, 317, 21-24.

Olenik, C., Barth, H., Just, I., Aktories, K. and Meyer, D.K. (1997) Gene expression of the small GTP-binding proteins RhoA, RhoB, Rac1, and Cdc42 in adult rat brain. Brain Res Mol Brain Res, 52, 263-269.

Olofsson, B. (1999) Rho guanine dissociation inhibitors: pivotal molecules in cellular signalling. Cell Signal, 11, 545-554.

Olson, E.C. and Walsh, C.A. (2002) Smooth, rough and upside-down neocortical development. Curr Opin Genet Dev, 12, 320-327.

Ozdinler, P.H. and Erzurumlu, R.S. (2001) Regulation of neurotrophin-induced axonal responses via Rho GTPases. J Comp Neurol, 438, 377-387.

Patel, T.D., Jackman, A., Rice, F.L., Kucera, J. and Snider, W.D. (2000) Development of sensory neurons in the absence of NGF/TrkA signaling in vivo. Neuron, 25, 345-357.

Paterson, H.F., Self, A.J., Garrett, M.D., Just, I., Aktories, K. and Hall, A. (1990) Microinjection of recombinant p21rho induces rapid changes in cell morphology. J Cell Biol, 111, 1001-1007.

Peterson, D.A., Dickinson-Anson, H.A., Leppert, J.T., Lee, K.F. and Gage, F.H. (1999) Central neuronal loss and behavioral impairment in mice lacking neurotrophin receptor p75. J Comp Neurol, 404, 1-20.

Polleux, F., Dehay, C. and Kennedy, H. (1998) Neurogenesis and commitment of corticospinal neurons in reeler. J Neurosci, 18, 9910-9923.

Ramakers, G.J. (2002) Rho proteins, mental retardation and the cellular basis of cognition. Trends Neurosci, 25, 191-199.

Read, P.W., Liu, X., Longenecker, K., Dipierro, C.G., Walker, L.A., Somlyo, A.V., Somlyo, A.P. and Nakamoto, R.K. (2000) Human RhoA/RhoGDI complex expressed in yeast: GTP exchange is sufficient for translocation of RhoA to liposomes. Protein Sci, 9, 376-386.

Ren, X.D., Kiosses, W.B. and Schwartz, M.A. (1999) Regulation of the small GTP-binding protein Rho by cell adhesion and the cytoskeleton. Embo J, 18, 578-585.

Reymond, C.D., Gomer, R.H., Mehdy, M.C. and Firtel, R.A. (1984) Developmental regulation of a Dictyostelium gene encoding a protein homologous to mammalian ras protein. Cell, 39, 141-148.

Ridley, A.J., Paterson, H.F., Johnston, C.L., Diekmann, D. and Hall, A. (1992) The small GTP-binding protein rac regulates growth factor-induced membrane ruffling. Cell, 70, 401-410.

Ridley, A.J. and Hall, A. (1992a) The small GTP-binding protein rho regulates the assembly of focal adhesions and actin stress fibers in response to growth factors. Cell, 70, 389-399.

Ridley, A.J. and Hall, A. (1992b) Distinct patterns of actin organization regulated by the small GTP-binding proteins Rac and Rho. Cold Spring Harb Symp Quant Biol, 57, 661-671.

Rossman, K.L. and Sondek, J. (2005) Larger than Dbl: new structural insights into RhoA activation. Trends Biochem Sci, 30, 163-165.

Ruchhoeft, M.L., Ohnuma, S., McNeill, L., Holt, C.E. and Harris, W.A. (1999) The neuronal architecture of Xenopus retinal ganglion cells is sculpted by rho-family GTPases in vivo. J Neurosci, 19, 8454-8463.

Sahay, A., Kim, C.H., Sepkuty, J.P., Cho, E., Huganir, R.L., Ginty, D.D. and Kolodkin, A.L. (2005) Secreted semaphorins modulate synaptic transmission in the adult hippocampus. J Neurosci, 25, 3613-3620.

Sasaki, T., Kato, M. and Takai, Y. (1993) Consequences of weak interaction of rho GDI with the GTP-bound forms of rho p21 and rac p21. J Biol Chem, 268, 23959-23963.

Sasaki, T. and Takai, Y. (1998) The Rho small G protein family-Rho GDI system as a temporal and spatial determinant for cytoskeletal control. Biochem Biophys Res Commun, 245, 641-645.

Sasaki, Y., Cheng, C., Uchida, Y., Nakajima, O., Ohshima, T., Yagi, T., Taniguchi, M., Nakayama, T., Kishida, R., Kudo, Y., Ohno, S., Nakamura, F. and Goshima, Y. (2002) Fyn and Cdk5 mediate semaphorin-3A signaling, which is involved in regulation of dendrite orientation in cerebral cortex. Neuron, 35, 907-920.

Schlaggar, B.L. and O'Leary, D.D. (1991) Potential of visual cortex to develop an array of functional units unique to somatosensory cortex. Science, 252, 1556-1560.

Schmidt, A. and Hall, A. (2002) Guanine nucleotide exchange factors for Rho GTPases: turning on the switch. Genes Dev, 16, 1587-1609.

Sekine, A., Fujiwara, M. and Narumiya, S. (1989) Asparagine residue in the rho gene product is the modification site for botulinum ADP-ribosyltransferase. J Biol Chem, 264, 8602-8605.

Serini, G., Valdembri, D., Zanivan, S., Morterra, G., Burkhardt, C., Caccavari, F., Zammataro, L., Primo, L., Tamagnone, L., Logan, M., Tessier-Lavigne, M., Taniguchi, M., Puschel, A.W. and Bussolino, F. (2003) Class 3 semaphorins control vascular morphogenesis by inhibiting integrin function. Nature, 424, 391-397.

Silos-Santiago, I., Molliver, D.C., Ozaki, S., Smeyne, R.J., Fagan, A.M., Barbacid, M. and Snider, W.D. (1995) Non-TrkA-expressing small DRG neurons are lost in TrkA deficient mice. J Neurosci, 15, 5929-5942.

Smeyne, R.J., Klein, R., Schnapp, A., Long, L.K., Bryant, S., Lewin, A., Lira, S.A. and Barbacid, M. (1994) Severe sensory and sympathetic neuropathies in mice carrying a disrupted Trk/NGF receptor gene. Nature, 368,

246-249.

Smithies, O. (2005) Many little things: one geneticist's view of complex diseases. Nat Rev Genet, 6, 419-425.

Song, H.J. and Poo, M.M. (1999) Signal transduction underlying growth cone guidance by diffusible factors. Curr Opin Neurobiol, 9, 355-363.

Sordella, R., Classon, M., Hu, K.Q., Matheson, S.F., Brouns, M.R., Fine, B., Zhang, L., Takami, H., Yamada, Y. and Settleman, J. (2002) Modulation of CREB activity by the Rho GTPase regulates cell and organism size during mouse embryonic development. Dev Cell, 2, 553-565.

Stemple, D.L. and Anderson, D.J. (1992) Isolation of a stem cell for neurons and glia from the mammalian neural crest. Cell, 71, 973-985.

Suidan, H.S., Stone, S.R., Hemmings, B.A. and Monard, D. (1992) Thrombin causes neurite retraction in neuronal cells through activation of cell surface receptors. Neuron, 8, 363-375.

Sun, Y.E. and Wu, H. (2006) The ups and downs of BDNF in Rett syndrome. Neuron, 49, 321-323.

Takai, Y., Sasaki, T. and Matozaki, T. (2001) Small GTP-binding proteins. Physiol Rev, 81, 153-208.

Taniguchi, M., Yuasa, S., Fujisawa, H., Naruse, I., Saga, S., Mishina, M. and Yagi, T. (1997) Disruption of semaphorin III/D gene causes severe abnormality in peripheral nerve projection. Neuron, 19, 519-530.

Taniguchi, S., Liu, H., Nakazawa, T., Yokoyama, K., Tezuka, T. and Yamamoto, T. (2003) p250GAP, a neural RhoGAP protein, is associated with and phosphorylated by Fyn. Biochem Biophys Res Commun, 306, 151-155.

Tapon, N. and Hall, A. (1997) Rho, Rac and Cdc42 GTPases regulate the organization of the actin cytoskeleton. Curr Opin Cell Biol, 9, 86-92.

Tarabykin, V., Stoykova, A., Usman, N. and Gruss, P. (2001) Cortical upper layer neurons derive from the subventricular zone as indicated by Svet1 gene expression. Development, 128, 1983-1993.

Tessarollo, L., Vogel, K.S., Palko, M.E., Reid, S.W. and Parada, L.F. (1994) Targeted mutation in the neurotrophin-3 gene results in loss of muscle sensory neurons. Proc Natl Acad Sci U S A, 91, 11844-11848.

Threadgill, R., Bobb, K. and Ghosh, A. (1997) Regulation of dendritic growth and remodeling by Rho, Rac, and Cdc42. Neuron, 19, 625-634.

Tucker, K.L., Meyer, M. and Barde, Y.A. (2001) Neurotrophins are required for nerve growth during development. Nat Neurosci, 4, 29-37.

Tucker, K.L. (2002) Neurotrophins and the control of axonal outgrowth. Panminerva Med, 44, 325-333.

Ueda, T., Kikuchi, A., Ohga, N., Yamamoto, J. and Takai, Y. (1990) Purification and characterization from bovine brain cytosol of a novel regulatory protein inhibiting the dissociation of GDP from and the subsequent binding of GTP to rhoB p20, a ras p21-like GTP-binding protein. J Biol Chem, 265, 9373-9380.

Ulupinar, E., Datwani, A., Behar, O., Fujisawa, H. and Erzurumlu, R. (1999) Role of semaphorin III in the developing rodent trigeminal system. Mol Cell Neurosci, 13, 281-292.

Van Aelst, L. and D'Souza-Schorey, C. (1997) Rho GTPases and signaling networks. Genes Dev, 11, 2295-2322.

Vastrik, I., Eickholt, B.J., Walsh, F.S., Ridley, A. and Doherty, P. (1999) Sema3A-induced growth-cone collapse is mediated by Rac1 amino acids 17-32. Curr Biol, 9, 991-998.

von Bartheld, C.S., Heuer, J.G. and Bothwell, M. (1991) Expression of nerve growth factor (NGF) receptors in the brain and retina of chick embryos: comparison with cholinergic development. J Comp Neurol, 310, 103-129.

Wahl, S., Barth, H., Ciossek, T., Aktories, K. and Mueller, B.K. (2000) Ephrin-A5 induces collapse of growth cones by activating Rho and Rho kinase. J Cell Biol, 149, 263-270.

Ward, N.L. and Hagg, T. (1999) p75(NGFR) and cholinergic neurons in the developing forebrain: a re-examination. Brain Res Dev Brain Res, 118, 79-91.

Welker, E., Armstrong-James, M., Bronchti, G., Ourednik, W., Gheorghita-Baechler, F., Dubois, R., Guernsey, D.L., Van der Loos, H. and Neumann, P.E. (1996) Altered sensory processing in the somatosensory cortex of the mouse mutant barrelless. Science, 271, 1864-1867.

Wiegers, W., Just, I., Muller, H., Hellwig, A., Traub, P. and Aktories, K. (1991) Alteration of the cytoskeleton of mammalian cells cultured in vitro by Clostridium botulinum C2 toxin and C3 ADP-ribosyltransferase. Eur J Cell Biol, 54, 237-245.

Woo, S. and Gomez, T.M. (2006) Rac1 and RhoA promote neurite outgrowth through formation and stabilization of growth cone point contacts. J Neurosci, 26, 1418-1428.

Wu, K.Y., Hengst, U., Cox, L.J., Macosko, E.Z., Jeromin, A., Urquhart, E.R. and Jaffrey, S.R. (2005) Local translation of RhoA regulates growth cone collapse. Nature, 436, 1020-1024.

Yamashita, T., Tucker, K.L. and Barde, Y.A. (1999) Neurotrophin binding to the p75 receptor modulates Rho activity and axonal outgrowth. Neuron, 24, 585-593.

Yamashita, T. and Tohyama, M. (2003) The p75 receptor acts as a displacement factor that releases Rho from Rho-GDI. Nat Neurosci, 6, 461-467.

Yeo, T.T., Chua-Couzens, J., Butcher, L.L., Bredesen, D.E., Cooper, J.D., Valletta, J.S., Mobley, W.C. and Longo, F.M. (1997) Absence of p75NTR causes increased basal forebrain cholinergic neuron size, choline acetyltransferase activity, and target innervation. J Neurosci, 17, 7594-7605.

8 PUBLICATIONS

Sanno, H., Komljenovic, D., and Tucker, KL. RhoGTPases play a role in proper formation of layers IV and V in somatosensory cortex. *In preparation*